

ผลกระทบบของวิวิธพันธุ์ของแหล่งกักเก็บต่อการผลิตน้ำมัน



นายศฤษดี สุวรรณมณี

ศูนย์วิทยทรัพยากร
จุฬาลงกรณ์มหาวิทยาลัย

วิทยานิพนธ์นี้เป็นส่วนหนึ่งของการศึกษาตามหลักสูตรปริญญาวิศวกรรมศาสตรมหาบัณฑิต

สาขาวิชาวิศวกรรมปิโตรเลียม ภาควิชาวิศวกรรมเหมืองแร่และปิโตรเลียม

คณะวิศวกรรมศาสตร์ จุฬาลงกรณ์มหาวิทยาลัย

ปีการศึกษา 2551

ลิขสิทธิ์ของจุฬาลงกรณ์มหาวิทยาลัย

EFFECT OF RESERVOIR HETEROGENEITY ON OIL PRODUCTION

Mr. Sarit Suwanmanee

ศูนย์วิทยทรัพยากร
จุฬาลงกรณ์มหาวิทยาลัย

A Thesis Submitted in Partial Fulfillment of the Requirements
for the Degree of Master of Engineering Program in Petroleum Engineering

Department of Mining and Petroleum Engineering

Faculty of Engineering

Chulalongkorn University

Academic Year 2008

Copyright of Chulalongkorn University

Thesis Title EFFECT OF RESERVOIR HETEROGENEITY
 ON OIL PRODUCTION

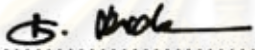
By Mr. Sarit Suwanmanee

Field of Study Petroleum Engineering

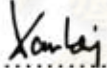
Advisor Assistant Professor Suwat Athichanagorn, Ph.D.


Co-Advisor Assistant Professor Sunthorn Pumjan, Ph.D.

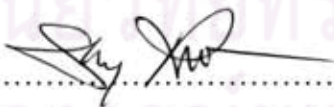
Accepted by the Faculty of Engineering, Chulalongkorn University in
 Partial Fulfillment of the Requirements for the Master's Degree



Dean of the Faculty of Engineering
 (Associate Professor Boonsom Lerthirunwong, Dr.Ing.)

THESIS COMMITTEE


Chairman
 (Associate Professor Sarithdej Pathanasethpong)


 Advisor
 (Assistant Professor Suwat Athichanagorn, Ph.D.)


 Co-Advisor
 (Assistant Professor Sunthorn Pumjan, Ph.D.)


 Examiner
 (Jirawat Chewarongroj, Ph.D.)

ศฤงค์ สุวรรณมณี: ผลกระทบของวิวิธพันธุ์ของแหล่งกักเก็บต่อการผลิตน้ำมัน. (EFFECT OF RESERVOIR HETEROGENEITY ON OIL PRODUCTION) อ.ที่ปรึกษาวิทยานิพนธ์
 หลัก: ผศ. ดร. สุวัฒน์ อธิษฐานกร, อ.ที่ปรึกษาวิทยานิพนธ์ร่วม: ผศ. ดร. สุนทร พุ่มจันทร์,
 96 หน้า.

ค่าความซึมผ่านของหินเป็นตัวแปรที่มีวิวิธพันธุ์สูงสุด และยังเป็นตัวแปรที่มีความสำคัญมากค่าหนึ่ง ซึ่งมีผลกระทบต่อความสามารถในการผลิตของแหล่งกักเก็บ ไม่ว่าจะเป็นในส่วนของการอัตราการผลิตและกระบวนการให้ได้น้ำมัน เพื่อจะศึกษาผลกระทบของวิวิธพันธุ์ต่อการผลิต จึงได้มีการสร้างแหล่งกักเก็บที่มีค่าวิวิธพันธุ์ที่แตกต่างกัน

ในการศึกษานี้ ได้นำขั้นตอนการจำลองด้วยวิธีการโดยลำดับเกาส์เขียนมาสร้างแบบจำลองแหล่งกักเก็บที่มีความแตกต่างกัน นอกจากนั้นยังได้ศึกษาถึงค่าความไม่แน่นอนของตัวแปรต่างๆ ที่ใช้ในการสร้างการจำลองแบบ โดยลำดับเกาส์เขียน เมื่อได้แบบจำลองมาแล้ว เราจะคำนวณค่าซึ่งแสดงถึงวิวิธพันธุ์คือ สัมประสิทธิ์โคสตราพาสันของแต่ละแหล่งกักเก็บ

การจำลองการไหลในแหล่งกักเก็บถูกนำมาศึกษาผลกระทบของวิวิธพันธุ์ต่อความสามารถในการผลิตหลังจากได้สร้างชั้นกักเก็บต่างๆ ที่มีการกระจายตัวของค่าความซึมผ่านของหินต่างกัน ซึ่งเราได้วิเคราะห์ผลกระทบของวิวิธพันธุ์ต่อความสามารถในการผลิต โดยการขับเคลื่อนด้วยก๊าซที่ละลายในน้ำมันในแหล่งกักเก็บ นอกจากนั้น ได้มีการประเมินความไม่แน่นอนของผลการจำลองที่เกิดจากค่าวิวิธพันธุ์ต่าง

อัตราส่วนของปริมาณน้ำมันที่เรานำขึ้นมาได้ต่อปริมาณทั้งหมดที่มีอยู่ในแหล่ง ได้ถูกนำมาเป็นตัวกำหนดในการเปรียบเทียบ กล่าวคือ อัตราส่วนของปริมาณน้ำมันที่เรานำขึ้นมาได้ต่อปริมาณทั้งหมดที่มีอยู่ในแหล่ง มีค่าลดลงเล็กน้อย เมื่อแหล่งกักเก็บมีวิวิธพันธุ์มากขึ้น นอกจากนั้นแล้วยังได้มีการนำระยะเวลาในการผลิตมาใช้ในการประเมิน พบว่าแหล่งกักเก็บที่มีค่าวิวิธพันธุ์สูงสุดจะใช้เวลาในการผลิตยาวนานที่สุด แต่ในทางตรงกันข้ามกลับให้อัตราส่วนของปริมาณน้ำมันที่เรานำขึ้นมาได้ต่อปริมาณทั้งหมดที่มีอยู่ในแหล่งน้อยที่สุด ค่าวิวิธพันธุ์ที่เพิ่มขึ้นจะทำให้ระยะเวลาในการผลิตเพื่อให้ได้น้ำมันมานั้นมีค่าสูงขึ้นด้วย

ภาควิชา วิศวกรรมเหมืองแร่และปิโตรเลียม
 สาขาวิชา วิศวกรรมปิโตรเลียม
 ปีการศึกษา 2551

ลายมือชื่อนิสิต.....*ศฤงค์ สุวรรณมณี*.....

ลายมือชื่อ.ที่ปรึกษาวิทยานิพนธ์หลัก.....*สุวัฒน์ อธิษฐานกร*.....

ลายมือชื่อ.ที่ปรึกษาวิทยานิพนธ์ร่วม.....*สุทร พุ่มจันทร์*.....

4871609821 : MAJOR PETROLEUM ENGINEERING

KEYWORDS : STOCHASTIC SIMULATION / GEOSTATISTICS / SEQUENTIAL GAUSSIAN SIMULATION / DYKSTRA-PARSONS COEFFICIENT

SARIT SUWANMANEE : EFFECT OF RESERVOIR HETEROGENEITY ON OIL PRODUCTION. ADVISOR: ASST. PROF. SUWAT ATHICHANAGORN, Ph.D., CO-ADVISOR : ASST. PROF. SUNTHORN PUMJAN, Ph.D., 96 pp.

Permeability which has the highest level of heterogeneity is one of the most important parameters which affect reservoir performance such as production profile and recovery processes. To study such effect, reservoirs with different degrees of reservoir heterogeneity were created and studied.

In this thesis, Sequential Gaussian Simulation (SGS) is used to generate maps of the reservoir. Moreover, sensitivity analysis of spatial continuity and SGS is performed to assess uncertainties by varying range, nugget and random seed. When the reservoir model is generated, Dykstra-Parsons coefficient (V_{DP}) is computed to measure the degree of heterogeneity.

Then, reservoir simulation is performed to study the effect of heterogeneity on reservoir performance for reservoirs with different permeability distributions that have been generated. The effect of heterogeneity on performance prediction for solution gas drive reservoir is quantified. The uncertainties associated with the results obtained from the heterogeneity are assessed.

The oil recovery factors (RF) at abandonment are compared. As V_{DP} increases, RF slightly decreases. When considered the time to abandonment, reservoir with the highest V_{DP} takes the longest time to produce oil. In general, the more heterogeneity, the longer time it takes to recover the fluid.

Department: Mining and Petroleum Engineering

Field of Study: Petroleum Engineering

Academic Year: 2008

Student's Signature.....*S. A. Suwanmanee*.....

Advisor's Signature.....*Suwat Athichanagorn*.....

Co-Advisor's Signature.....*Sunthorn Pumjan*.....

ACKNOWLEDGEMENTS

I would like to express my appreciation to my advisor, Dr. Suwat Athichanagorn, for providing me with knowledge of petroleum engineering and invaluable guidance during this study. I am also grateful to Dr. Sunthorn Pumjan my thesis co-advisor for creative suggestions and invaluable advice.

I wish to thank the thesis committee members for their comments and recommendations.

I would like to further mention my deep appreciation to my family and my friends who offered me their undivided attention, endless love, encouragement, and support.



ศูนย์วิทยทรัพยากร
จุฬาลงกรณ์มหาวิทยาลัย

CONTENTS

	Page
Abstract (in Thai)	iv
Abstract (in English)	v
Acknowledgements	vi
Contents	vii
List of Tables	ix
List of Figures	x
List of Abbreviations	xv
Nomenclature	xvi
 CHAPTER	
I Introduction	1
1.1 Introduction.....	1
1.2 Thesis Outline.....	2
 II Literature Review	 3
2.1 Literature Review.....	3
 III Theories and Concepts	 6
3.1 Structural Analysis.....	6
3.2 Kriging Concepts.....	10
3.2.1 Ordinary Kriging (OK) Algorithm.....	10
3.3 Conditional Simulation.....	13
3.3.1 Sequential Gaussian Simulation Procedure.....	15
3.4 Dykstra-Parsons Coefficient.....	16
 IV Reservoir Model Construction	 18
4.1 Base Model.....	18
4.2 Reservoir Model with Different Degrees of Heterogeneity.....	23
4.2.1 Sensitivity Analysis of Variogram.....	27
4.2.2 Sensitivity Analysis of Realizations.....	38

CHAPTER	Page
V Reservoir Performance Prediction.....	58
5.1 Performance of Reservoir having Different Levels of Heterogeneity.....	58
VI Conclusions and Recommendations.....	74
6.1 Conclusions.....	74
6.2 Recommendations.....	75
References.....	76
Appendices.....	78
Appendix A.....	79
Appendix B.....	87
Vitae.....	96



 ศูนย์วิทยทรัพยากร
 จุฬาลงกรณ์มหาวิทยาลัย

LIST OF TABLES

		Page
Table 4.1	Permeability and porosity of input data	20
Table 4.2	Statistical results of eight main models.....	26
Table 4.3	Comparison of eight-model normal score transform variogram data...37	
Table 4.4	SGS results of eight models by varying parameters.....	54
Table 5.1	Statistical results of oil recovery and reservoir pressure of different models.....	63
Table 5.2	Comparison of statistical results of oil recovery factor and V_{DP} of each model.....	65
Table B1	Comparison of oil recovery and reservoir pressure at different degrees of heterogeneity.....	95



 ศูนย์วิทยทรัพยากร
 จุฬาลงกรณ์มหาวิทยาลัย

LIST OF FIGURES

	Page
Figure 3.1 Variogram models with a sill	8
Figure 3.2 Power variogram models without a sill	9
Figure 3.3 Transform of original data to a normal score	14
Figure 3.4 SGS algorithm procedure	16
Figure 3.5 Dykstra-Parsons plot	17
Figure 4.1 Assumed distribution (a) and location map (b) of permeability of base model.....	19
Figure 4.2 Permeability histograms of original data.....	22
Figure 4.3 Location maps of each model	24
Figure 4.4 Probability plot of permeability of 109-wells in the base case.....	25
Figure 4.5 Normal score transform of omni-directional spherical variograms of main model varied nuggets and ranges using number of lags of 32, lag distance of 60 m.....	29
Figure 4.6 Normal score transform of omni-directional spherical variograms of the model I varied nuggets and ranges using number of lags of 35, lag distance of 70 m.....	30
Figure 4.7 Normal score transform of omni-directional spherical variograms of the model II varied nuggets and ranges using number of lags of 35, lag distance of 74 m.....	31
Figure 4.8 Normal score transform of omni-directional Gaussian variograms of the model III varied nuggets and ranges using number of lags of 38, lag distance of 48 m.....	32
Figure 4.9 Normal score transform of omni-directional spherical variograms of the model IV varied nuggets and ranges using number of lags of 37, lag distance of 80 m.....	33
Figure 4.10 Normal score transform of omni-directional spherical variograms of the model V varied nuggets and ranges using number of lags of 34, lag distance of 58 m.....	34

Figure 4.11	Normal score transform of omni-directional spherical variograms of the model VI varied nuggets and ranges using number of lags of 40, lag distance of 50 m.....	35
Figure 4.12	Normal score transform of omni-directional spherical variograms of the model VII varied nuggets and ranges using number of lags of 30, lag distance of 58 m.....	36
Figure 4.13	Relationship between number of lags and lag distance.....	38
Figure 4.14	Flow sheet to obtain realizations with different degrees of heterogeneity.....	39
Figure 4.15	SGS of the main model varied nuggets and ranges at the seed number of 106236.....	40
Figure 4.16	SGS of the main model varied nuggets and ranges at the seed number of 1299460.....	40
Figure 4.17	SGS of the main model varied nuggets and ranges at the seed number of 4211847.....	41
Figure 4.18	SGS of the main model varied nuggets and ranges at the seed number of 5209254.....	41
Figure 4.19	SGS of the model I varied nuggets and ranges at the seed number of 153567.....	42
Figure 4.20	SGS of the model I varied nuggets and ranges at the seed number of 896078.....	42
Figure 4.21	SGS of the model I varied nuggets and ranges at the seed number of 4773049.....	43
Figure 4.22	SGS of the model I varied nuggets and ranges at the seed number of 5237802.....	43
Figure 4.23	SGS of the model II varied nuggets and ranges at the seed number of 3782386.....	44
Figure 4.24	SGS of the model II varied nuggets and ranges at the seed number of 4574483.....	44
Figure 4.25	SGS of the model II varied nuggets and ranges at the seed number of 6768113.....	45

Figure 4.26	SGS of the model III varied nuggets and ranges at the seed number of 218583.....	45
Figure 4.27	SGS of the model III varied nuggets and ranges at the seed number of 2904965.....	46
Figure 4.28	SGS of the model III varied nuggets and ranges at the seed number of 7497676.....	46
Figure 4.29	SGS of the model IV varied nuggets and ranges at the seed number of 2895849.....	47
Figure 4.30	SGS of the model IV varied nuggets and ranges at the seed number of 6259246.....	47
Figure 4.31	SGS of the model IV varied nuggets and ranges at the seed number of 9451304.....	48
Figure 4.32	SGS of the model V varied nuggets and ranges at the seed number of 69069.....	48
Figure 4.33	SGS of the model V varied nuggets and ranges at the seed number of 5027296.....	49
Figure 4.34	SGS of the model V varied nuggets and ranges at the seed number of 7301294.....	49
Figure 4.35	SGS of the model VI varied nuggets and ranges at the seed number of 1042094.....	50
Figure 4.36	SGS of the model VI varied nuggets and ranges at the seed number of 6160440.....	50
Figure 4.37	SGS of the model VI varied nuggets and ranges at the seed number of 8275380.....	51
Figure 4.38	SGS of the model VII varied nuggets and ranges at the seed number of 307057.....	51
Figure 4.39	SGS of the model VII varied nuggets and ranges at the seed number of 5280856.....	52
Figure 4.40	SGS of the model VII varied nuggets and ranges at the seed number of 8326199.....	52

Figure 5.1	Reservoir model with 32 producers.....	59
Figure 5.2	Relationship between oil recovery factor and V_{DP} at 5,160 days.....	61
Figure 5.3	Relationship between oil recovery factor and V_{DP} at abandonment....	61
Figure 5.4	Relationship between time to abandonment and V_{DP}	62
Figure 5.5	Relationship between oil recovery and time to abandonment.....	62
Figure 5.6	Relationship between field oil production rate and time of 9 models with different values of V_{DP} using 32 producers.....	68
Figure 5.7	Relationship between reservoir pressure and time of 9 models with different values of V_{DP} using 32 producers.....	68
Figure 5.8	Relationship between cumulative oil production and time of 9 models with different values of V_{DP} using 32 producers.....	69
Figure 5.9	Comparison of hydrocarbon pore volume and time.....	69
Figure 5.10	Reservoir model with 15 producers.....	70
Figure 5.11	Relationship between field oil production rate and time of 9 models with different values of V_{DP} using 15 producers.....	70
Figure 5.12	Relationship between field oil production rate and time using 32 and 15 producers.....	71
Figure 5.13	Relationship between reservoir pressure and time of 9 models with different values of V_{DP} using 15 producers.....	71
Figure 5.14	Relationship between reservoir pressure and time using 32 and 15 producers.....	72
Figure 5.15	Relationship between cumulative oil production and time of 9 models with different values of V_{DP} using 15 producers.....	72
Figure 5.16	Relationship between cumulative oil production and time using 32 and 15 producers.....	73
Figure 5.17	Relationship between oil recovery and time using 32 and 15 producers.....	73
Figure A1	Omni-directional spherical variograms of main model varied nuggets and ranges using number of lags of 32, lag distance of 60 m.....	79

Figure A2	Omni-directional spherical variograms of the model I varied nuggets and ranges using number of lags of 35, lag distance of 70 m.....	80
Figure A3	Omni-directional spherical variograms of the model II varied nuggets and ranges using number of lags of 35, lag distance of 74 m.....	81
Figure A4	Omni-directional Gaussian variograms of the model III varied nuggets and ranges using number of lags of 38, lag distance of 48 m.....	82
Figure A5	Omni-directional spherical variograms of the model IV varied nuggets and ranges using number of lags of 37, lag distance of 80 m.....	83
Figure A6	Omni-directional spherical variograms of the model V varied nuggets and ranges using number of lags of 34, lag distance of 58 m.....	84
Figure A7	Omni-directional spherical variograms of the model VI varied nuggets and ranges using number of lags of 40, lag distance of 50 m.....	85
Figure A8	Omni-directional spherical variograms of the model VII varied nuggets and ranges using number of lags of 30, lag distance of 58 m.....	86

LIST OF ABBREVIATIONS

CV	coefficient of variation
CS	conditional simulation
HPV	hydrocarbon pore volume
MVUE	minimum variance unbiased estimation
NS	normal score transform
OK	Ordinary Kriging
PVT	pressure-volume-temperature
RF	recovery factor
SD	standard deviation
SGCOSIM	sequential Gaussian cosimulation
SGS	sequential Gaussian simulation
MVUE	minimum variance unbiased estimation



ศูนย์วิทยทรัพยากร
จุฬาลงกรณ์มหาวิทยาลัย

NOMENCLATURE

a	range
C_0	nugget effect
cdf	cumulative distribution function
E	expected value
$F^{-1}(p)$	inverse cumulative distribution function for the probability value
$F_Y(y)$	cumulative distribution function of a random variable Y
$F_Z(y)$	cumulative distribution function of a random variable Z
$G(\cdot)$	standard Gaussian distribution
$G(y)$	standard normal cumulative distribution function
$G^{-1}(p)$	standard normal p-quartile function
h	lag distance
k	permeability
m	mean
$m(u)$	local mean within a search neighborhood
N	number of sample size
$N(h)$	total number of sample pairs for the lag interval h
RF	random function
RV	random variable
u_i	sampled location
u_j	sampled location
u_0	unsampled location
V_{DP}	Dykstra-Parsons coefficient
$Y(u)$	generic variable function of location u
$Z(u)$	generic random variable at location u
$z(u)$	generic variable function of location u
$z^{(l)}(u)$	l -th realizations of the random function $Z(u)$ at location u
$Z(x_i + \vec{h})$	value of sample located at point $x_i + \vec{h}$
$Z(x_i)$	value of sample located at point x_i

GREEK LETTERS

Φ	porosity
∞	infinity
σ	standard deviation
σ^2	variance
σ_E^2	error variance
$\gamma(h)$	variogram at distance h
$\mu(u)$	Lagrange parameter
λ_i	weight assigned to each sample
λ_0	a constant



ศูนย์วิทยทรัพยากร
จุฬาลงกรณ์มหาวิทยาลัย

CHAPTER I

INTRODUCTION

1.1 Introduction

In reality, reservoir performance prediction always deals with a lot of uncertainties involving internal variables such as fluids and rock properties and the heterogeneity of the reservoir, and external variables such as oil price, operating cost, and capital expenditure. Specifically, the internal variable, namely, heterogeneity is one of the most important measures for geologists, geophysicists and reservoir engineers to quantify in order to generate an acceptable reservoir model for predicting the reservoir performance. The main point of this work is to assess uncertainties in the simulation results when the reservoir has a different degree of heterogeneity.

The variable that has highest level of heterogeneity is permeability. It is an important parameter that affects flow and displacement processes due to its variation. Therefore, in reservoir analysis, the measures of heterogeneity are almost exclusively focused and applied to permeability data because permeability variations are typically much larger than variations of other properties. Thus, changes in permeability can easily dominate the influence of variations in other properties. The most common method that has been used to measure such complexity is Dykstra-Parsons coefficient. Not only can it help engineers to quantify and measure the heterogeneity but also help them to understand the performance of the natural drive mechanism.

Before performing the reservoir simulation, it is necessary to quantify the distribution of permeability at the grid cells. Therefore, Geostatistical methods are frequently used to do the task because they offer the advantages of linking statistical methods with the position of variables in space and direction compared with other methods which do not.

After generating realizations with different permeability distributions, reservoir simulation is performed to study the effect of heterogeneity on reservoir performance. In this study, we are interested in the effect of heterogeneity on oil

recovery based on natural depletion. The uncertainties associated with the results obtained from this recovery schemes will be assessed.

1.2 Thesis Outline

The thesis report consists of six chapters and the outlines of each chapter are listed below.

Chapter II reviews literature that are involved with stochastic techniques by mentioning the advantages, drawback and application of each algorithm such as Kriging and Sequential Gaussian Simulation (SGS). In addition, it also mentions the application of Dykstra-Parsons coefficient (V_{DP}).

Chapter III presents theories and concepts related with this study.

Chapter IV shows how to prepare and obtain the extra seven models and compares statistical results of all models varied uncertainties in spatial continuity models and random number seed of SGS. In addition, it mentions how to determine V_{DP} value from permeability distributions. Finally, this chapter also examines the simulation studies from the SGS technique at different degrees of heterogeneity.

Chapter V examines and compares the simulation results in reservoir performance based on specific abandonment times at different degrees of V_{DP} .

Chapter VI provides conclusions of the study and recommendations for future work.

ศูนย์วิทยทรัพยากร
จุฬาลงกรณ์มหาวิทยาลัย

CHAPTER II

LITERATURE REVIEW

2.1 Literature Review

An accurate understanding of the description of a reservoir is required to improve production forecasts. Due to the lack of information between wells, a geostatistical model is used to generate equiprobable lithofacies simulations between wells. It has also been widely used in the petroleum industry because it can integrate geological, geophysical, and petrophysical data for building a more realistic reservoir model. Considering the complex behavior of the spatial distributions of petrophysical variables and the limited number of samples used in estimation, a smooth deterministic model, such as the one derived from Kriging, may not yield a realistic level of heterogeneity. To represent such heterogeneity, stochastic modeling based on conditional simulation has been increasingly used in recent years, Journel (1990) and Srivastava (1994). Using these techniques, a variable value at a location in space is determined by first obtaining the probability distribution at that location, and then drawing a number (i.e. simulated value) at random from this distribution. The simulated values do not only reproduce statistical and spatial patterns of the input data, but also honor this data at the sampling locations. Unlike Kriging, stochastic modeling provides a range of equi-probable realizations or models of reservoir, each comprising more realistic levels of heterogeneity. Such multiple models provide valuable information to assess the uncertainty, and hence are of considerable help in reservoir management, Journel (1994). Therefore, the conditional simulation is considered more appropriate for the simulation of the reservoir data.

Poquioma, P., and Mohan Kelkar (1994) presented the results for applying geostatistical techniques (Ordinary Kriging and conditional simulation) to generate distribution of permeability in order to improve the simulation of the fluid flow. The comparison indicates that conditional simulation techniques can be effectively used to represent the variability of the reservoir properties.

Paul J. Hicks studied the ability of three-dimensional fluid flow simulations using 3-D porosity distributions generated from unconditional sequential Gaussian simulation (SGS) to match the result of fluid flow simulations using the experimental 3-D porosity distribution. He mentioned that the SGS technique has an advantage over Krigging and other linear interpolation techniques because they maintain the spatial variability of the property being simulated. Any number of possibilities for the spatial distribution of permeability, or other unknown properties, can be generated as opposed to Krigging which generates one estimation.

Al-Khalifa (2006) studied and estimated hydrocarbon in-place using SGS with different uncertainties of the input data such as core data, facies based and well logs. There were two stochastic porosity models built using the same input data, but one model was based on a conceptual model and the other was not. The results showed that the use of conceptual models has given higher oil and gas estimates. He pointed out that the uniqueness of stochastic modeling methods has the ability to create many equi-probable realizations from the same geological data.

Kirk B. Hird investigated the effect of areal permeability heterogeneities on well performance and explained that stochastic simulation techniques can generate equally probable permeability realizations which result in widely varying simulated well performance under normal waterflood conditions.

Baker, R.O., and Moore, R.G (1997) mentioned the heterogeneity is a key factor in predicting waterflood or EOR recovery. It is not possible to make accurate performance predictions for EOR or waterflood schemes without adequate reservoir characterization.

Jerry Lucia, F., and Graham E. Fogg used conditional simulation to simulate permeability distribution and explained that realization having low permeability has low recovery and production efficiency.

Sahni, A., and Dehghani K (2005) focused a workflow for benchmarking reservoir model heterogeneity from production logs and core data by varying the level of heterogeneity using Dykstra Parsons coefficient (V_{DP}). V_{DP} determined from production logs was used to estimate flow near the well and to calibrate a simulation model while V_{DP} measured from core data was used to quantify permeability heterogeneity trends. He also investigated the workflow how a history matched

simulation model could be used to predict displacement performance at any given heterogeneity level.

Jakobsen, S.R (1994) applied Dykstra Parsons coefficient to reduce the error of relative permeability data obtained on heterogeneous cores. He demonstrated that the results of displacement efficiency, wettability and reservoir performance can be improved if relative permeability is correct. The Johnson-Bossler-Nauman (JBN) technique is a conventional method that is only applicable to homogeneous core material. As a result, flow behavior investigated by JBN method to derive relative permeability curves is incorrect. The true curve must be taken into account for the impact of heterogeneities depending on V_{DP} . For example, the deviation of relative permeability decreases with decreasing V_{DP} .

Karn B., Jakarrin A. and Atjana L. (2005) determined sets of permeability data with V_{DP} values of 0.1, 0.2 and 0.9. by using $V_{DP} = 1 - e^{-\sigma}$. When V_{DP} was first selected, standard deviation (SD) of its model could be calculated and then permeability of 100 wells was randomly generated by the Monte Carlo simulation where permeability distribution trends of each data set was assumed in increasing the value from Northwest to Southeast in which the well locations were also randomly selected. They used SGS to generate multiple maps for reducing uncertainty in performance prediction. The results showed that the higher heterogeneity, the lower oil recovery it will be. Moreover, they mentioned that If V_{DP} value is greater than 0.5, it should not be used to simulate as a homogeneous reservoir because it has a wider range of standard deviation which has more effect on oil recovery factor.

ศูนย์วิทยทรัพยากร
จุฬาลงกรณ์มหาวิทยาลัย

CHAPTER III

THEORIES AND CONCEPTS

Geostatistical techniques have been used extensively in the mining industry since the early 1950's. It was initially developed to evaluate the ore reserves in the mining industry.

In the petroleum industry, this technique was introduced in the 1970's and has been widely applied and developed to predict the reservoir properties because it can generate multiple realizations that can account for the uncertainty and spatial variability of the key reservoir parameters such as porosity or permeability. Spatial continuity or variation is modeled in geostatistics by the variogram. The relative degree of continuity or spatial correlation between different directions is one of the most important aspects of the spatial continuity model. In this approach, the unsampled values are implicitly assumed to be correlated with each other. To study such a correlation, structural analysis is first used to quantify; the predictions at unsampled locations are then made using kriging technique or it can be simulated using conditional simulations.

3.1 Structural Analysis

Structural analysis, variogram or correlogram is used to measure and study spatial variability or continuity of a particular variable and also to quantify spatial correlation of data as a function of distance and direction. It can be applied to determine cross-continuity of different variables at different locations. The variogram is calculated from the data as the variance of difference between data separated a certain distance apart. When the data is bigger in difference, the variance is larger. The most important factor in estimating the variogram is to use the information to estimate variable values at unsampled locations. The first step in performing the spatial analysis is to estimate the value of the variograms using the well data. These variograms are usually mentioned as the conditioning or experimental variograms.

Estimating the conditioning variograms in practice requires great care and caution due to some problems such as lack of data pairs at certain lag distance, e.g., due to well spacing, selective well location, and biased sampling. The variogram solution is presented below

$$\gamma(\bar{h}) = \frac{1}{2N(\bar{h})} \sum_{i=1}^N [Z(x_i) - Z(x_i + \bar{h})]^2 \quad (3.1)$$

where $\gamma(\bar{h})$ = variogram value at distance h
h = lag distance
 $Z(x_i)$ = value of sample located at point x_i
 $Z(x_i + \bar{h})$ = value of sample located at point $x_i + \bar{h}$
 $N(\bar{h})$ = total number of sample pairs for the lag interval \bar{h}

The variogram is an important input into stochastic modeling. Proper variogram modeling is a key factor to get a realistic reservoir characterization model. It is a mathematical tool that quantifies spatial correlation and continuity of a variable. Equation 3.1 defines that any function of two random variables located \bar{h} distance apart is independent of the location and is a function of only the distance and the direction between the two locations. In addition, it is a plot of the average squared difference in value between data points against their separation distance. It is computed as half the average squared difference between the components of every data pair. The geostatistical model states that nearby sample points have more influence on the result of simulation than those far apart; in fact, if the separation between two sample points is beyond the range of influence, they have no spatial correlation. The variogram model that is normally used to study the spatial variability can be classified into 2 categories which are models with a sill and without as presented in Equations 3.2 to 3.5. Models with a sill, or transition models, are used when the variogram reaches a constant value after a certain lag distance including the spherical, exponential, Gaussian, and hole effect model. Usually, the sill is close to the variance. And those without a sill include the power, nugget effect and linear

models. Some of the variogram models that have commonly seen are sketched in Figures 3.1 and 3.2.

(i) Spherical Model

$$\gamma(\bar{h}) = \begin{cases} C_0 + C_1 \left[1.5 \left(\frac{\bar{h}}{a} \right) - 0.5 \left(\frac{\bar{h}}{a} \right)^3 \right] & \text{where } \bar{h} \leq a \\ C_0 + C_1 & \text{where } \bar{h} > a \end{cases} \quad (3.2)$$

where a = range

C_0 = nugget effect

$C_0 + C_1$ = sill

(ii) Exponential Model

$$\gamma(\bar{h}) = \begin{cases} C_0 + C_1 \left[1 - \exp\left(-\frac{\bar{h}}{a}\right) \right] & \text{where } \bar{h} \leq a \\ C_0 + C_1 & \text{where } \bar{h} > a \end{cases} \quad (3.3)$$

(iii) Gaussian Model

$$\gamma(\bar{h}) = \begin{cases} C_0 + C_1 \left[1 - \exp\left(-\frac{\bar{h}^2}{a^2}\right) \right] & \text{where } \bar{h} \leq a \\ C_0 + C_1 & \text{where } \bar{h} > a \end{cases} \quad (3.4)$$

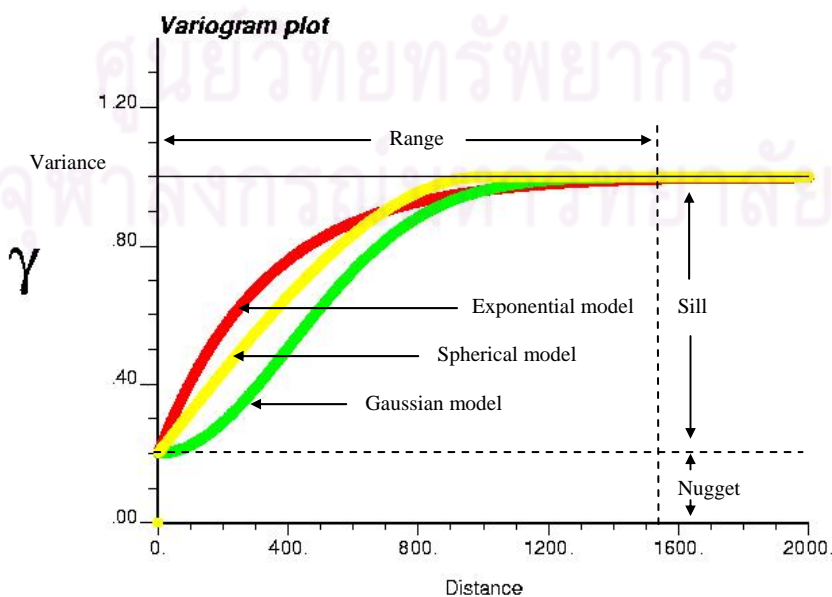


Figure 3.1 : Variogram models with a sill

(iv) Power Model

$$\gamma(\bar{h}) = C_0 + W \cdot \bar{h}^a \quad \text{where } W = \text{slope at origin} \quad (3.5)$$

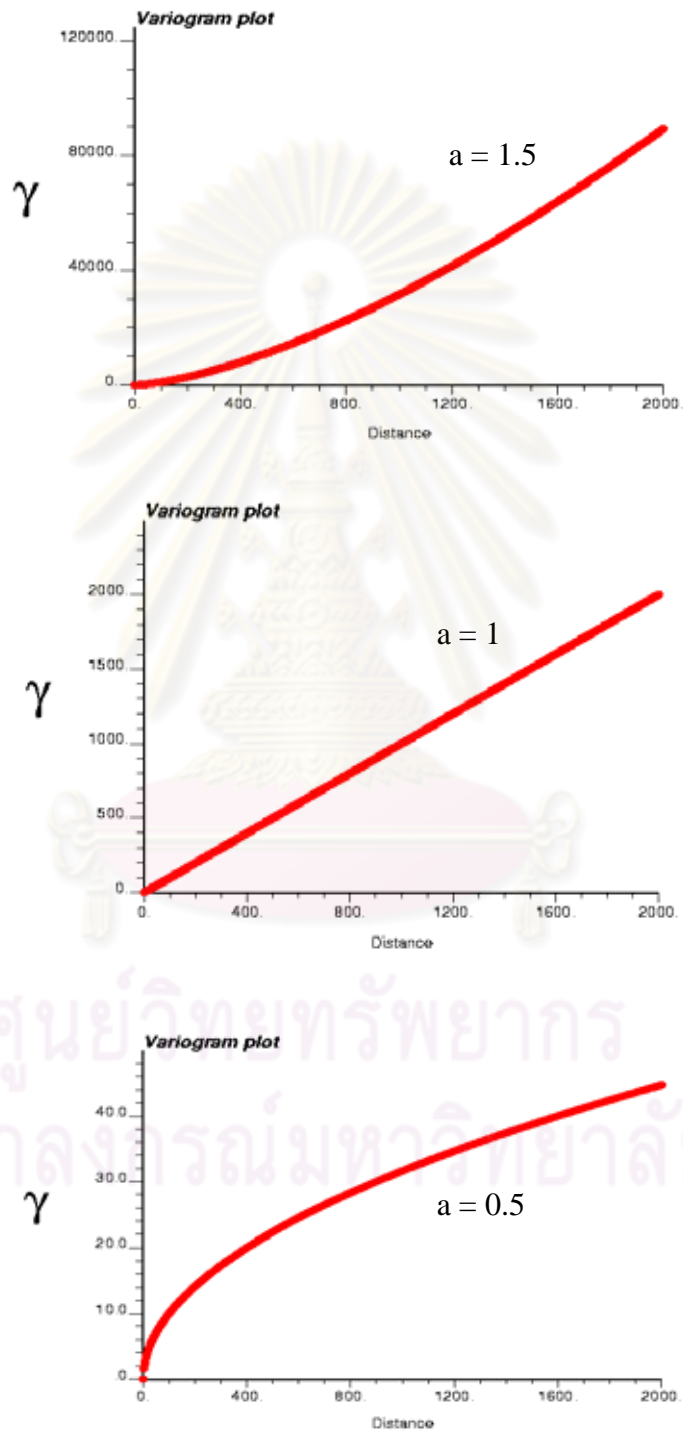


Figure 3.2 : Power variogram models without a sill

3.2 Kriging Concepts

The concept of Kriging assumes that the estimated value of the variable is linearly related to the nearby samples by using the minimum variance unbiased estimation technique to estimate the weights. That is to say, the estimated value is unbiased and will result in minimum error variance. One of the disadvantages of Kriging technique is that it can produce only one reservoir model. Selecting only one reservoir model could lead to errors in the prediction of the production and not allow an assessment of uncertainty in prediction. Normally, we would expect larger uncertainty in areas that are farther away from the control data.

Typically, there are several Kriging procedures to estimate the sampled variable, for example, “*Simple Kriging*” is the simplest one but it is not practical because it requires a knowledge of population mean. In practice, the true global may not be known without a prior assumption, “*Ordinary Kriging or Conventional Kriging*” is more flexible than simple Kriging and allows for variations in local change. It is most widely used in the Kriging technique because it does not require the knowledge of mean at unsampled locations, “*Co-Kriging*” allows the estimation of one variable based on the spatial information of other related variables. This procedure is useful when there is one extensively sampled variable and one sparsely sampled variable, and they are spatially related. And, “*Universal Kriging*” is used when the sample data exhibits a trend in a particular direction.

As stated above, Ordinary Kriging is the algorithm that is most widely used to define unsampled values. The derivation of the OK system and its solution will be explained, and it will be used in the conventional simulation subroutine.

3.2.1 Ordinary Kriging (OK) Algorithm

The objective is to find the estimate Z_0^* at an unknown location from a weighted sum of Z_i 's at known locations. We will first come up with the solution as shown below.

$$Z^*(u_0) = \sum_{i=1}^n \lambda_i Z(u_i) + \lambda_0 \quad (3.6)$$

At unbiased condition requires that

$$E[Z(u_0) - Z^*(u_0)] = 0 \quad (3.7)$$

By substituting Eq. 3.6 into Eq. 3.7, we obtain

$$E[Z(u_0)] = \lambda_0 + \sum_{i=1}^n \lambda_i E[Z(u_i)] \quad (3.8)$$

The assumption of OK is that $E[Z(u_0)] = E[Z(u_i)] = m(u_0)$, where $m(u_0)$ is the local mean within the search neighborhood, we can express Eq. 3.8 as

$$\lambda_0 = m(u_0) \left(1 - \sum_{i=1}^n \lambda_i \right) \quad (3.9)$$

In practice, we do not know the value of $m(u_0)$, we can force λ_0 to be zero. Then,

$$\sum_{i=1}^n \lambda_i = 1 \quad (3.10)$$

As a result, the value at the unknown location is estimated by

$$Z^*(u_0) = \sum_{i=1}^n \lambda_i Z(u_i) \quad (3.11)$$

In order to estimate the weights of the neighboring values that have influence with the unknown data, the minimum variance unbiased estimation (MVUE) is used for the Kriging algorithm.

$$\sigma_E^2 = \text{Var}[Z(u_0) - Z^*(u_0)] = \text{Var}\left[Z(u_0) - \sum_{i=1}^n \lambda_i Z(u_i)\right] \quad (3.12)$$

Expanding,

$$\sigma_E^2 = \gamma(u_0, u_0) + \sum_{i=1}^n \sum_{j=1}^n \lambda_i \lambda_j \gamma(u_i, u_j) - 2 \sum_{i=1}^n \lambda_i \gamma(u_i, u_0) \quad (3.13)$$

We must minimize the error variance with a constraint defined in Eq. 3.10. To do so, the Lagrange multiplier method is used. As a result, we define the function, F , as

$$\begin{aligned} F &= \sigma_E^2 + \left(\sum_{i=1}^n \lambda_i - 1 \right) \\ &= \gamma(u_0, u_0) + \sum_{i=1}^n \sum_{j=1}^n \lambda_i \lambda_j \gamma(u_i, u_j) - 2 \sum_{i=1}^n \lambda_i \gamma(u_i, u_0) + 2u \left(\sum_{i=1}^n \lambda_i - 1 \right) \end{aligned} \quad (3.14)$$

where u is a Lagrange parameter

Taking the derivatives to minimize the error variance, we will obtain

$$\frac{\partial F}{\partial \lambda_i} = 0 = 2 \sum_{j=1}^n \lambda_j \gamma(u_i, u_j) + 2u - 2\gamma(u_i, u_0) \quad \text{for } i = 1, \dots, n. \quad (3.15)$$

and

$$\frac{\partial F}{\partial u} = 0 = \sum_{i=1}^n \lambda_i - 1 \quad (3.16)$$

Rearranging Eq. 3.15, we can obtain it as

$$\sum_{j=1}^n \lambda_j \gamma(u_i, u_j) + u = \gamma(u_i, u_0) \quad \text{for } i = 1, \dots, n. \quad (3.17)$$

Eq. 3.17 can be expressed as a matrix form which results in the $(n+1) \times (n+1)$ matrix as shown below

$$\begin{bmatrix} \gamma(u_1, u_1) & \cdots & \gamma(u_1, u_n) & 1 \\ \vdots & & \vdots & \vdots \\ \gamma(u_n, u_1) & \cdots & \gamma(u_n, u_n) & 1 \\ 1 & \cdots & 1 & 0 \end{bmatrix} \begin{bmatrix} \lambda_1 \\ \vdots \\ \lambda_n \\ u \end{bmatrix} = \begin{bmatrix} \gamma(u_1, u_0) \\ \vdots \\ \gamma(u_n, u_0) \\ 1 \end{bmatrix} \quad (3.18)$$

By solving the matrix equation, we can get the values of λ_i and u .

Once λ_i is calculated, the estimated value of variable at u_0 , $Z^*(u_0)$, is reckoned with Eq. 3.11. The error variance is also estimated by using the equation below.

$$\sigma_E^2 = \gamma(u_0, u_0) - \sum_{i=1}^n \lambda_i \gamma(u_0, u_i) - u \quad (3.19)$$

ศูนย์วิทยทรัพยากร
จุฬาลงกรณ์มหาวิทยาลัย

3.3 Conditional Simulation

As discussed above, Kriging estimations are deterministic and cannot be used to quantify uncertainty because it creates a smooth picture. Although, Kriging which has a minimum error variance yields a unique realization, it does not reproduce spatial fluctuations. That is, it will normally preserve the large-scale features of variabilities and will eliminate the small features of variabilities. In addition, it produces conditional bias in the sense that through smoothing, small values are overestimated and large values are underestimated. Smoothed maps should not be used where spatial patterns of values are important. As a result, it is difficult and might not be adequate enough to properly capture local uncertainties and represent the real reservoir heterogeneity. Therefore, we need to choose the technique of conditional simulation (CS) which can provide a range of equi-probable realizations to generate stochastic random fields.

Sequential Gaussian Simulation (SGS) is the most popular algorithm to generate multiple realizations with the help of a random number generator. In addition, the unique point of SGS technique is that it samples a value and back transforms the value into the original domain after visiting every new unsampled location. This leads to adequately capturing the spatial relationship without losing the information in the class distribution. Therefore, in this thesis, SGS is used to generate the realization of permeability data. In addition, the variogram structure (nugget and range) are varied in order to observe their influence on the generated permeability field.

As mentioned before, in order to proceed with the SGS technique, multivariate Gaussian or normal score transform is required as it will transform the raw data into a new domain so that the data of each category in the Gaussian space can be easily defined. The condition of the Gaussian transform is said that random function RF $Y(u)$ of any original data needs to be normal as written in Eq. 3.20

$$\text{Pr ob}\{Y(u) \leq y\} = G(y) \forall y \quad (3.20)$$

where $G(\cdot)$ is the standard Gaussian distribution and $Y(u)$ is assumed to be standardized with a zero mean and unit variance.

Let Z and Y be the two data sets and their cumulative distribution function (cdf) are $F_Z(z)$ and $F_Y(y)$. The transform $Y = \psi(Z)$ identifies the cumulative probabilities which correspond to the Z and Y p-quantiles:

$$F_Y(y_p) = F_Z(z_p) = p, \forall p \in [0,1] \quad (3.21)$$

We can express p-quantile of $F_Y(y)$, y_p as,

$$y_p = F_Y^{-1}(F_Z(z_p)) = F_Y^{-1}(p), \forall p \in [0,1] \quad (3.22)$$

where $F_Y^{-1}(\cdot)$ is a quartile function of the random variable, RV Y .

If Y is standard normal with cdf $F_Y(y) = G(y)$, the transform $G^{-1}(F_Z(\cdot))$ is the normal score transform. Figure 3.3 shows an example of transforming original data to a normal score.

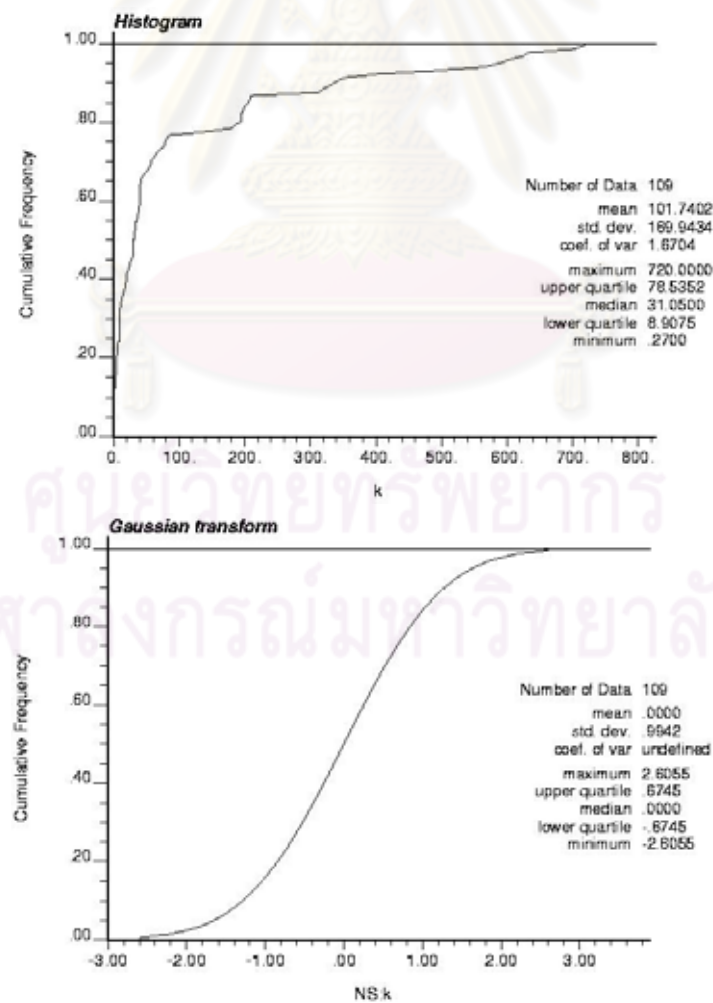


Figure 3.3 : Transform of original data to a normal score

3.3.1 Sequential Gaussian Simulation Procedure

Sequential Gaussian Simulation (SGS) is a procedure that uses the Kriging mean variance to generate and solve a Gaussian field where unsampled locations are sequentially visited in random order until all unsampled data are simulated or visited. The SGS procedure will be explained in details below:

1. Transform the data set into a Gaussian distribution or standard normal data
2. Construct variogram analysis to fit with a proper model.
3. Select grid node at random.
4. Perform Ordinary Kriging at the grid cell to estimate mean and variance of normal distribution.
5. Draw a simulated data from $N(\mu, \sigma^2)$ and add the simulated data to the data set.
6. Select another grid node at random and repeat the procedure for Ordinary Kriging until all grid nodes are visited or simulated.
7. Back transform the simulated data to the original space, and the realization map is created.
8. Provide different random number sequences for random visited nodes and repeat the same procedure for additional realization maps.

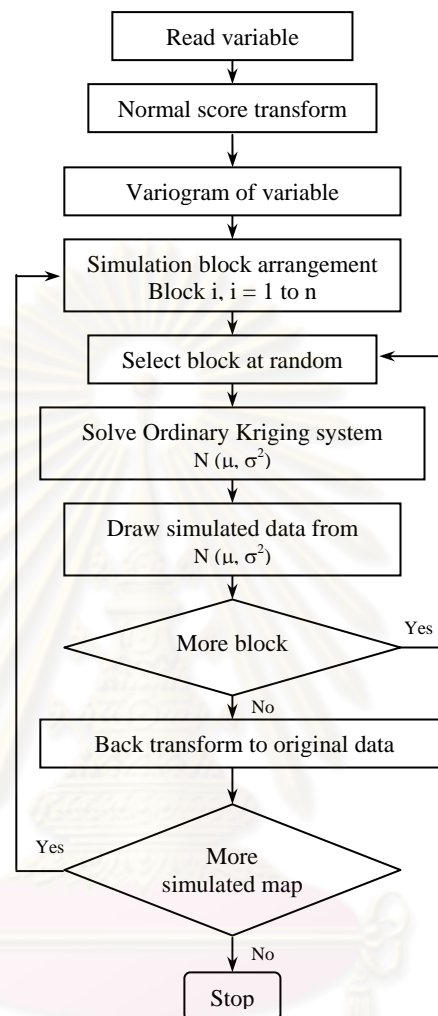


Figure 3.4 : SGS algorithm procedure

3.4 Dykstra-Parsons Coefficient

In order to investigate a degree of heterogeneity in a reservoir, Dykstra-Parson coefficient is used. In the petroleum industry, Dykstra-Parsons coefficient, sometimes called coefficient of permeability variation, or variance, V_{DP} , is the most common method used to measure the variation of permeability. Permeability typically has a log normal distribution. The Dykstra-Parsons coefficient is defined as follows:

$$V_{DP} = \frac{k_{0.50} - k_{0.16}}{k_{0.50}} \quad (3.23)$$

where $k_{0.50}$ is the median permeability and $k_{0.16}$ is the permeability one standard deviation below $k_{0.50}$ on a log-probability plot. The variation of V_{DP} ranges from 0 (uniform) to 1 (infinitely heterogeneous). The lower values (0 to 0.5) represent cases of low heterogeneity, while the higher values (0.7 to 1.0) reflect reservoirs with large to extremely large levels of heterogeneity according to Larry W. Lake and Jerry L. Jensen. Most reservoirs have the V_{DP} values of 0.5 to 0.9 according to Wilhite, G. Paul (1986).

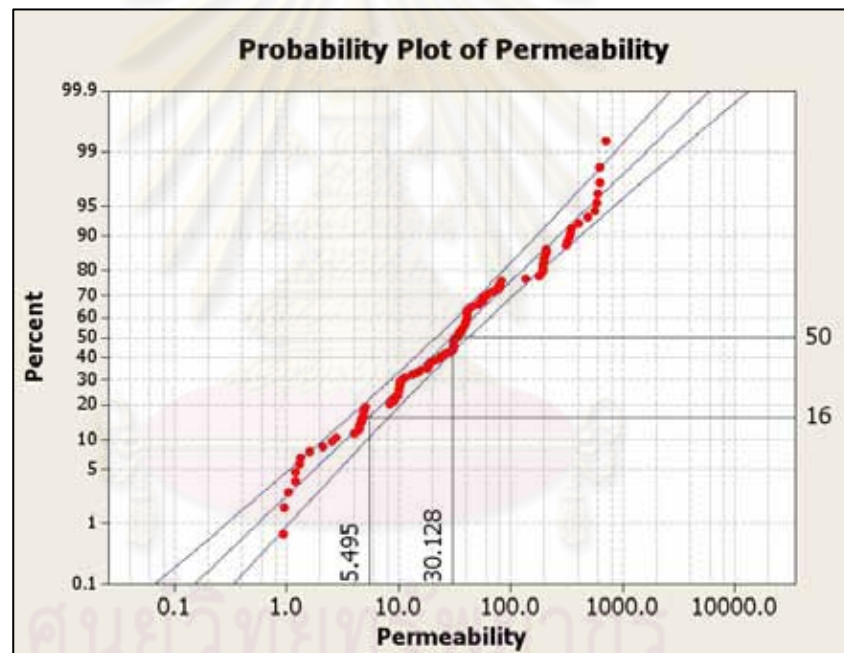


Figure 3.5 : Dykstra-Parsons plot

The Dykstra-Parsons coefficient is determined from a set of permeability data ordered in increasing value as shown in Figure 3.5. Dykstra and Parsons (1950) state that the values to be used in the definition are taken from a “best-fit” line through the data when they are plotted on a log-probability plot. If the points do not fall approximately on a straight line, more weight is to be given to the central points than the points at the extremities.

CHAPTER IV

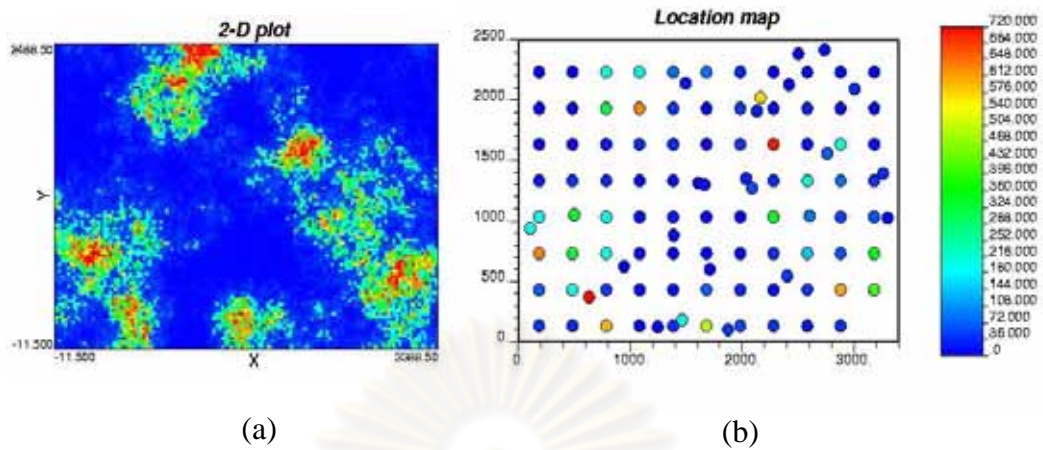
Reservoir Model Construction

This chapter is divided into two sections which are a base model and a reservoir model with a different degree of heterogeneity. The base model section explains how to prepare and formulate the base case and the next section shows how to generate maps from the original data and assess uncertainties using Sequential Gaussian Simulation Technique (SGS) as well as measuring the heterogeneity using Dykstra-Parsons coefficient.

4.1 Base Model

This study investigated the effect of areal permeability heterogeneities on well performance where thickness was assumed to be constant and porosity was assumed to be correlated with permeability. The permeability distribution of base case was assumed with a known spatial correlation of lognormal frequency distribution as shown in Figures 4.1 (a) and 4.2 (a). 109 wells were also assumed to be drilled in the base model where the well locations were illustrated in Figure 4.1 (b). The assigned locations of 109 wells will help us obtain different maps with degrees of heterogeneity as explained in detail in the next section.

As shown in Figures 4.1 (a) and (b), the permeability data cover an area of 2500 x 3400 square-meter. The distributions of reservoir rock properties were generated for a rectangular reservoir with dimensions of 136 x 100 x 1 blocks with a block size equal to 25 x 25 x 7 m. in the x, y and z directions, respectively.



(a) (b)
Figure 4.1 : Assumed distribution (a) and location map
(b) of permeability of base model

Table 4.1 shows the x and y coordinates of the original data, permeability and porosity, from the 109 wells which have the minimum and maximum values of 0.27 md., 720 md. and 0.15 and 0.27 respectively. In addition, the names of each well are assigned as well 1 to well 109, respectively where the well names were ordered in increasing values of permeability. The correlation that we used to determine porosity value from the permeability value is shown in Equation 4.1.

$$\phi = \frac{1}{43.586} \times \left[\ln \left(\frac{k}{0.0057} \right) \right] \quad (4.1)$$

ศูนย์วิทยทรัพยากร
จุฬาลงกรณ์มหาวิทยาลัย

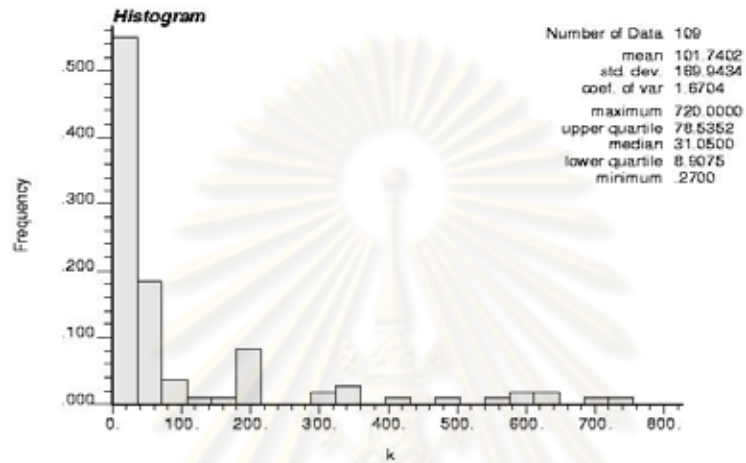
Table 4.1 : Permeability and porosity of input data

Well name	x- coordinate (m.)	y- coordinate (m.)	Permeability, md.	Normal score transform of permeability	Porosity, (%)
1	2500	2380	0.27	-2.605	0.15
2	1680	1930	0.39	-2.204	0.10
3	1244	120	0.47	-1.997	0.16
4	1680	730	0.53	-1.851	0.10
5	2416	2124	0.80	-1.736	0.17
6	1980	730	0.87	-1.640	0.12
7	1380	730	0.94	-1.558	0.12
8	180	1630	0.96	-1.485	0.12
9	3180	2230	1.04	-1.419	0.12
10	180	1930	1.20	-1.358	0.12
11	1680	1030	1.21	-1.303	0.12
12	1707	599	1.30	-1.251	0.18
13	1980	1030	1.34	-1.202	0.13
14	942	623	1.61	-1.156	0.15
15	2280	2230	2.10	-1.112	0.14
16	480	2230	2.56	-1.070	0.14
17	180	2230	2.75	-1.031	0.14
18	1080	130	4.05	-0.992	0.15
19	1606	1312	4.47	-0.955	0.20
20	3180	1930	4.47	-0.920	0.15
21	2738	2411	4.68	-0.885	0.19
22	480	1630	4.70	-0.851	0.15
23	1080	430	4.84	-0.819	0.15
24	2580	2230	4.90	-0.787	0.15
25	3301	1024	4.93	-0.756	0.19
26	1080	1330	5.10	-0.726	0.16
27	1384	881	8.42	-0.696	0.20
28	1380	1330	9.07	-0.667	0.17
29	2880	1930	9.08	-0.639	0.17
30	2880	2230	9.79	-0.611	0.17
31	1080	1030	9.87	-0.583	0.17
32	2280	1930	10.01	-0.556	0.17
33	2280	430	10.13	-0.530	0.17
34	480	1930	10.21	-0.503	0.17
35	1380	430	10.28	-0.477	0.17
36	1080	730	10.33	-0.452	0.17
37	1664	1301	10.78	-0.427	0.24
38	1680	1630	11.40	-0.401	0.17
39	3180	1630	13.12	-0.377	0.18
40	1495	2138	14.65	-0.352	0.14
41	180	1330	15.78	-0.328	0.18
42	2580	1630	18.13	-0.304	0.19
43	2580	130	18.52	-0.280	0.19
44	1380	1030	18.91	-0.256	0.19
45	780	1630	19.07	-0.232	0.19
46	2131	1909	21.25	-0.208	0.19
47	2031	1345	23.44	-0.185	0.22
48	2580	1930	23.78	-0.162	0.19
49	1980	2230	25.81	-0.138	0.19
50	1980	430	28.48	-0.115	0.20
51	1080	1630	30.43	-0.092	0.20
52	3262	1394	30.93	-0.069	0.20
53	1380	1630	31.00	-0.046	0.20
54	480	130	31.03	-0.023	0.20

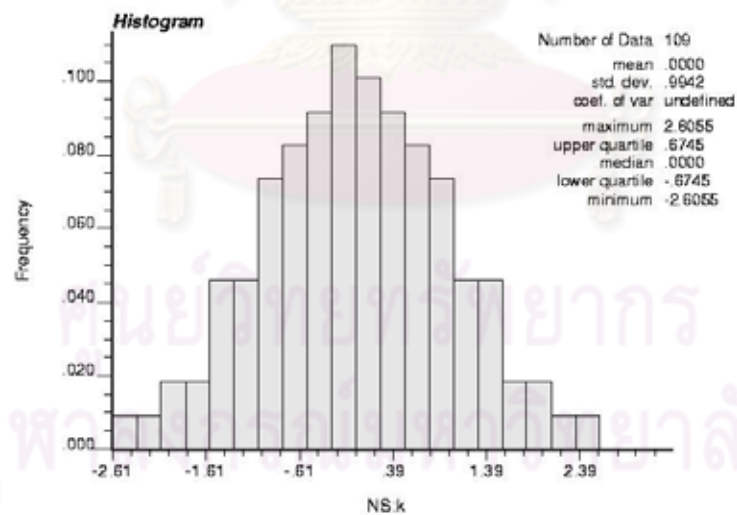
Table 4.1 : Permeability and porosity of input data (continued)

Well name	x-coordinate (m.)	y-coordinate (m.)	Permeability, md.	Normal score transform of permeability	Porosity, (%)
55	780	1330	31.05	0.000	0.20
56	2280	730	31.30	0.023	0.20
57	3008	2092	31.71	0.046	0.23
58	2880	130	33.50	0.069	0.20
59	1380	130	33.94	0.092	0.20
60	2280	1330	34.27	0.115	0.20
61	180	130	36.73	0.138	0.20
62	2280	130	36.97	0.162	0.20
63	480	1330	38.31	0.185	0.20
64	3180	1330	38.72	0.208	0.20
65	1870	100	39.67	0.232	0.24
66	1980	1930	40.05	0.256	0.20
67	2580	430	40.44	0.280	0.20
68	1380	1930	40.86	0.304	0.20
69	780	430	40.92	0.328	0.20
70	1980	1930	41.05	0.352	0.20
71	2400	547	41.08	0.377	0.23
72	1980	1630	42.70	0.401	0.20
73	2880	1030	45.67	0.427	0.21
74	1980	130	51.79	0.452	0.21
75	2086	1272	53.35	0.477	0.21
76	3180	1030	57.15	0.503	0.21
77	2880	730	57.43	0.530	0.21
78	180	430	62.24	0.556	0.21
79	2757	1554	64.77	0.583	0.21
80	1680	430	69.85	0.611	0.22
81	2880	1330	77.44	0.639	0.22
82	1380	2230	77.71	0.667	0.22
83	1680	2230	81.01	0.696	0.22
84	2601	1041	83.29	0.726	0.21
85	2580	730	135.74	0.756	0.23
86	180	1030	180.02	0.787	0.24
87	480	430	186.16	0.819	0.24
88	100	940	194.10	0.851	0.27
89	780	730	194.52	0.885	0.24
90	780	1030	196.19	0.920	0.24
91	1080	2230	197.75	0.955	0.24
92	2580	1330	200.27	0.992	0.24
93	2880	1630	204.35	1.031	0.24
94	780	2230	208.13	1.070	0.24
95	1462	178	208.78	1.112	0.23
96	780	1930	313.07	1.156	0.25
97	480	730	320.20	1.202	0.25
98	2280	1030	332.05	1.251	0.25
99	496	1053	339.40	1.303	0.24
100	3180	730	351.31	1.358	0.25
101	3180	430	403.28	1.419	0.26
102	1680	130	486.93	1.485	0.26
103	2161	2017	565.05	1.558	0.27
104	780	130	590.61	1.640	0.26
105	2880	430	602.47	1.736	0.27
106	1080	1930	625.15	1.851	0.27
107	180	730	630.27	1.997	0.27
108	2280	1630	702.73	2.204	0.27
109	632	369	720.00	2.605	0.27

In reality, permeability distribution typically exhibits as a log-normal. In order to quantify the statistical data, permeabilities of the original data were plotted into the histogram as it shows a log-normal distribution in which the mean is 101.7402 md. and standard deviation is 169.9434 md. Figure 4.2 illustrates permeability histogram of the original data.



(a) Histogram



(b) Normal score transform histogram

Figure 4.2 : Permeability histograms of original data

4.2 Reservoir Model with Different Degrees of Heterogeneity

As mentioned before, to study the effect of heterogeneity, it becomes difficult to get the wide range of permeability which can represent all degrees of heterogeneity in one field. As a result, seven extra models are generated to support the study.

Reducing the numbers of wells is performed manually so that the mean can be controlled as close as possible to the base case. In this study, seven other models are created where the wells of each model are taken out gradually from their maximum and minimum values until their means are close to 101.74. For example, when well 1 to well 12, lower tail, and well 108 and well 109, upper tail, were taken out from the base model, model I would be created and have the mean of 101.65. In this case, care should be taken. That is to say that if we took out the maximum value of only well 109 instead of both well 108 and well 109, the mean of the Model I would be 107.91 where then the new mean value is beyond the mean of the base case. As a result, the comparison may be difficult when explaining the performance of different cases. Therefore, the same method is applied to all the remaining models which can represent different degrees of heterogeneity. That is, after wells of each model had been taken out from both lower tail and upper tail to get their means close to the base case mean, Model I, II, III, IV, V, VI and VII then only used wells 13 to 107, 24 to 105, 34 to 103, 44 to 101, 51 to 99, 58 to 97 and 64 to 95, respectively as seen in Table 4.2. After all other seven models were created, the location maps of each model is illustrated in Figure 4.3.

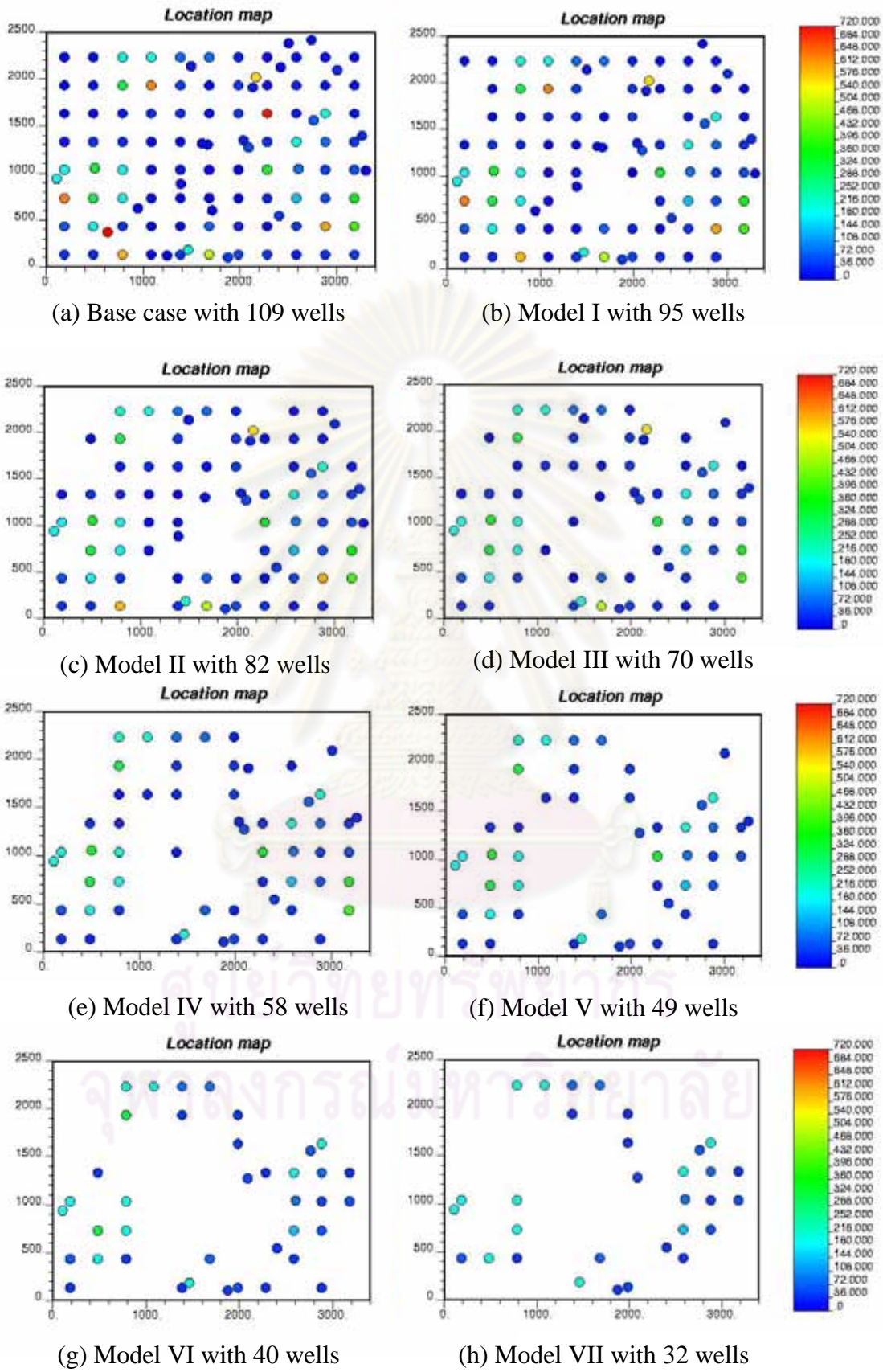


Figure 4.3 : Location maps of each model

After the new seven models were created, we would measure the degree of heterogeneity. Theoretically, there are many methods to measure the degree of heterogeneity. In this case, Dykstra-Parsons coefficient (V_{DP}) is used. In this study, permeability distribution of each model was plotted into a log-normal probability scale. To quantify the permeability values at the probability of 16% and 50%, MINITAB program, a statistical software, is used. The uniqueness of this program is to choose the exact value at a given probability without any bias. Figure 4.4 shows the example of 109-well permeability data obtained from the base case and how to obtain the V_{DP} value from the probability plot.

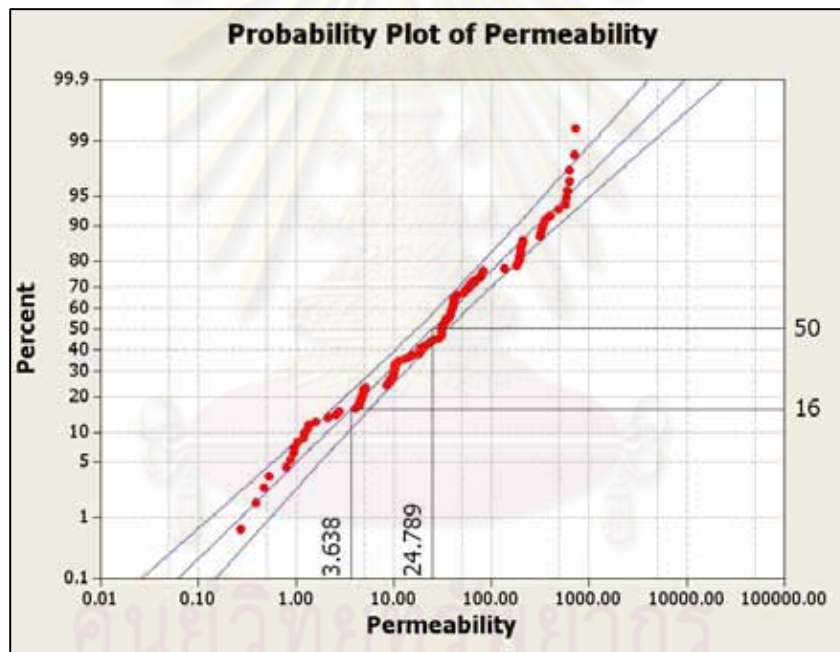


Figure 4.4 : Probability plot of permeability of 109-wells in the base case

Table 4.2 : Statistical results of eight main models

Model name	Base case	Model I	Model II	Model III	Model IV	Model V	Model VI	Model VII
Used well name	1 to 109	13 to 107	24 to 105	34 to 103	44 to 101	51 to 99	58 to 97	64 to 95
Number of well	109	95	82	70	58	49	40	32
Mean (md.)	101.7402	101.6523	101.9997	101.280	101.8003	101.8182	102.5048	101.6620
Std. dev.	169.9434	155.0001	140.6738	122.2001	102.0488	91.1697	81.0508	67.1185
Coef. of var	1.6704	1.5248	1.3792	1.2066	1.0024	0.8954	0.7907	0.6602
Skewness	2.26	2.16	2.10	1.90	1.45	1.31	1.15	0.66
Kurtosis	4.35	3.98	3.94	3.28	1.00	0.60	0.27	-1.45
Maximum	720	630.27	602.47	565.05	403.28	339.4	320.2	208.78
Upper quartile	78.5352	82.72	135.7415	180.0185	186.1601	188.1451	190.1301	190.13
Median	31.05	34.27	39.195	40.89	44.185	53.35	59.835	67.31
Lower quartile	8.9075	10.4425	18.91	30.43	33.5	37.975	40.65	41.89
Minimum	0.27	1.34	4.9	10.21	18.91	30.43	33.5	38.72
V_{DP}	0.853	0.779	0.713	0.656	0.59	0.551	0.52	0.482

As the number of wells and means of each model were deduced and controlled, Model VI gave the maximum mean value of 102.51 md. while Model III give the minimum mean value of 101.28 md. The means of the new seven models are close to the base case mean of 101.74 md. In this regard the recovery factor in reservoir simulation which we will later be performed can be easily compared.

After all the models were created, the coefficients of variation (V_{DP}) could be found in the ranges of 0.853 to 0.482 from the base case to model VII, respectively. Table 4.2 shows that V_{DP} decreases as standard deviation decreases.

As seen in Table 4.2, the upper, median and lower quartile values gradually increase from the base model to model VII. This could represent that their values rely very much on the standard deviation. The lower the value of standard deviation, the higher the value at given quartiles will be. The coefficient of variation (CV) is a normalized measure of dispersion of a probability distribution. It is defined as the ratio of the standard deviation to the mean. Typically, distributions with CV less than one are considered low-variance while those with CV greater than one are considered high-variance because standard deviation alone normally has little interpretable meaning unless the mean value is also reported.

Again, at CV greater than one, the standard deviation tends to have a wider range started from the Model IV upwards to the Base case. This could represent that the large level of heterogeneity would start from the V_{DP} of 0.59 to 0.853 in this case.

Skewness is a measure of the asymmetry of the probability distribution of a real-valued random variable. All models in our study provide the positive skewness in which the mass of the distribution is concentrated on the left. In other words, this kind of distributions is said to be right-skewed. Moreover, kurtosis is a measure of the peakedness of the probability distribution of a real-valued random variable. In this case, the higher kurtosis, the higher variance.

4.2.1 Sensitivity Analysis of Variogram

As illustrated in Figure 4.3, we generated seven more models at different degrees of heterogeneity varying V_{DP} values from 0.853 to 0.482. Geostatistically, there is not enough information to represent reservoir uncertainty characteristic and its effect on reservoir performance. Therefore, sensitivity analysis will be conducted in order to assess uncertainty of the model reservoirs. We will first study the effect of variogram in which it comprises of nugget and range and secondly investigate random number seed by using SGS.

To find spatial variability of its data as a function of distance and direction, in this case, omni-directional variogram is applied as it includes both vertical and horizontal directions. Tolerances with respect to distance and direction are used and given as a half of lag distance and ± 22.5 degree of direction, respectively.

Nugget effects are chosen as the uncertainty in the values of 0.1 and 0.3. Practically, nugget value of zero is very difficult to obtain due to the limited data for capturing the spatial relationship in petroleum field. In this case, variogram does not exhibit a clearly defined nugget and structure or shows too many fluctuations. Theoretically, the nugget effect value should not be greater than 0.3. Otherwise, it would be unacceptable data or statistical random value. Range is varied from 300 m. to 900 m. depending on variogram characteristics. Theoretically, the range is to use half the maximum possible distance within the region of interest. The reason is to ensure that representative pairs are collected on both sides of a given location. As

referred to the location maps, 2,500 m. is the maximum distance between any two sample points within the region of interest. As a result, the variogram estimation is restricted to a maximum lag distance or range of 1,250 m. There are three ranges fitted in variograms such as 300-600 m., 500-800 m., and 600-900 m. The different of 300 m.-range is given to be the uncertainty. The reason to come up with the value is that we normally get an erratic variogram result, particularly, in petroleum field due to the lack of a sample. Thus, range, in this case, is quite difficult to define and cannot preserve the correct behavior. If the range is set too large, we might get an outside sample of the local stationary region. On the other hand, if it is given too small, we may not have enough data to represent a good estimation. Therefore, 300 m.-range is given to be the range of the uncertainty as it can help us to cover and represent a better result.

Before SGS has been used, Gaussian transformation is required to transform the cumulative distribution function to Gaussian variable in which its variability of the data set is restricted to -3 to +3 as seen in Figure 4.2 (b). Theoretically, SGS algorithm needs to be used in the Gaussian distribution to transform sample data into equivalent data. The advantage of the Gaussian transform is that it is easier to define the raw data into a normal score which has a mean of zero and a variance of one and can be also reduced the effect of extreme data on variogram. Therefore, normal score transform was defined. After performing SGS, we can backtransform the data to original values and will use SGS of the base case for generating multiple maps and sensitivity analysis as explained in the following details. The sensitivity analysis of normal score variograms is illustrated from Figures 4.5 to 4.12.

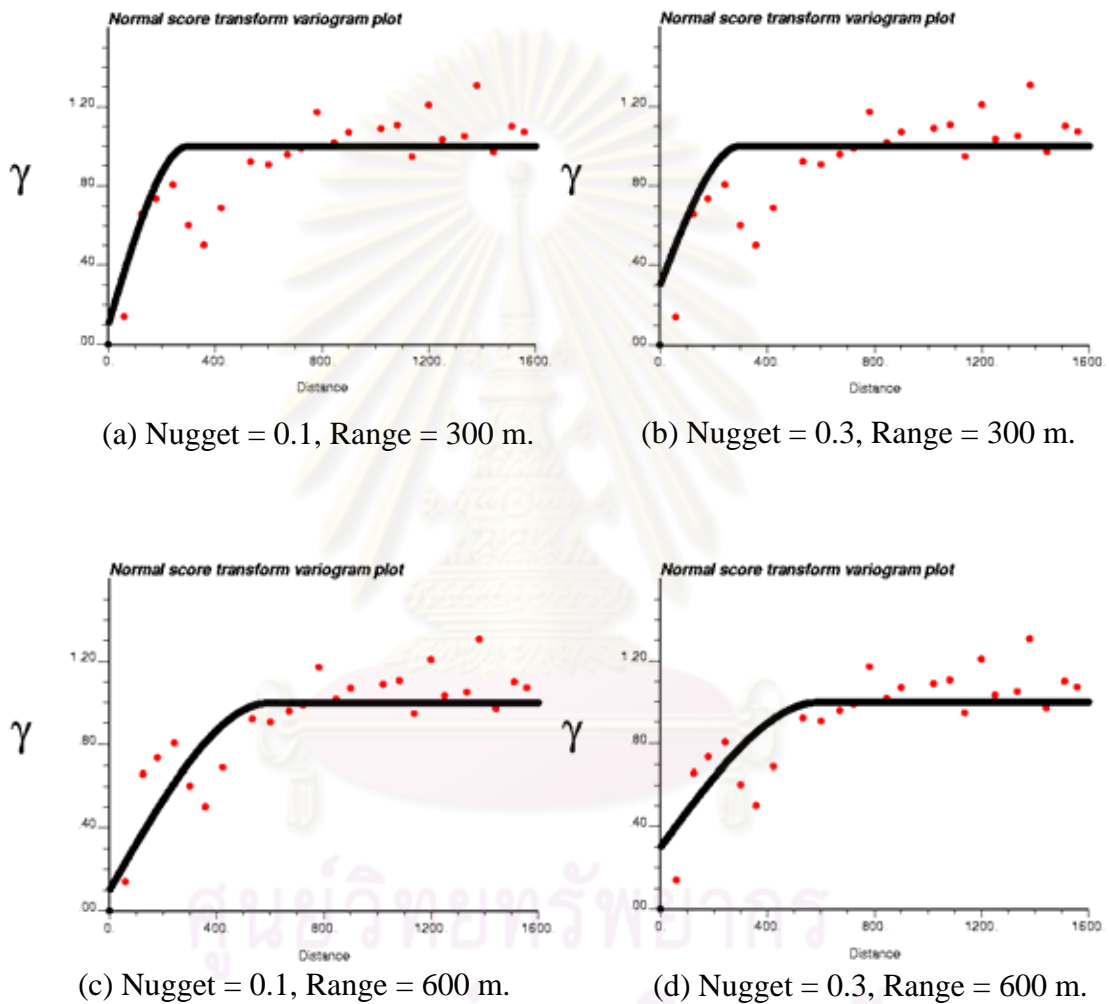


Figure 4.5 : Normal score transform of omni-directional spherical variograms of base case varied nuggets and ranges using number of lags of 32, lag distance of 60 m.

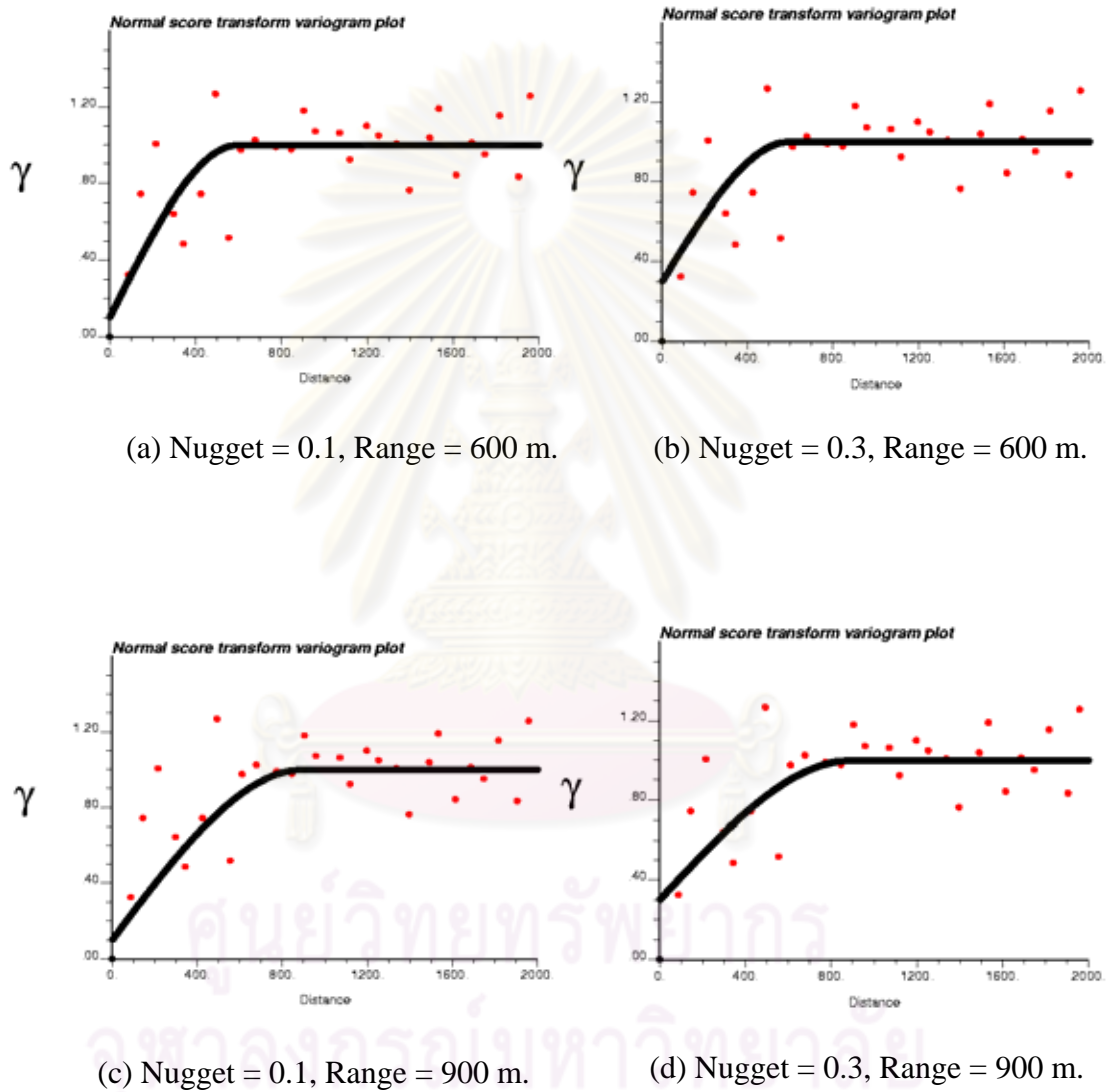


Figure 4.6 : Normal score transform of omni-directional spherical variograms of the model I varied nuggets and ranges using number of lags of 35, lag distance of 70 m.

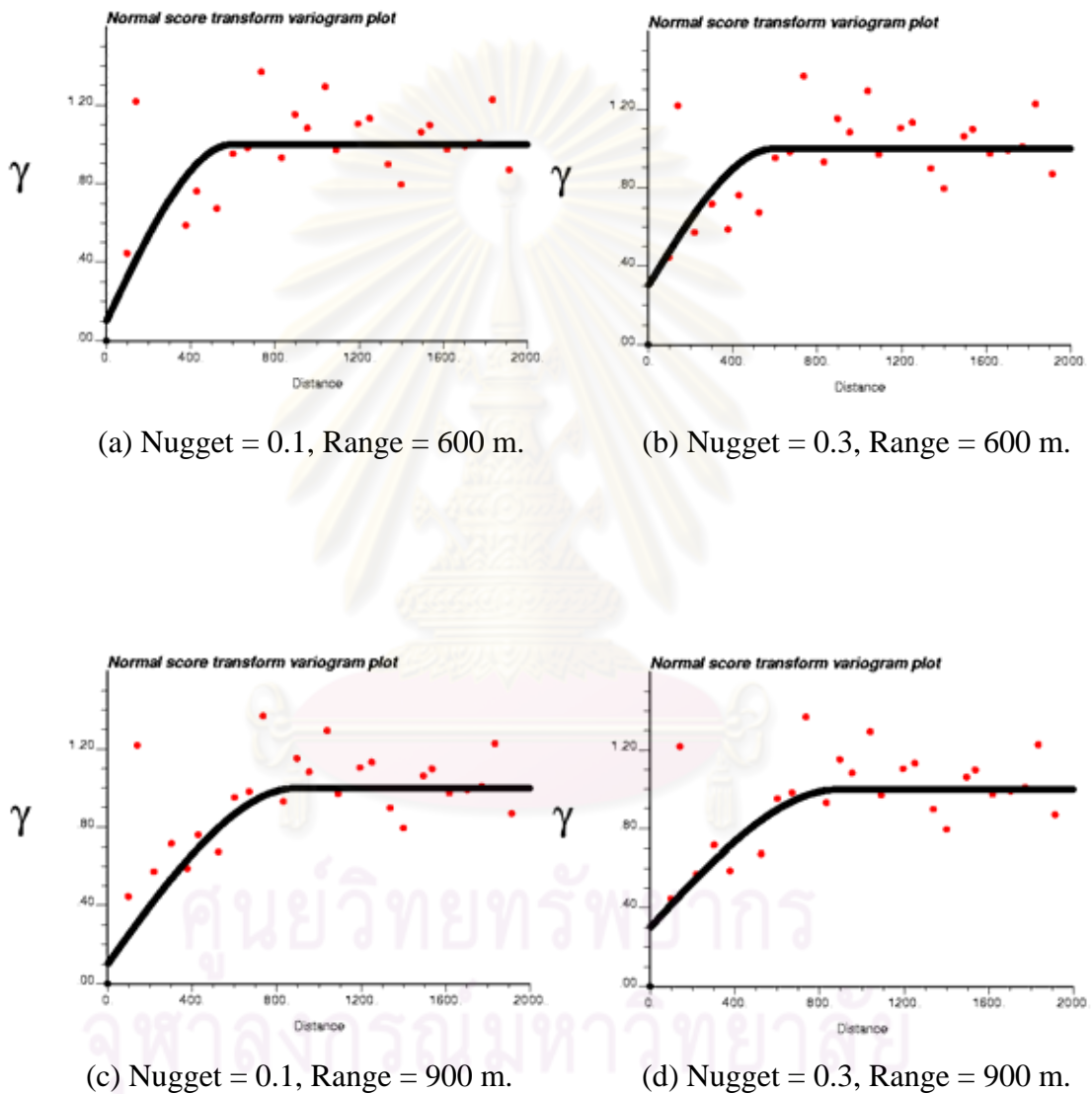


Figure 4.7 : Normal score transform of omni-directional spherical variograms of the model II varied nuggets and ranges using number of lags of 35, lag distance of 74 m.

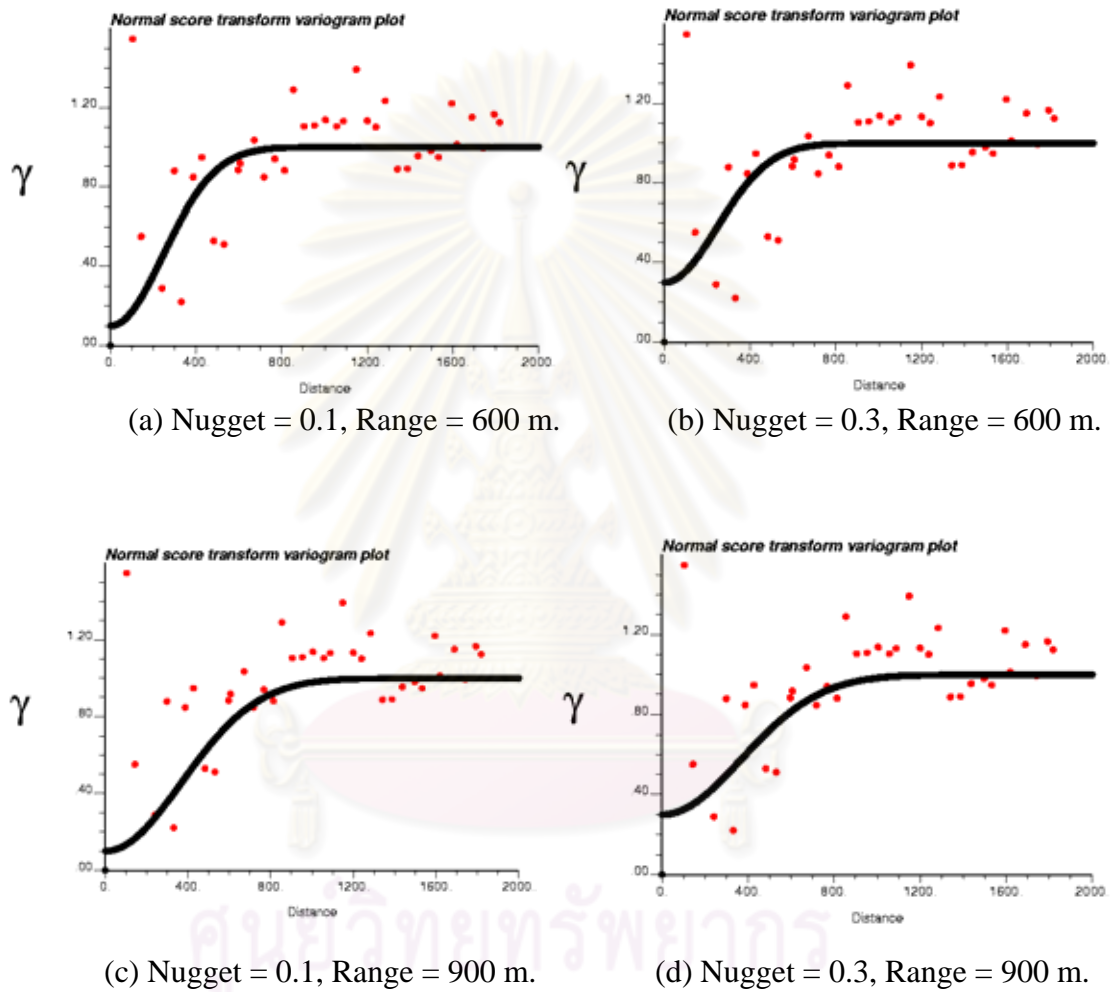


Figure 4.8 : Normal score transform of omni-directional Gaussian variograms of the model III varied nuggets and ranges using number of lags of 38, lag distance of 48 m.

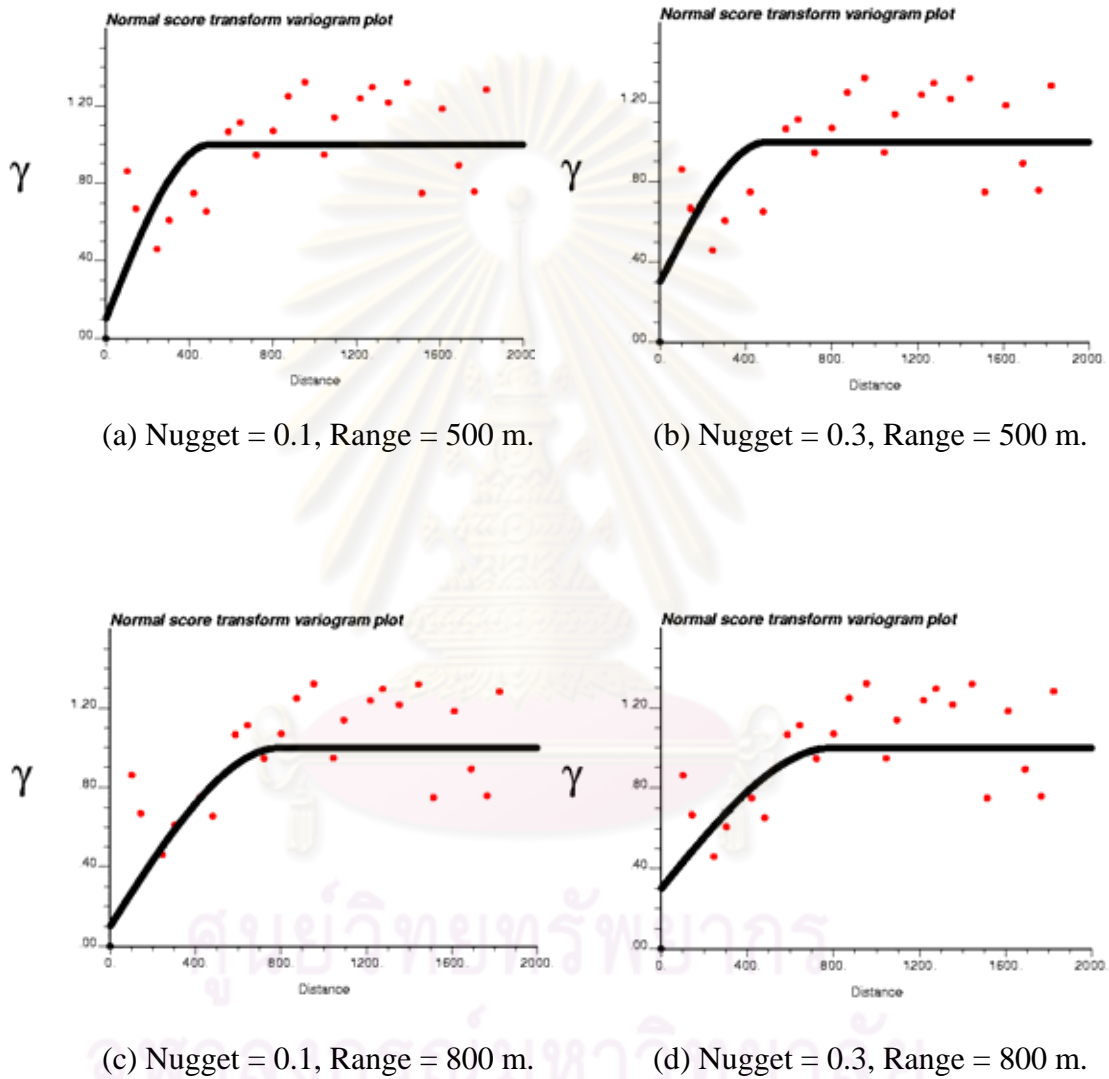


Figure 4.9 : Normal score transform of omni-directional spherical variograms of the model IV varied nuggets and ranges using number of lags of 37, lag distance of 80 m.

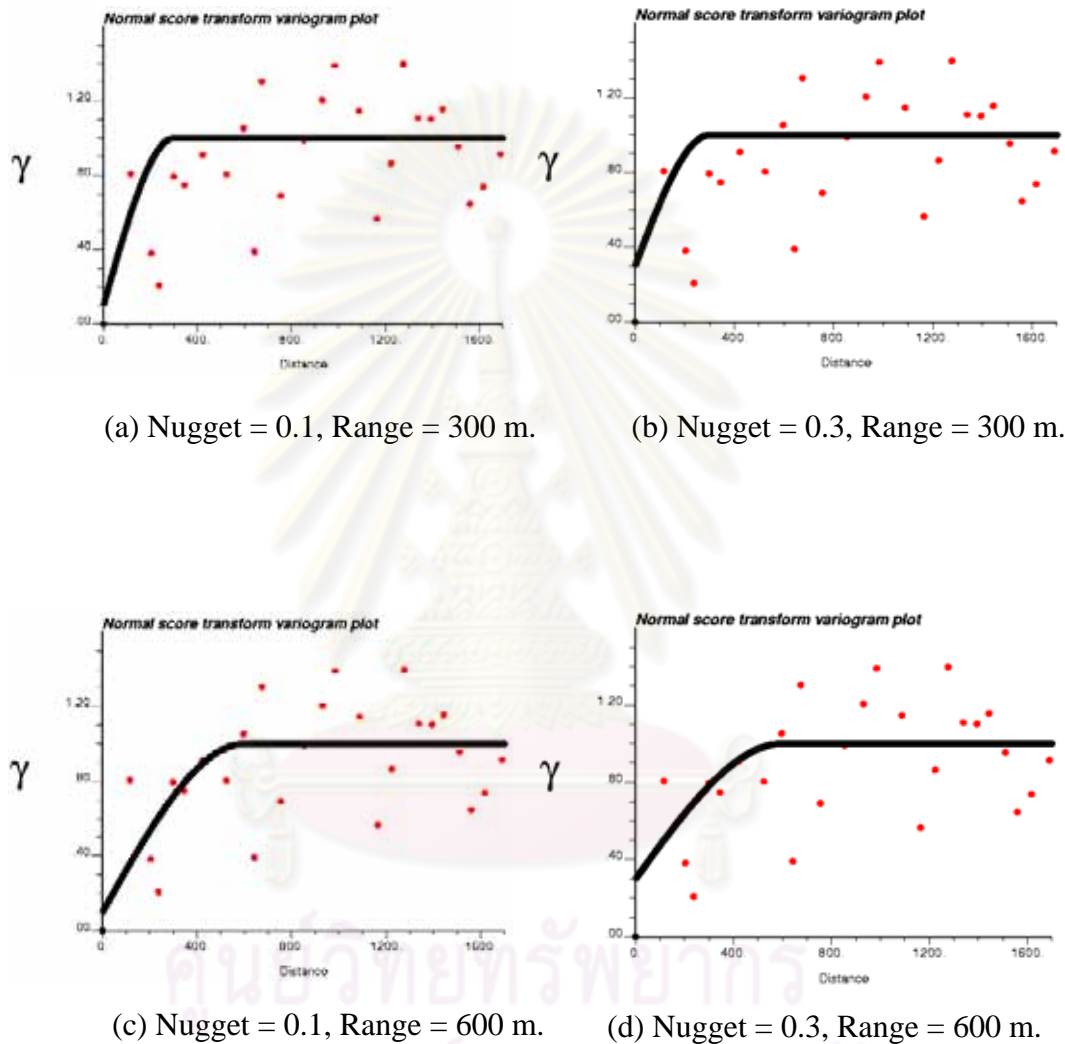


Figure 4.10 : Normal score transform of omni-directional spherical variograms of the model V varied nuggets and ranges using number of lags of 34, lag distance of 58 m.

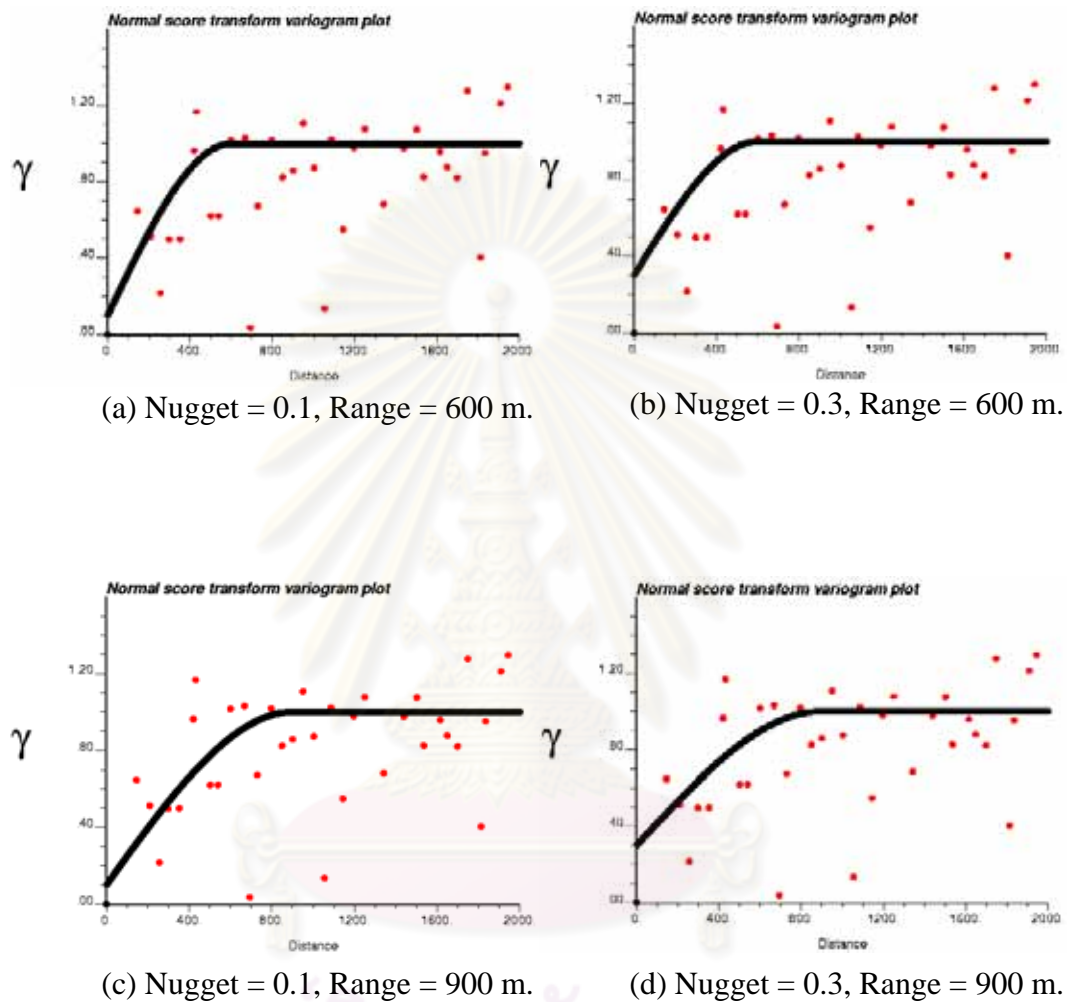


Figure 4.11 : Normal score transform of omni-directional spherical variograms of the model VI varied nuggets and ranges using number of lags of 40, lag distance of 50 m.

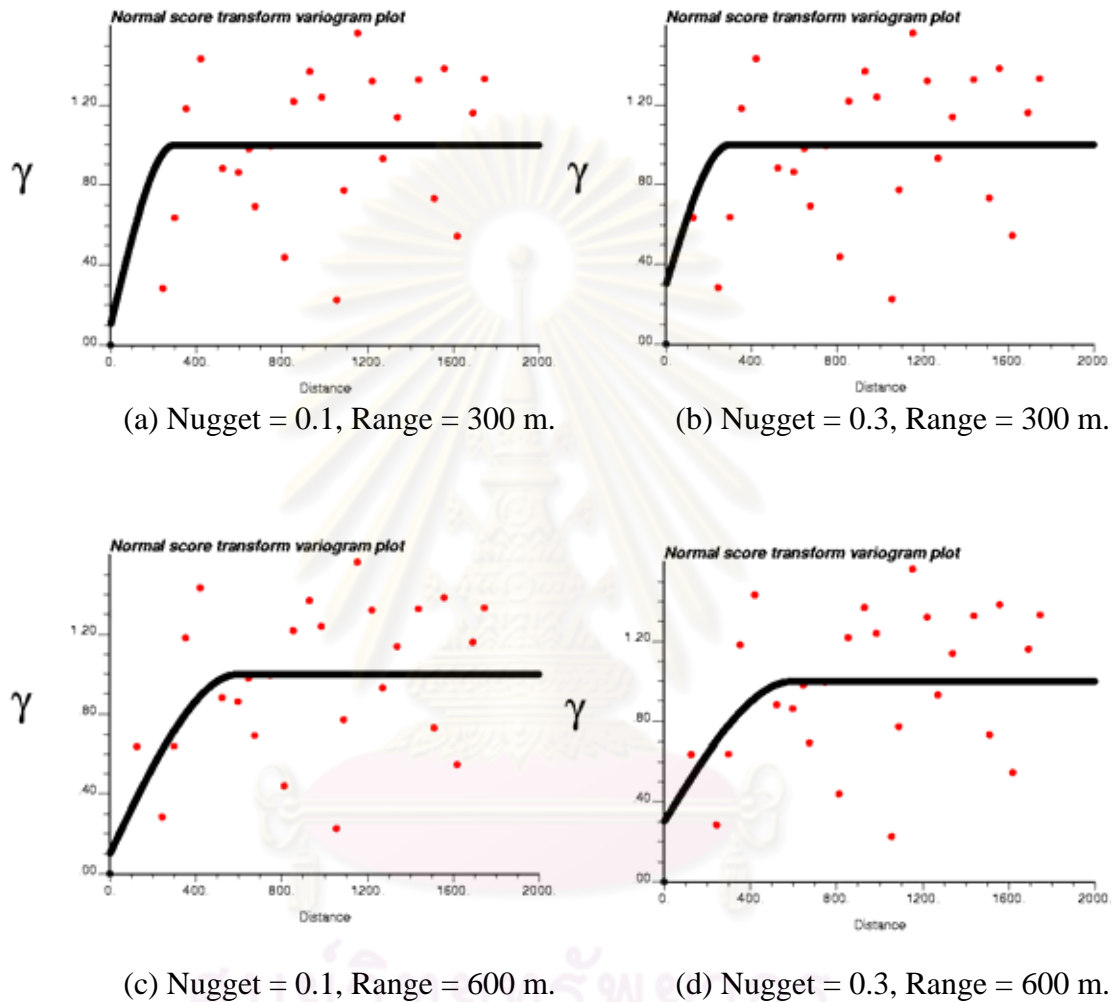


Figure 4.12 : Normal score transform of omni-directional spherical variograms of the model VII varied nuggets and ranges using number of lags of 30, lag distance of 58 m.

Table 4.3 : Comparison of eight-model normal score transform variogram data

Model Name	Variogram Type	Number of Lags	Lag Distance (m.)	Lags Tolerance (m.)	Ranges (m.)
Base case	Spherical	32	60	30	300, 600
Model I	Spherical	35	70	35	600, 900
Model II	Spherical	35	74	37	600, 900
Model III	Gaussian	38	48	24	600, 900
Model IV	Spherical	37	80	40	500, 800
Model V	Spherical	34	58	29	300, 600
Model VI	Spherical	40	50	25	600, 900
Model VII	Spherical	30	58	28	300, 600

As explained earlier, conventional variogram does not give a clear structural model to describe its spatial relationship in which it normally exhibits the most fluctuation. Thus, a normal score variogram is chosen for reducing that effect. Table 4.3 shows the comparison of eight-model normal score transform variogram data which are varied according to the parameters such as nugget effects and ranges.

There are two types of variogram used in this study such as spherical and Gaussian variograms. Spherical variogram characterizes all models except model III is fitted by the Gaussian variogram. All the models are generated using the nugget effects of 0.1 and 0.3. Base case, Model V and VII are fitted with the range of 300 to 600 m. Model IV is fitted with the range of 500 to 800 m. Model I, II, III and VI are fitted with the range of 600 to 900 m., respectively. As expected, the variogram starts with a zero value and increases as the lag distance between the two values increase. As a result, variance increases as lag distance increases. Lags tolerance is typically given half the lag distance to ensure that we can capture additional lags for a better estimate of the variogram. As seen from the normal score transform variogram plots, the base case to model IV give a clearly interpretable structure but model V to model VII still shows some fluctuation in the estimated values. This is because the lack of the data and/or spatial continuity should have significant effect on the interpretation. The relationship between number of lags and lag distance is shown in Figure 4.13.

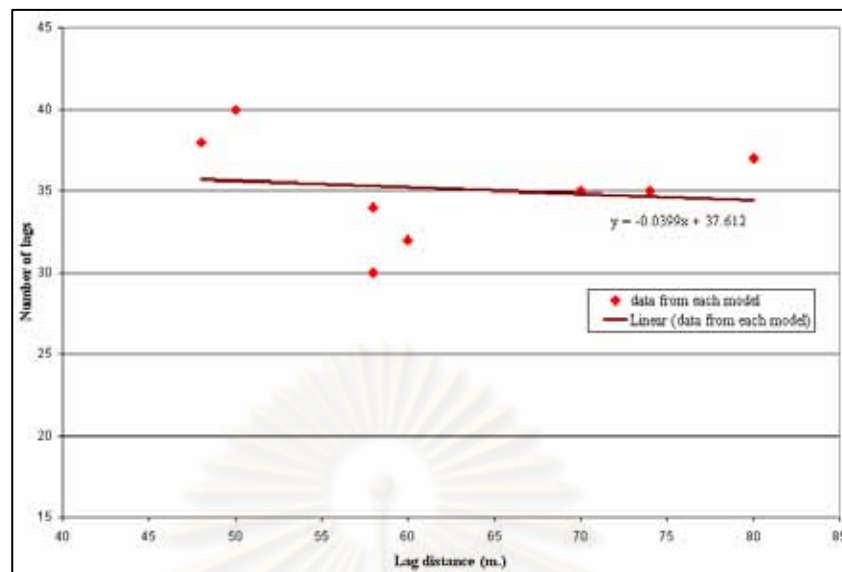


Figure 4.13 : Relationship between number of lags and lag distance

Figure 4.13 shows that the possible number of lags decrease as lag distance increases. Theoretically, at given lag distance, the more lags we have, the more accurate the estimate of the variogram.

4.2.2 Sensitivity Analysis of Realizations

In this study, we investigate only the effect of permeability on reservoir performance. Although, there are many factors which can help us in understanding more accurately such as porosity, water saturation etc., we assume that there are less effect than permeability. As a result, this study will be concerned with only parameter.

Geostatistically, multiple fine-scale stochastic realizations are generated by changing the random number seed in the SGS. Moreover, the variogram parameters which are range and nugget are varied. The realizations which give a different degree of heterogeneity are used to quantify uncertainty in performance predictions. As mentioned before, SGS has been widely used to assess spatial uncertainty in the reservoir performance because it can create the different schemes of reservoir characteristics in some global sense by giving the numbers of equiprobable images. Comparing with the Kriging method, it provides a single numerical image which is best in some local accuracy sense and does not represent the reality. In addition, it

only relies on neighborhood data which gives a smooth picture. Once, we use the Kriging model to study the effect on reservoir performance, it will not give us precise information. As a result, SGS is used to access reservoir uncertainty. Figure 4.14 illustrates the flow sheet to obtain realizations with different degrees of heterogeneity. Figures 4.15 to 4.40 show the result of 104 realizations generated by SGS.

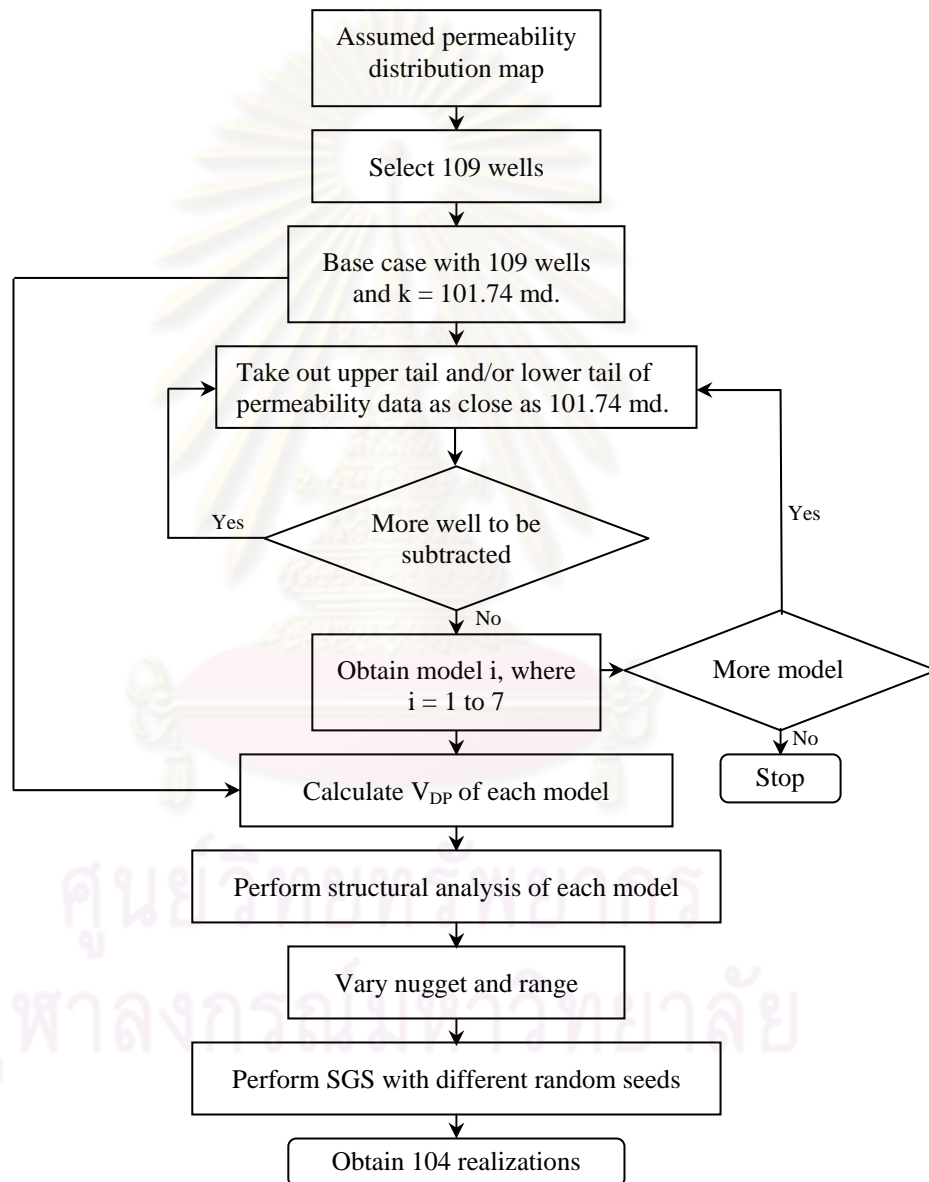
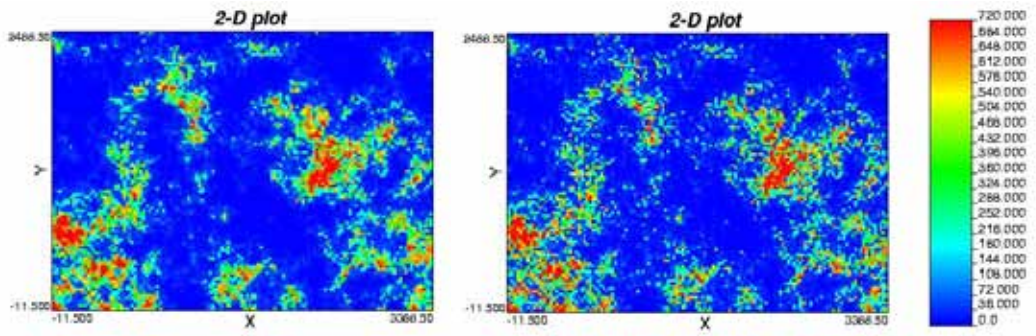
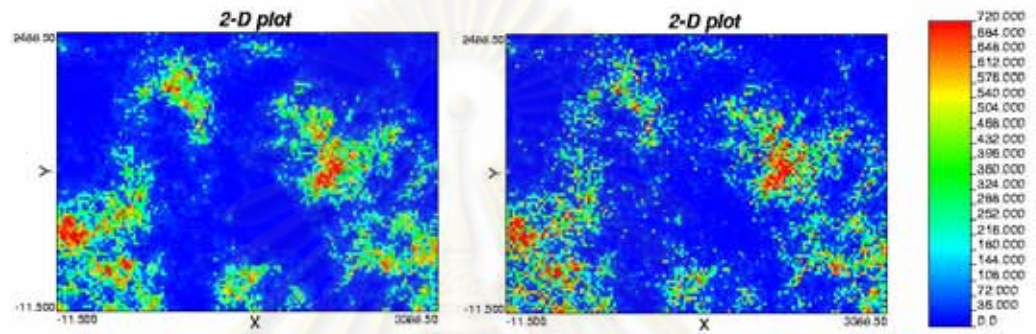


Figure 4.14 : Flow sheet to obtain realizations with different degrees of heterogeneity

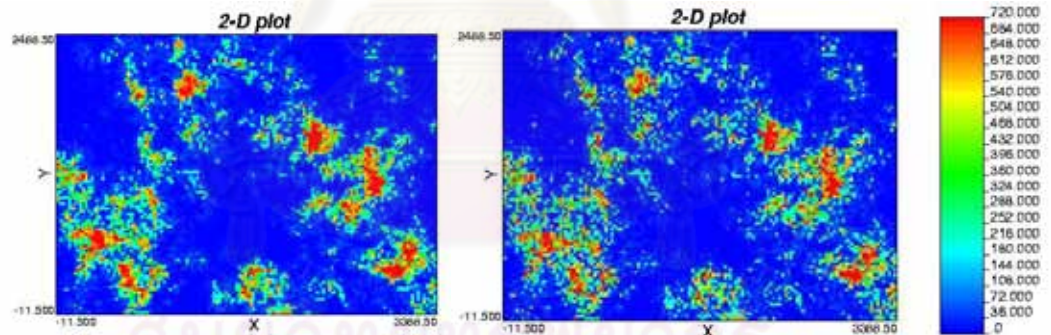


(a) Nugget = 0.1, Range = 300 m. (b) Nugget = 0.3, Range = 300 m.

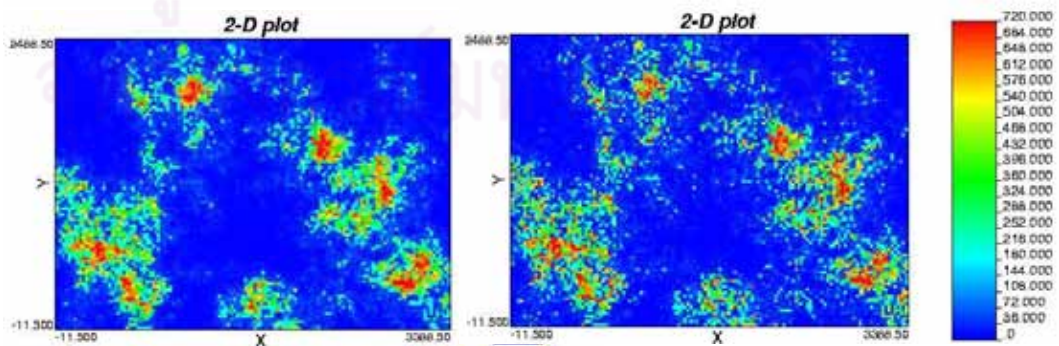


(c) Nugget = 0.1, Range = 600 m. (d) Nugget = 0.3, Range = 600 m.

Figure 4.15 : SGS of the base case varied nuggets and ranges at the seed number of 106236

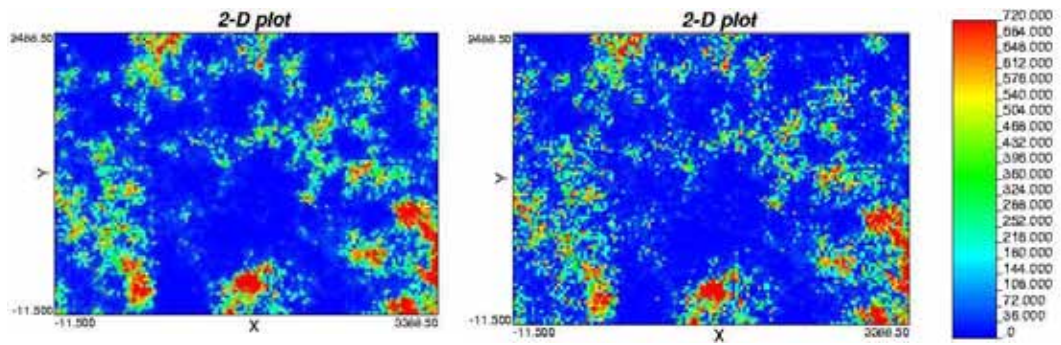


(a) Nugget = 0.1, Range = 300 m. (b) Nugget = 0.3, Range = 300 m.

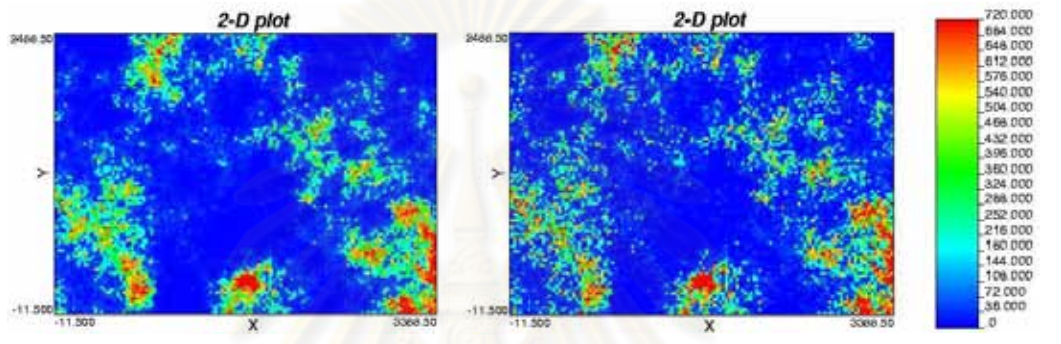


(c) Nugget = 0.1, Range = 600 m. (d) Nugget = 0.3, Range = 600 m.

Figure 4.16 : SGS of the base case varied nuggets and ranges at the seed number of 1299460

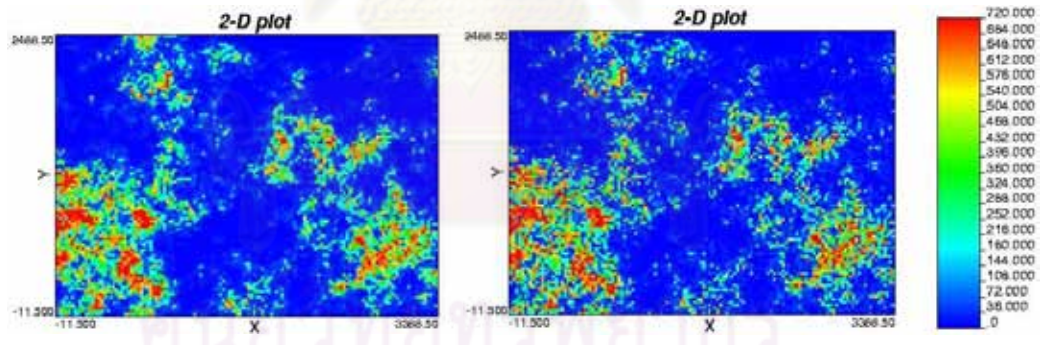


(a) Nugget = 0.1, Range = 300 m. (b) Nugget = 0.3, Range = 300 m.

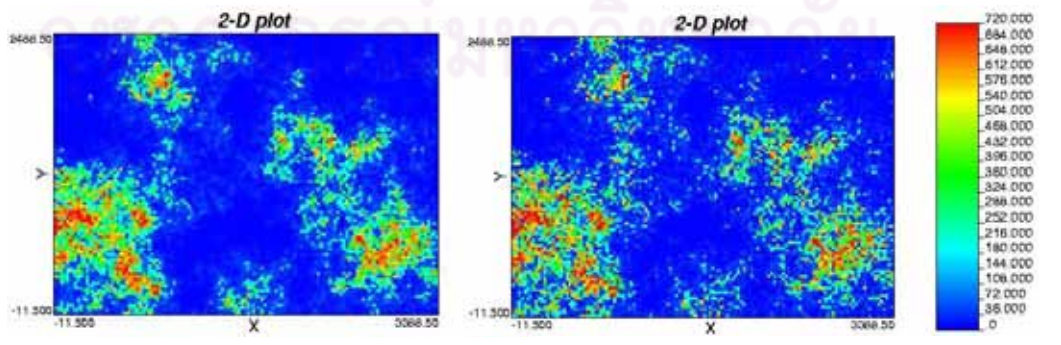


(c) Nugget = 0.1, Range = 600 m. (d) Nugget = 0.3, Range = 600 m.

Figure 4.17 : SGS of the base case varied nuggets and ranges at the seed number of 4211847

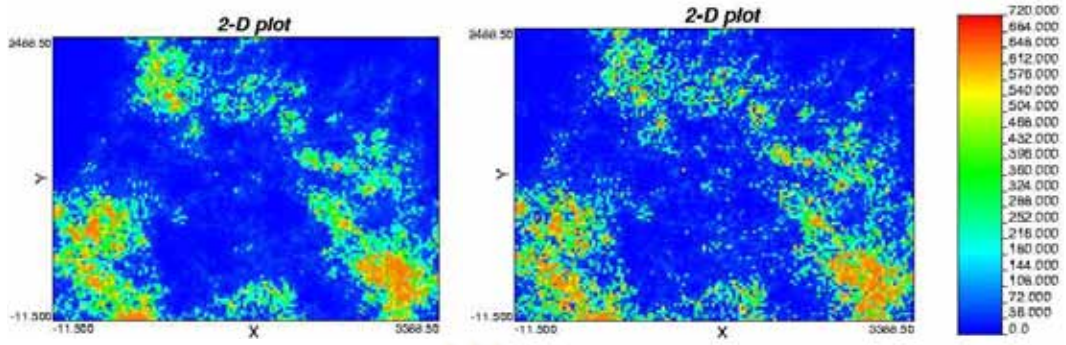


(a) Nugget = 0.1, Range = 300 m. (b) Nugget = 0.3, Range = 300 m.

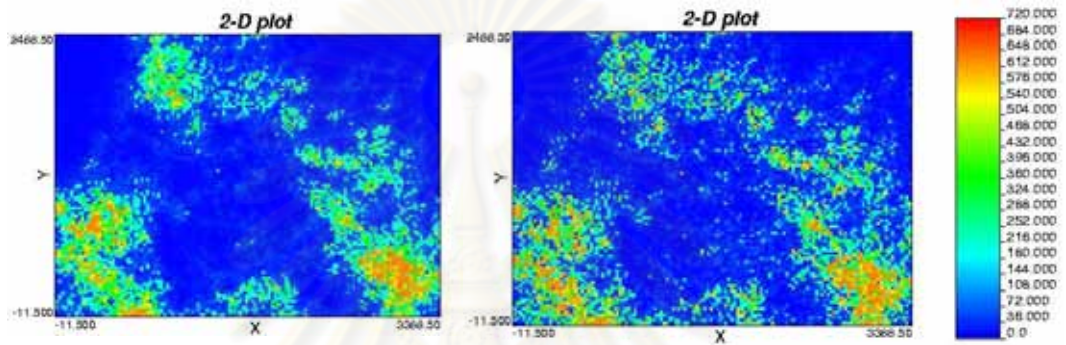


(c) Nugget = 0.1, Range = 600 m. (d) Nugget = 0.3, Range = 600 m.

Figure 4.18 : SGS of the base case varied nuggets and ranges at the seed number of 5209254

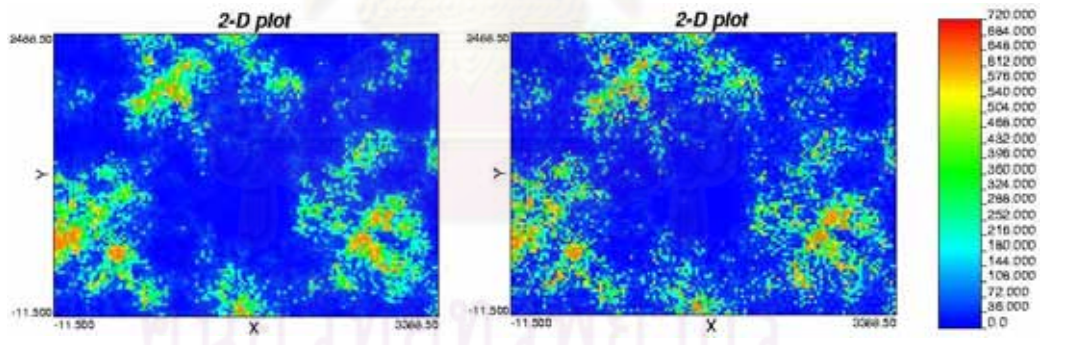


(a) Nugget = 0.1, Range = 600 m. (b) Nugget = 0.3, Range = 600 m.

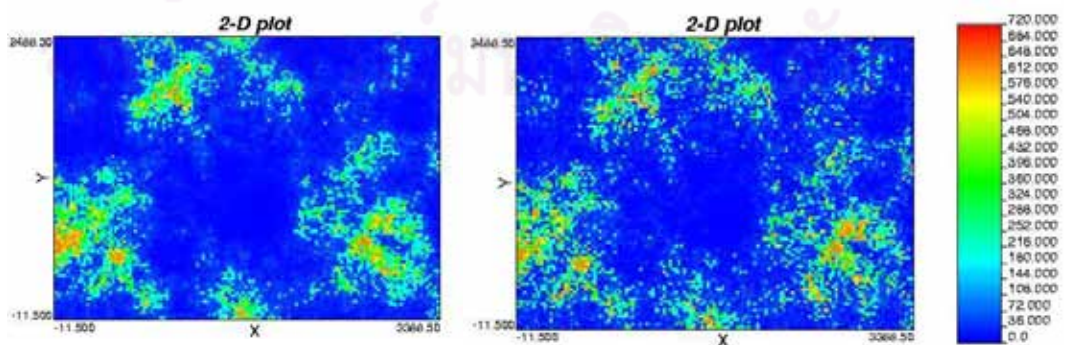


(c) Nugget = 0.1, Range = 900 m. (d) Nugget = 0.3, Range = 900 m.

Figure 4.19 : SGS of the model I varied nuggets and ranges at the seed number of 153567

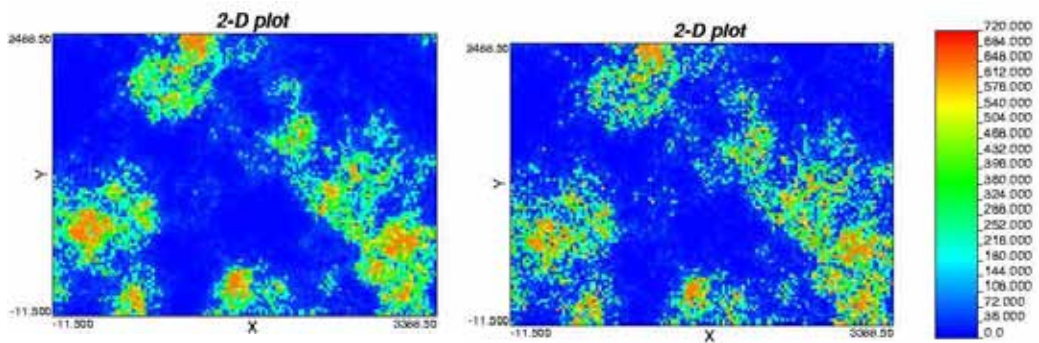


(a) Nugget = 0.1, Range = 600 m. (b) Nugget = 0.3, Range = 600 m.

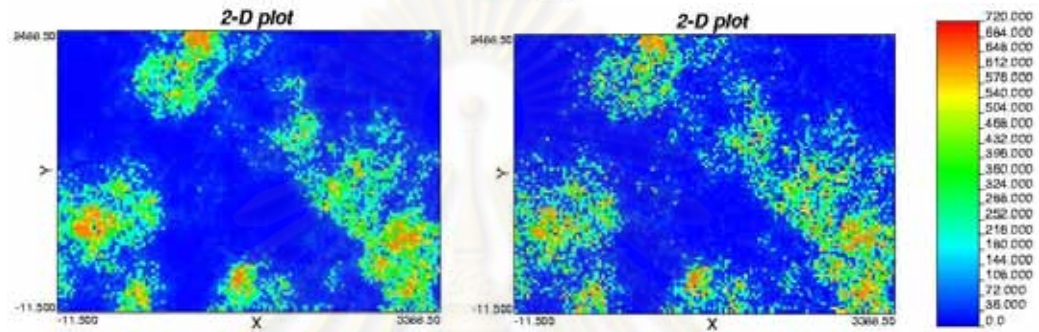


(c) Nugget = 0.1, Range = 900 m. (d) Nugget = 0.3, Range = 900 m.

Figure 4.20 : SGS of the model I varied nuggets and ranges at the seed number of 896078

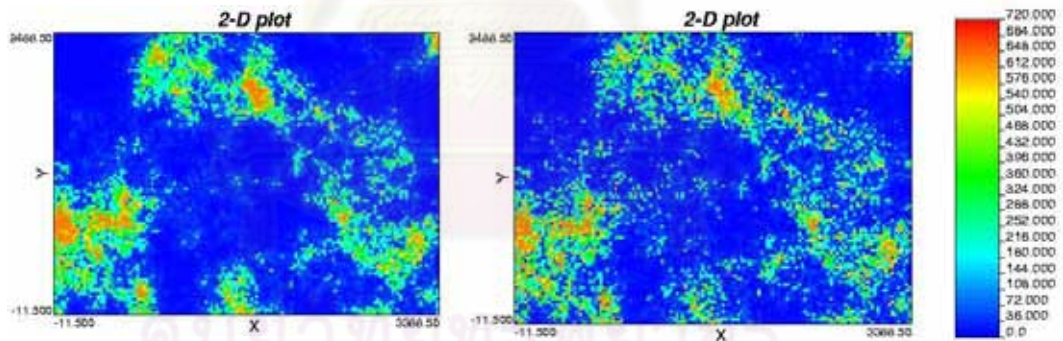


(a) Nugget = 0.1, Range = 600 m. (b) Nugget = 0.3, Range = 600 m.

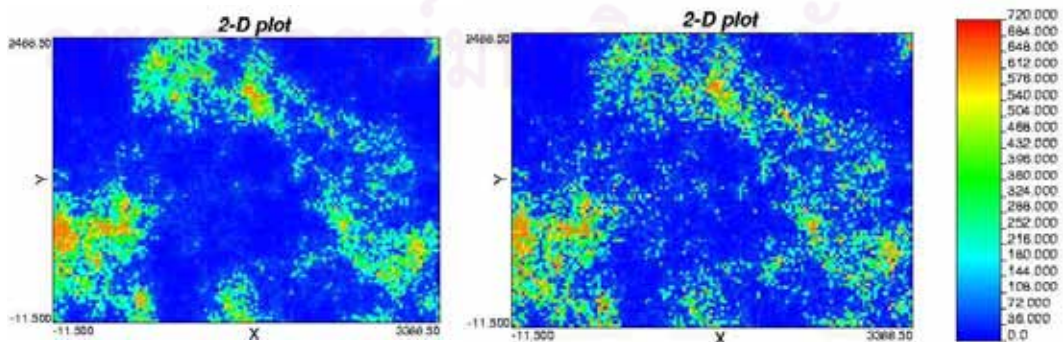


(c) Nugget = 0.1, Range = 900 m. (d) Nugget = 0.3, Range = 900 m.

Figure 4.21 : SGS of the model I varied nuggets and ranges at the seed number of 4773049



(a) Nugget = 0.1, Range = 600 m. (b) Nugget = 0.3, Range = 600 m.



(c) Nugget = 0.1, Range = 900 m. (d) Nugget = 0.3, Range = 900 m.

Figure 4.22 : SGS of the model I varied nuggets and ranges at the seed number of 5237802

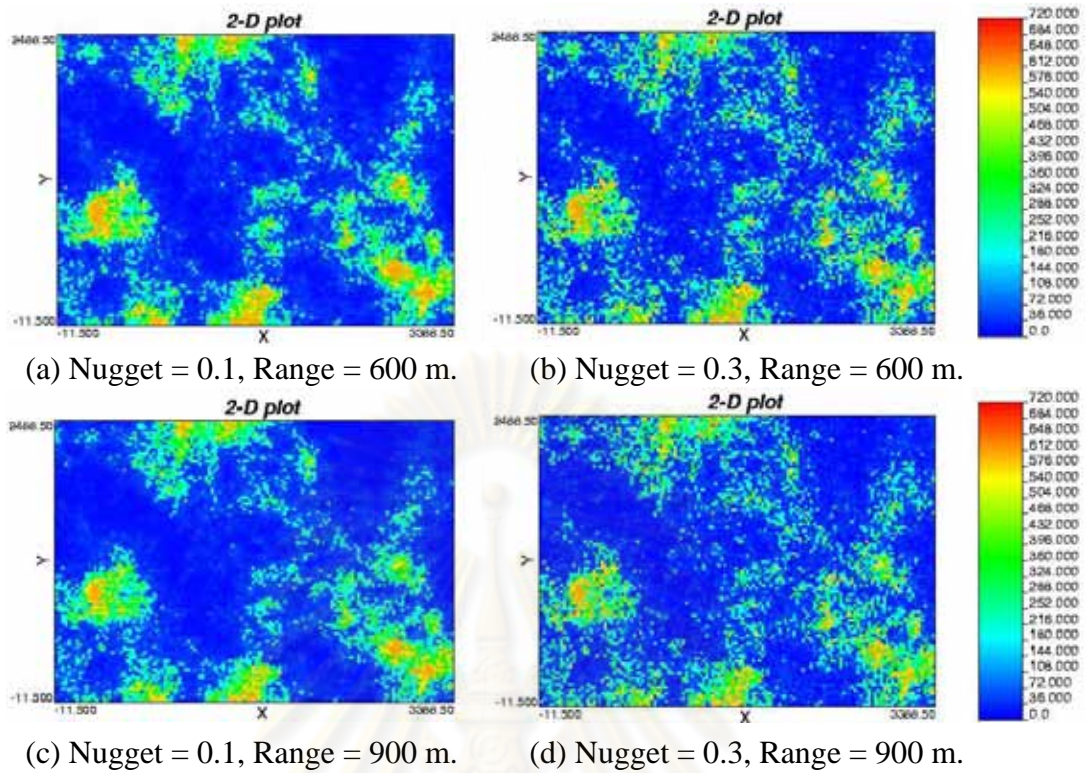


Figure 4.23 : SGS of the model II varied nuggets and ranges at the seed number of 3782386

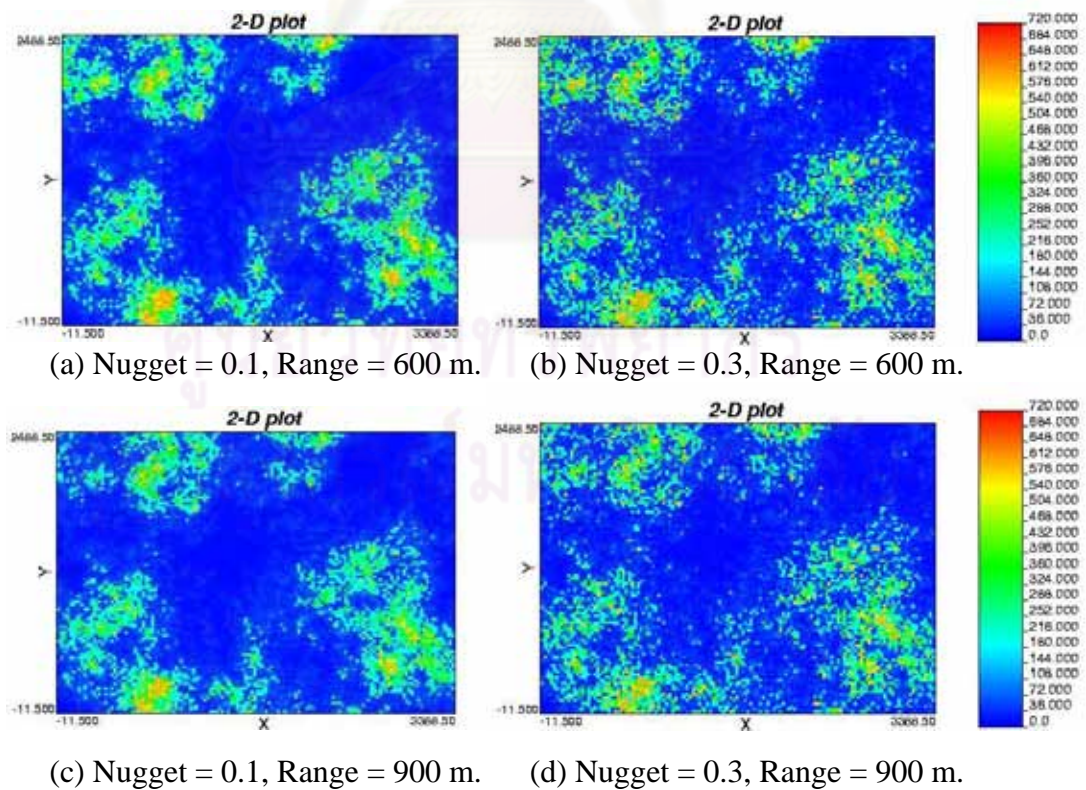


Figure 4.24 : SGS of the model II varied nuggets and ranges at the seed number of 4574483

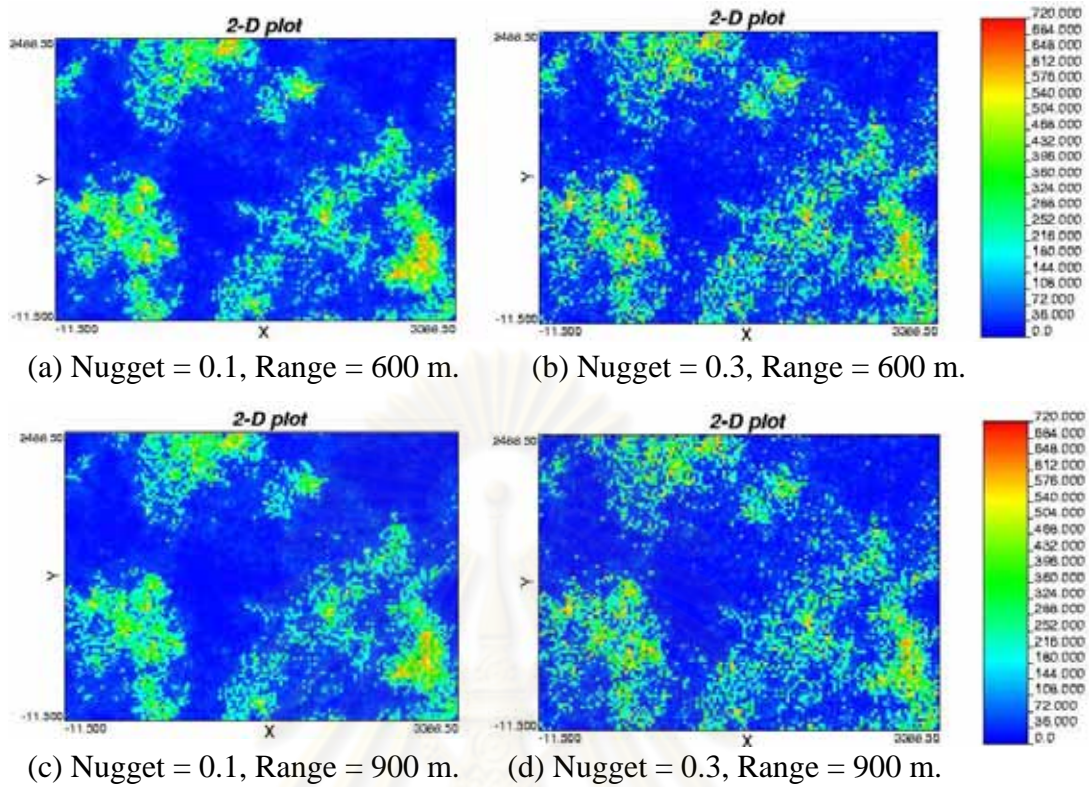


Figure 4.25 : SGS of the model II varied nuggets and ranges at the seed number of 6768113

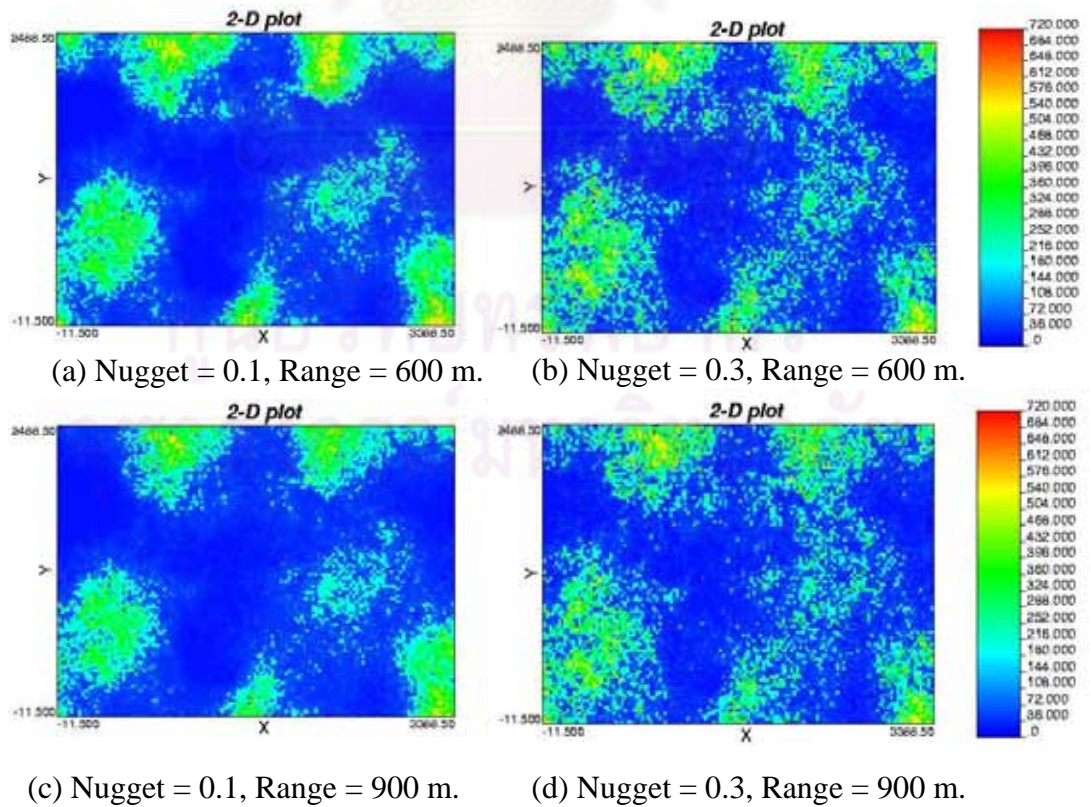


Figure 4.26 : SGS of the model III varied nuggets and ranges at the seed number of 218583

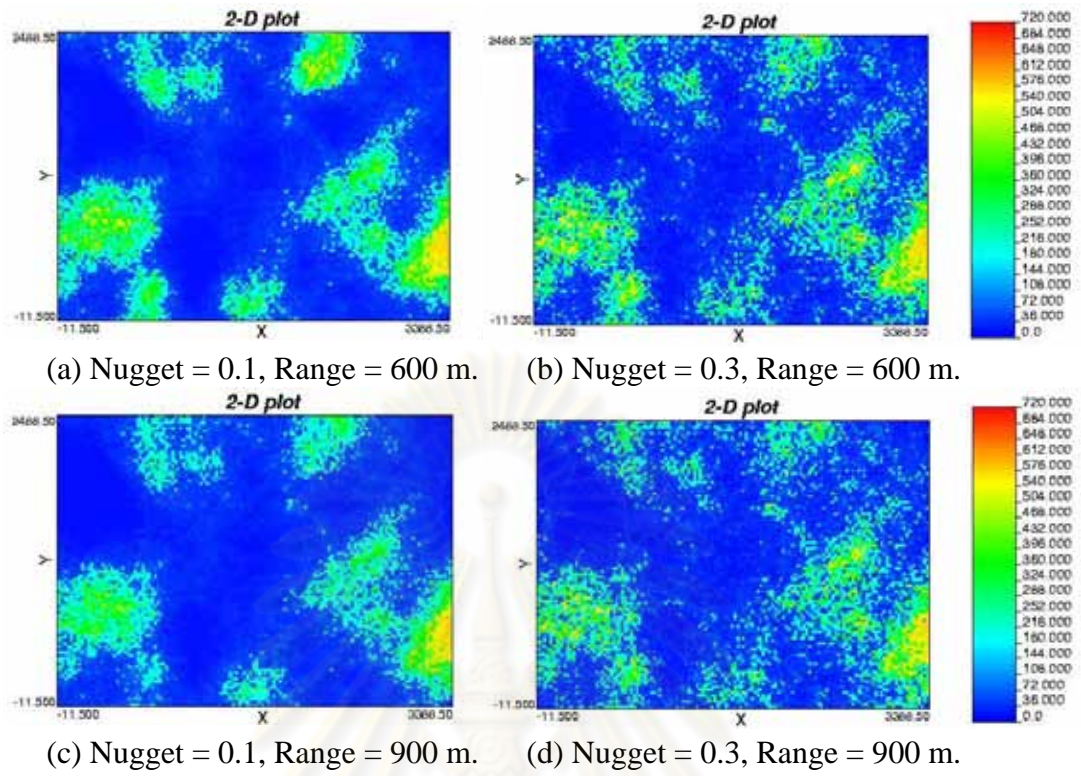


Figure 4.27 : SGS of the model III varied nuggets and ranges at the seed number of 2904965

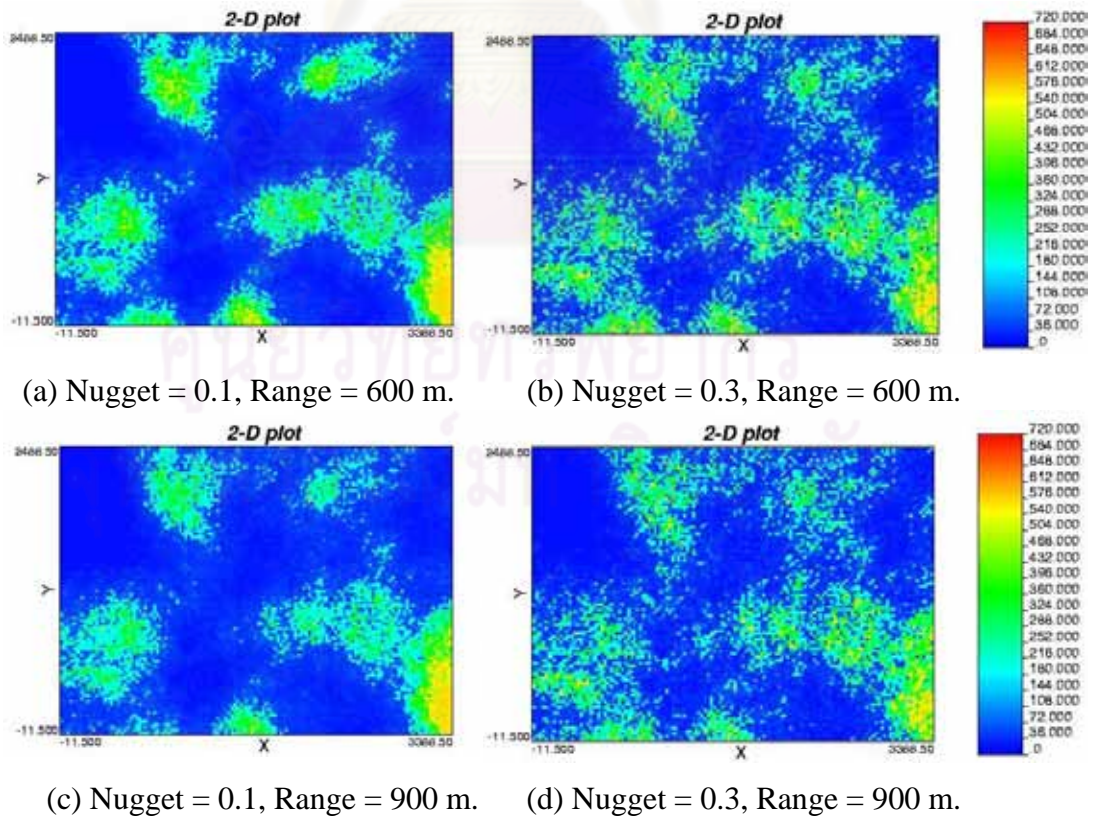


Figure 4.28 : SGS of the model III varied nuggets and ranges at the seed number of 7497676

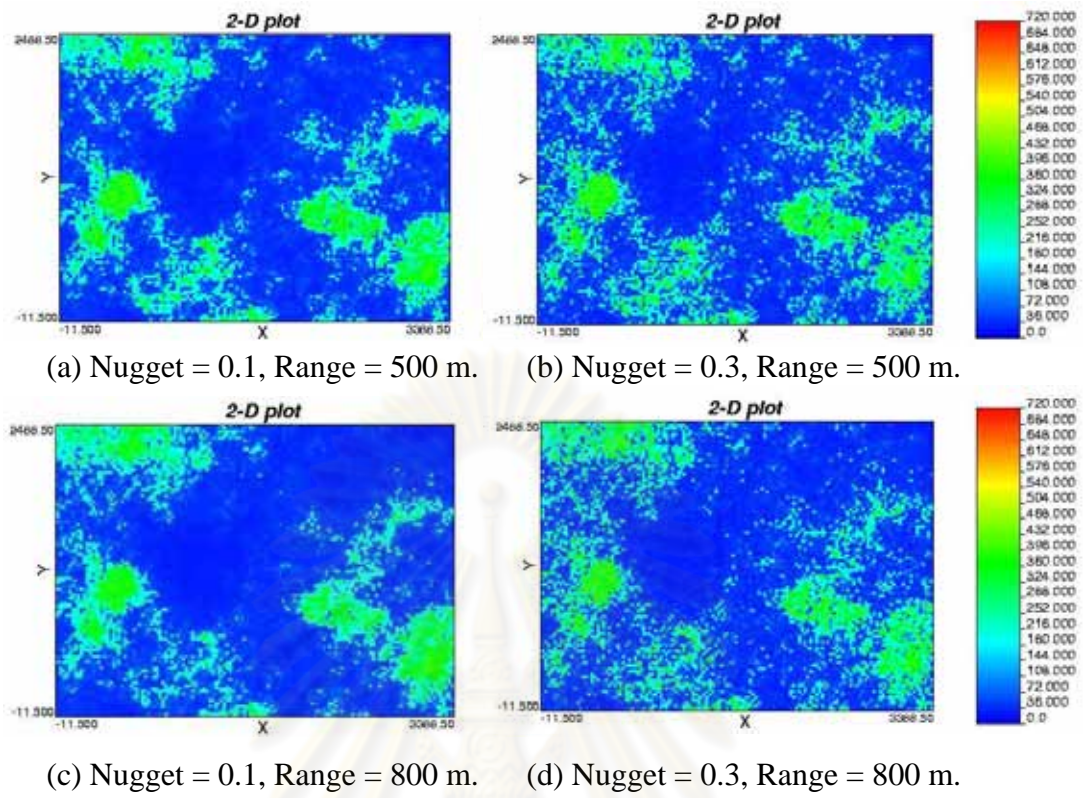


Figure 4.29 : SGS of the model IV varied nuggets and ranges at the seed number of 2895849

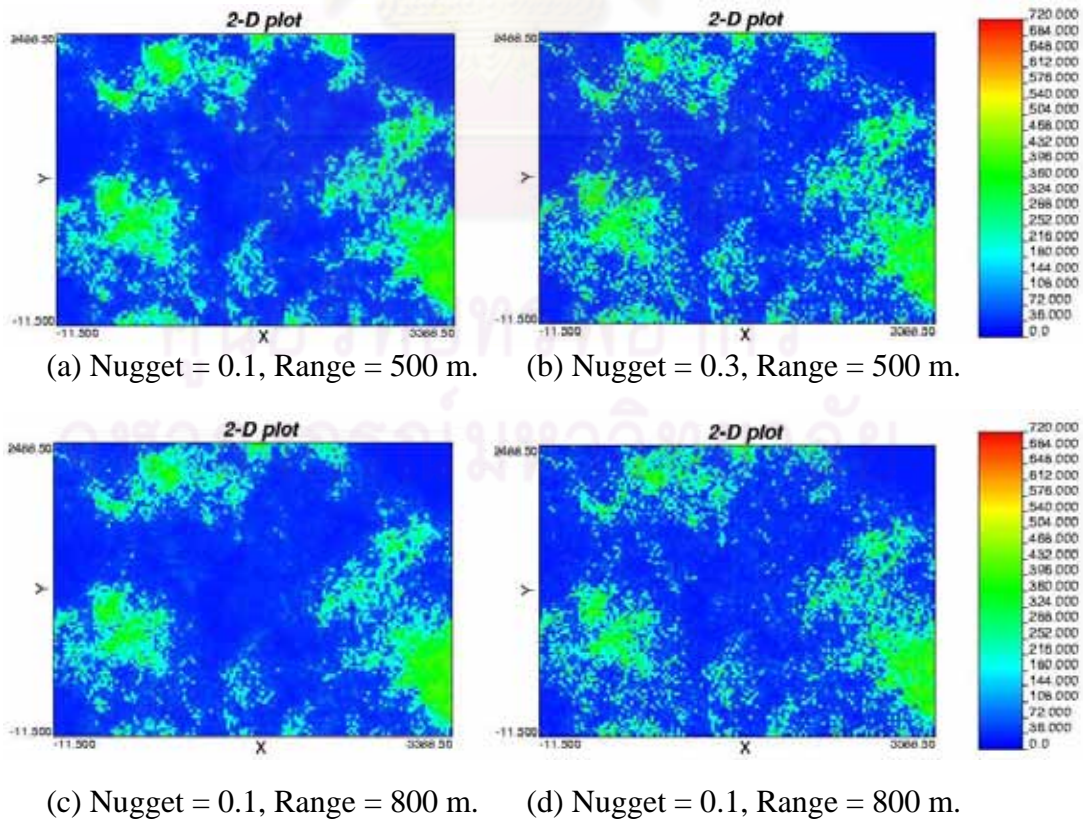
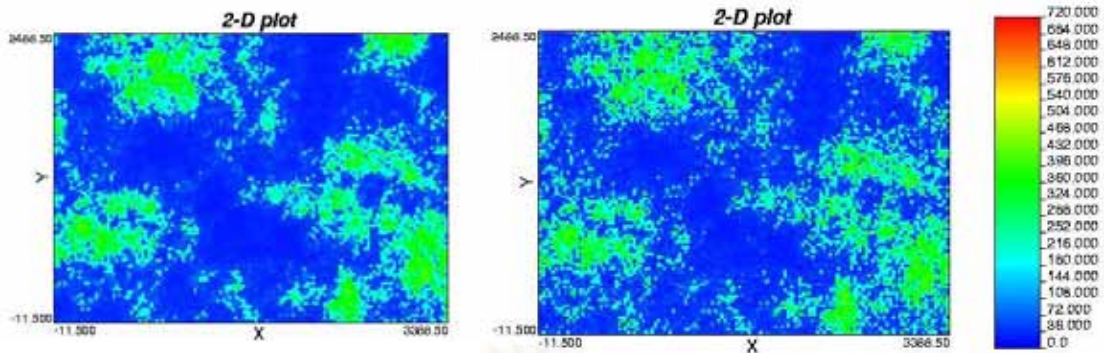
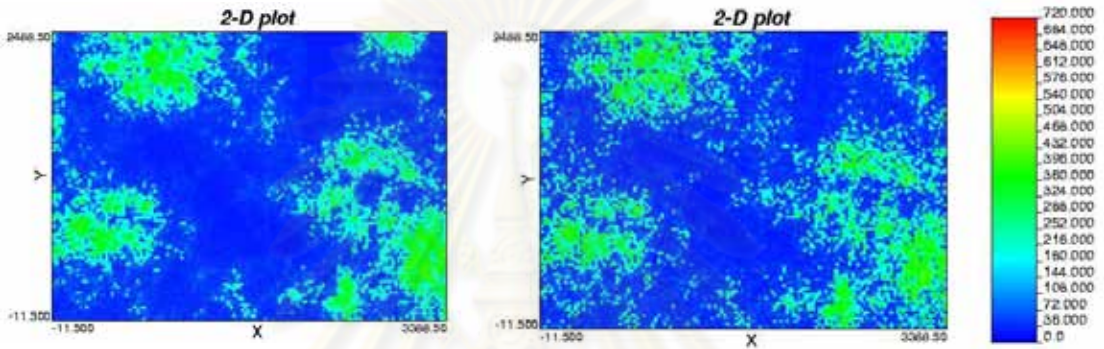


Figure 4.30 : SGS of the model IV varied nuggets and ranges at the seed number of 6259246



(a) Nugget = 0.1, Range = 500 m.

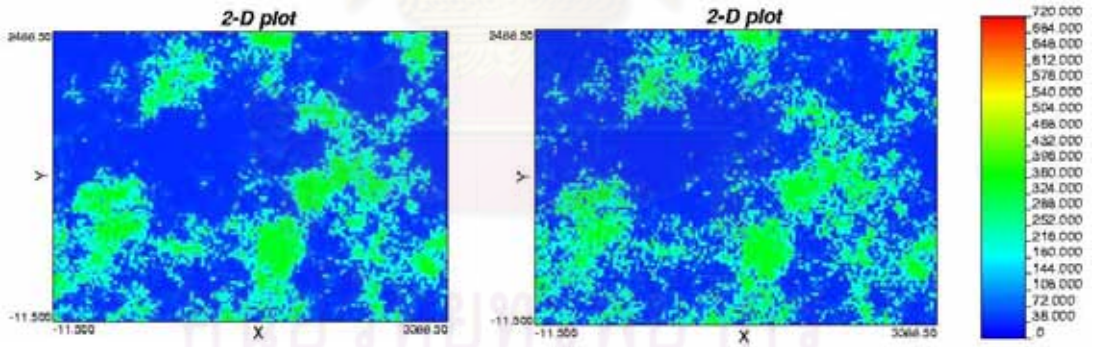
(b) Nugget = 0.3, Range = 500 m.



(c) Nugget = 0.1, Range = 800 m.

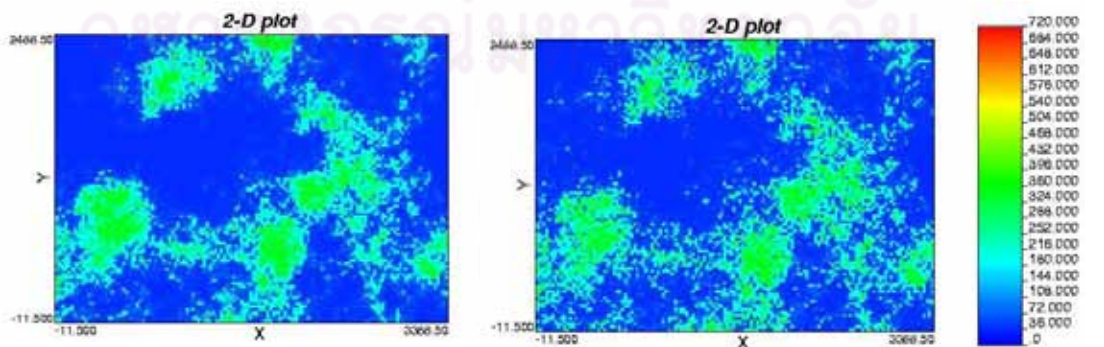
(d) Nugget = 0.3, Range = 800 m.

Figure 4.31 : SGS of the model IV varied nuggets and ranges at the seed number of 9451304



(a) Nugget = 0.1, Range = 300 m.

(b) Nugget = 0.3, Range = 300 m.



(c) Nugget = 0.1, Range = 600 m.

(d) Nugget = 0.3, Range = 600 m.

Figure 4.32 : SGS of the model V varied nuggets and ranges at the seed number of 69069

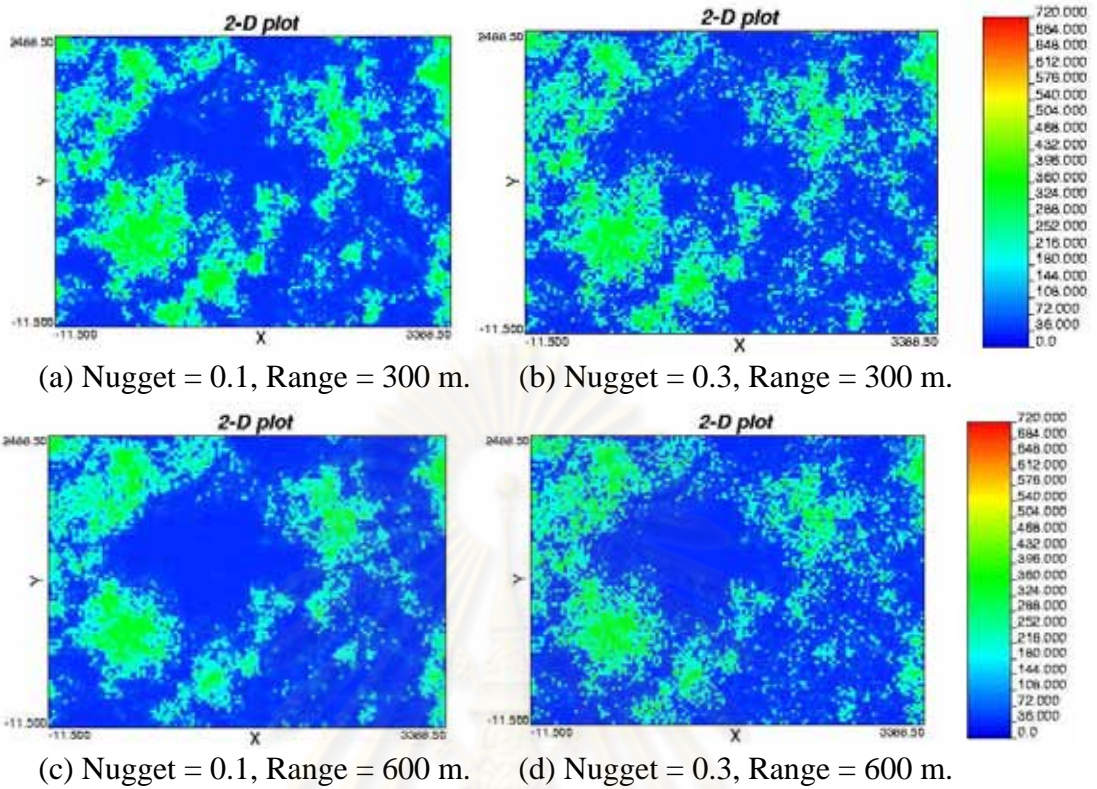


Figure 4.33 : SGS of the model V varied nuggets and ranges at the seed number of 5027296

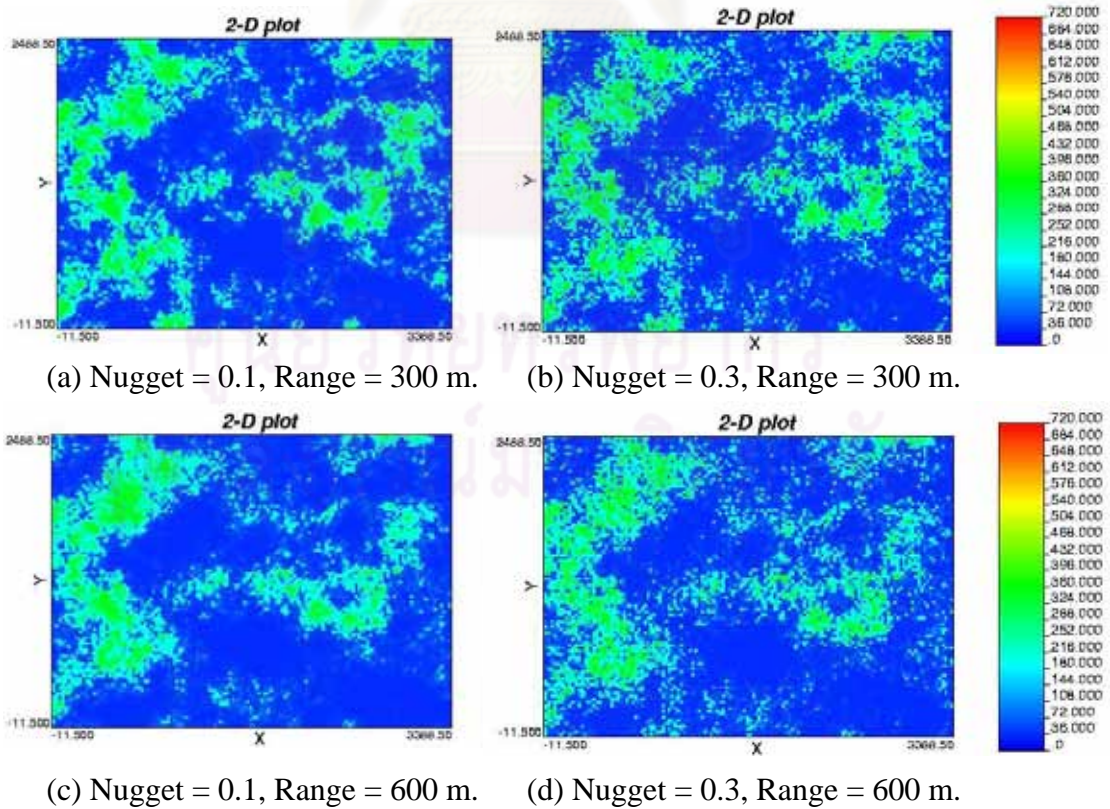


Figure 4.34 : SGS of the model V varied nuggets and ranges at the seed number of 7301294

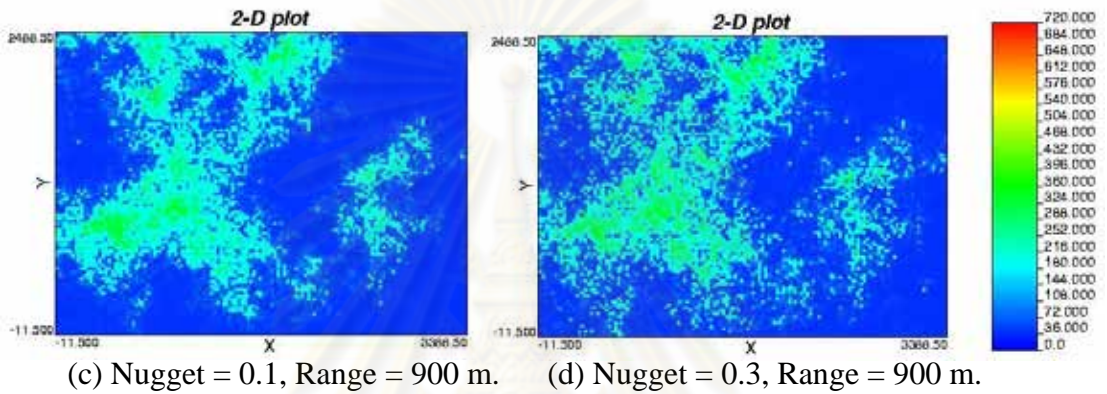
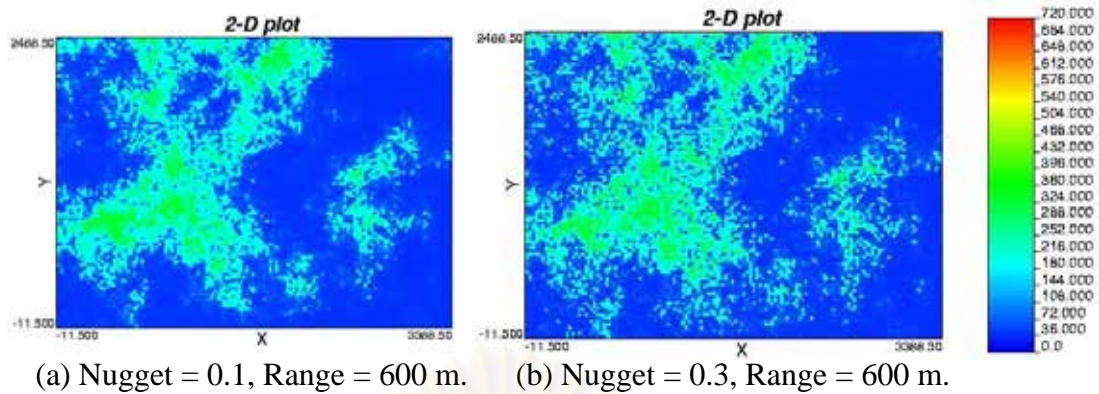


Figure 4.35 : SGS of the model VI varied nuggets and ranges at the seed number of 1042094

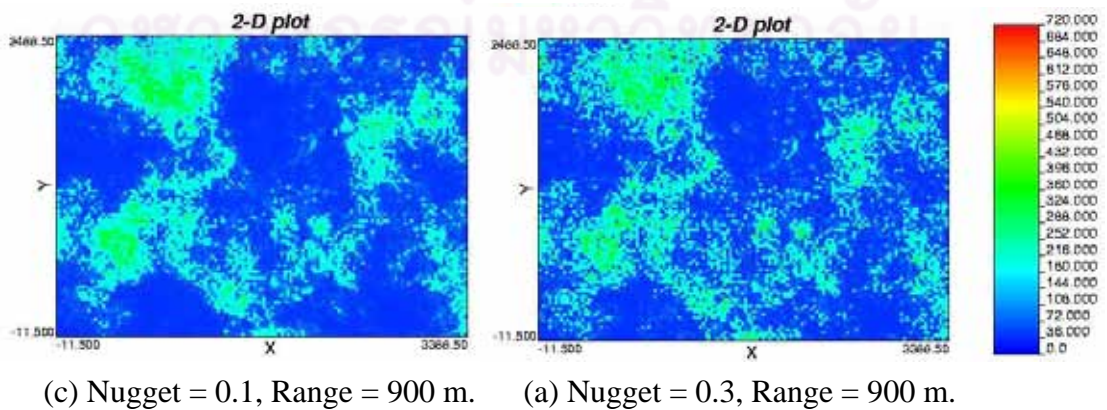
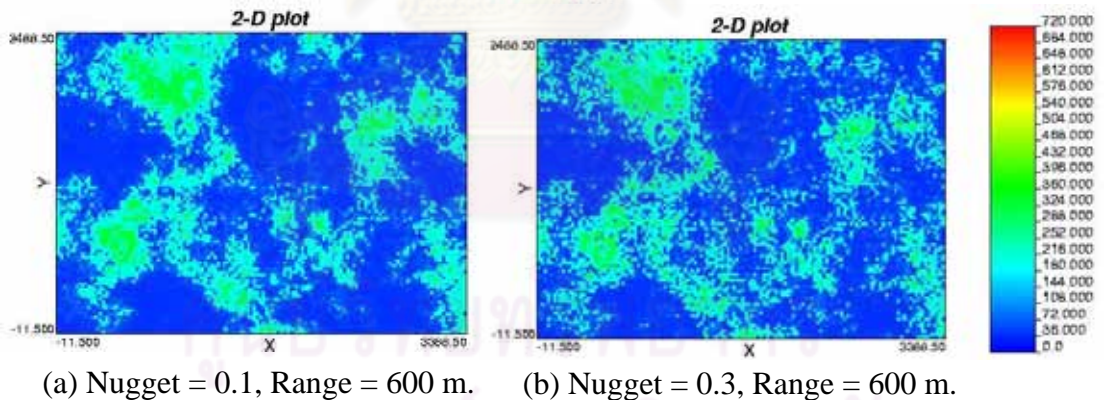
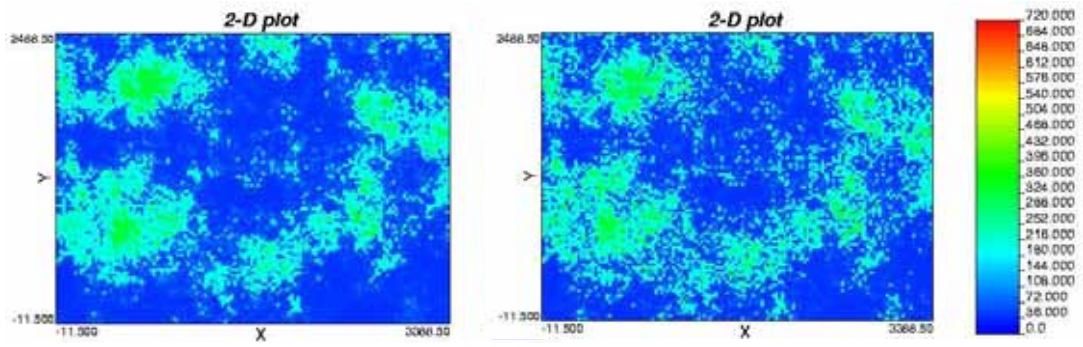
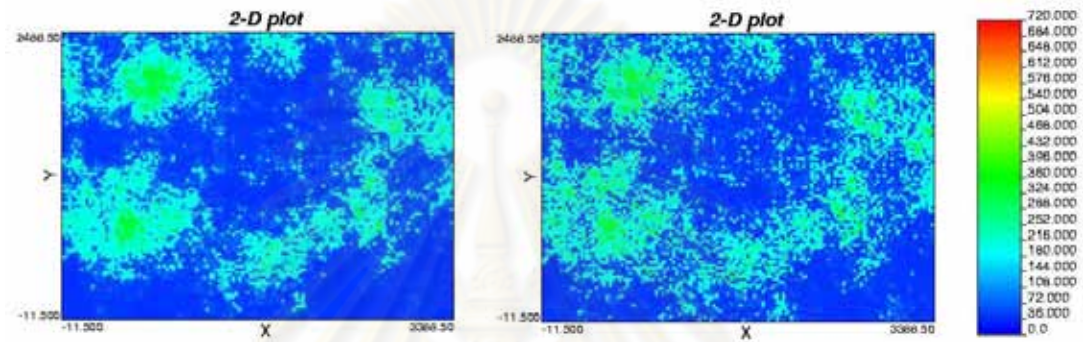


Figure 4.36 : SGS of the model VI varied nuggets and ranges at the seed number of 6160440

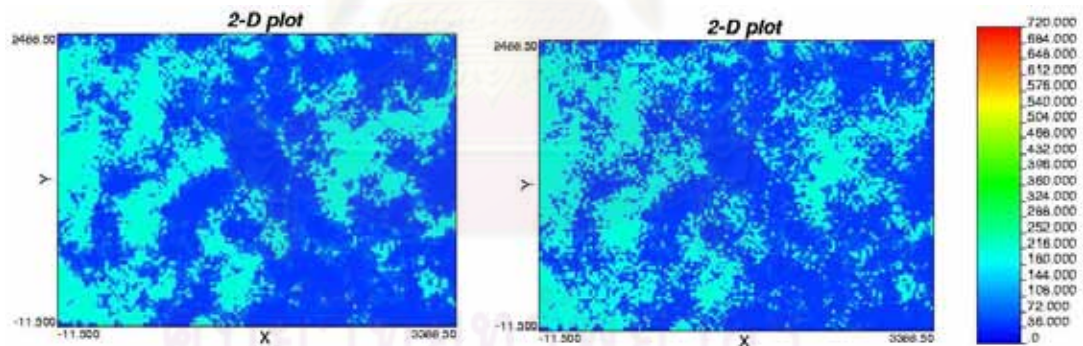


(a) Nugget = 0.1, Range = 600 m. (b) Nugget = 0.3, Range = 600 m.

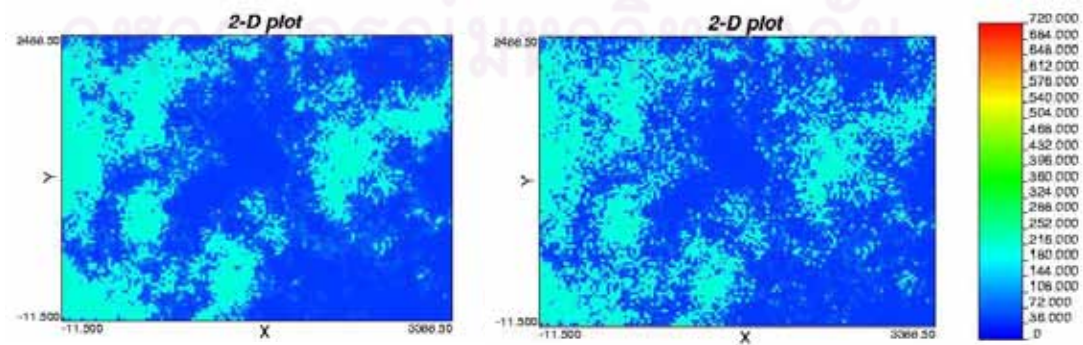


(c) Nugget = 0.1, Range = 900 m. (d) Nugget = 0.3, Range = 900 m.

Figure 4.37 : SGS of the model VI varied nuggets and ranges at the seed number of 8275380

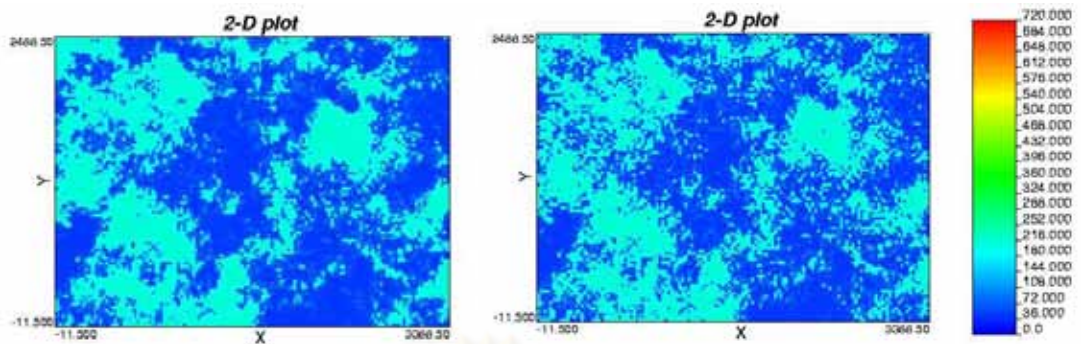


(a) Nugget = 0.1, Range = 300 m. (b) Nugget = 0.3, Range = 300 m.

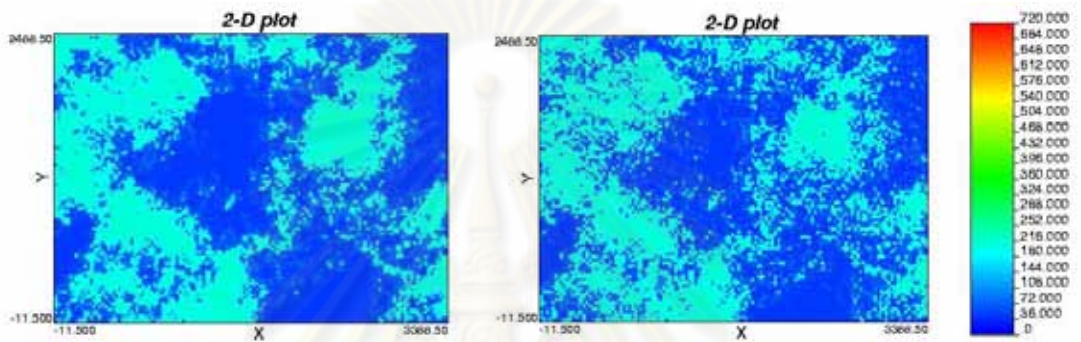


(c) Nugget = 0.1, Range = 600 m. (d) Nugget = 0.3, Range = 600 m.

Figure 4.38 : SGS of the model VII varied nuggets and ranges at the seed number of 307057

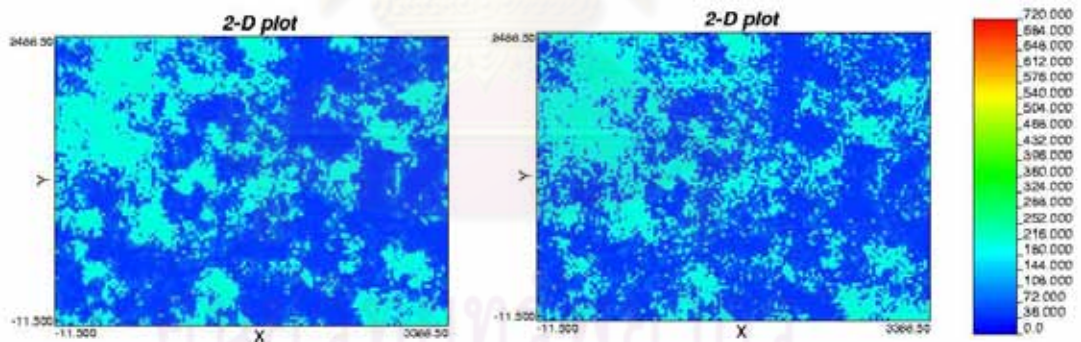


(a) Nugget = 0.1, Range = 300 m. (b) Nugget = 0.3, Range = 300 m

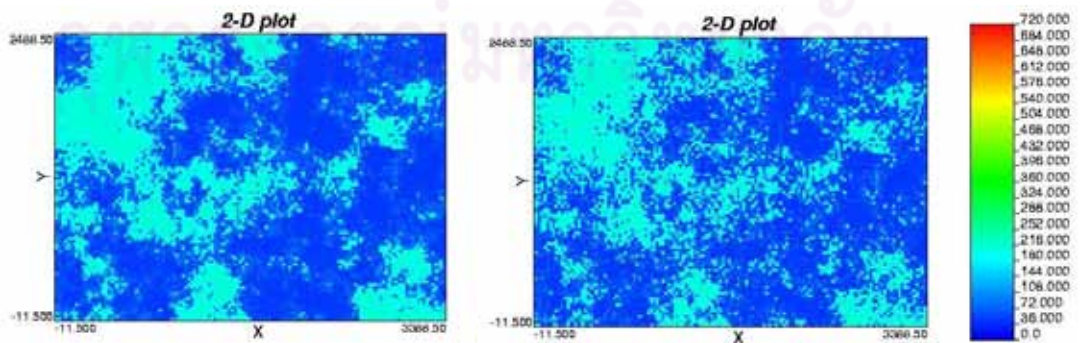


(c) Nugget = 0.1, Range = 600 m. (d) Nugget = 0.3, Range = 600 m.

Figure 4.39 : SGS of the model VII varied nuggets and ranges at the seed number of 5280856



(a) Nugget = 0.1, Range = 300 m. (b) Nugget = 0.3, Range = 300 m.



(c) Nugget = 0.1, Range = 600 m. (d) Nugget = 0.3, Range = 600 m.

Figure 4.40 : SGS of the model 7 varied nuggets and ranges at the seed number of 8326199

As shown from Figures 4.15 to 4.40, to assess the uncertainties, random number seed of 3 values are generated into SGS in which all simulated models use the number of grids of 13,600 except the Base case and model I are given random number seed of 4 values due to its wide range of standard deviation. As described earlier, nugget effects of 0.10 and 0.30 and ranges of 300-600 m., 500-800 m. and 600-900 m. are obtained to approach the spatial uncertainty. Thus, by varying all the parameters, 104 realizations are created. Table 4.4 summarizes statistical parameters of all realizations.



Table 4.4 : SGS results of eight models by varying parameters

Base case with 109 wells (Prior to simulation, $V_{DP} = 0.853$, mean = 101.74 md., and SD = 169.94)																
Seed no.	1299460				4211847				5209254				1062367			
Model type	Spherical				Spherical				Spherical				Spherical			
Distance (m.)	300	300	600	600	300	300	600	600	300	300	600	600	300	300	600	600
Nugget value (%)	10	30	10	30	10	30	10	30	10	30	10	30	10	30	10	30
V_{DP}	0.875	0.88	0.86	0.87	0.867	0.872	0.846	0.856	0.879	0.885	0.862	0.873	0.876	0.879	0.855	0.864
Mean	99.243	102.64	91.671	97.07	107.64	111.8	99.641	104.84	114.96	118.55	100.68	107.96	109.35	111.19	97.138	102.09
Std.dev.	175.8	180.94	159.02	169.5	178.77	185.18	164.23	173.93	186.46	194	165.81	179.57	182.05	186.06	159.93	171.4
Coef. of var	1.7714	1.7628	1.7346	1.7462	1.6608	1.6563	1.6482	1.6591	1.622	1.6364	1.647	1.6633	1.6648	1.6734	1.6464	1.6788
Maximum	720	720	720	720	720	720	720	720	720	720	720	720	720	720	720	720
Upper quartile	72.41	75.553	69.592	72.927	81.888	82.715	79.15	81.041	148.89	153.11	80.683	82.283	81.813	82.653	79.183	79.092
Median	28.309	26.611	30.788	30.296	31.127	31.155	31.403	31.163	31.035	31.012	31.02	31.002	31.008	30.992	31.032	31.009
Lower quartile	4.6879	4.5515	4.9038	4.7786	4.9916	4.9263	9.0744	8.4897	4.8685	4.7295	4.9287	4.8808	4.8503	4.8279	5.0528	4.9457
Minimum	0.27	0.27	0.27	0.27	0.27	0.27	0.27	0.27	0.27	0.27	0.27	0.27	0.27	0.27	0.27	0.27
Model I with 95 wells (Prior to simulation, $V_{DP} = 0.779$, mean = 101.65 md., and SD = 155.00)																
Seed no.	153567				896078				4773049				5237802			
Model type	Spherical				Spherical				Spherical				Spherical			
Distance (m.)	600	600	900	900	600	600	900	900	600	600	900	900	600	600	900	900
Nugget value (%)	10	30	10	30	10	30	10	30	10	30	10	30	10	30	10	30
V_{DP}	0.798	0.804	0.783	0.794	0.773	0.781	0.754	0.766	0.813	0.819	0.797	0.808	0.786	0.795	0.768	0.782
Mean	104.25	113.45	95.908	107.39	86.868	92.976	79.042	86.734	107.17	113.3	98.102	106.42	97.441	104.54	87.891	97.113
Std.dev.	158	170.92	145.23	162.68	134.29	145.24	121.58	135.54	162.22	171.68	148.37	162.36	146.81	157.08	131.71	146.24
Coef. of var	1.5156	1.5067	1.5143	1.5148	1.5459	1.5621	1.5382	1.5628	1.5137	1.5153	1.5124	1.5257	1.5067	1.5026	1.4986	1.5059
Maximum	630.27	630.27	630.27	630.27	630.27	630.27	630.27	630.27	630.27	630.27	630.27	630.27	630.27	630.27	630.27	630.27
Upper quartile	127.52	176.38	81.88	133	77.538	77.671	69.056	74.878	173.41	183.89	110.59	147.95	88.587	135.99	79.209	82.412
Median	33.992	34.23	33.918	34.216	32.468	33.53	32.061	33.427	32.031	32.389	31.684	33.113	33.907	34.212	33.856	34.216
Lower quartile	10.165	10.186	10.245	10.248	10.232	10.246	10.3	10.294	9.5808	9.5734	9.8599	9.8439	10.18	10.206	10.256	10.277
Minimum	1.34	1.34	1.34	1.34	1.34	1.34	1.34	1.34	1.34	1.34	1.34	1.34	1.34	1.34	1.34	1.34

ศูนย์วิทยทรัพยากร
จุฬาลงกรณ์มหาวิทยาลัย

Table 4.4 : SGS results of eight models by varying parameters (continued)

Model II with 82 wells (Prior to simulation, $V_{DP} = 0.713$, mean = 102.00 md., and SD = 140.67)												
Seed no.	3782386				4574483				6768113			
Model type	Spherical				Spherical				Spherical			
Distance (m.)	600	600	900	900	600	600	900	900	600	600	900	900
Nugget value (%)	10	30	10	30	10	30	10	30	10	30	10	30
V_{DP}	0.7	0.709	0.682	0.696	0.703	0.719	0.678	0.704	0.691	0.709	0.672	0.697
Mean	107.28	114.81	97.839	107.54	92.09	98.669	82.445	92.071	94.692	105.26	87.257	99.944
Std.dev.	143.06	149.94	130.48	140.58	122.17	134.81	107.85	125.29	123.05	137.84	111.37	129.89
Coef. of var	1.3335	1.306	1.3337	1.3072	1.3266	1.3663	1.3081	1.3608	1.2995	1.3095	1.2764	1.2996
Maximum	602.47	602.47	602.47	602.47	602.47	602.47	602.47	602.47	602.47	602.47	602.47	602.47
Upper quartile	179.98	190.55	90.943	181.47	104.4	129.12	78.613	82.3	119.81	181.98	81.855	157.46
Median	40.4	40.841	40.088	40.688	38.893	39.005	38.612	38.72	39.927	40.401	39.838	40.352
Lower quartile	23.471	23.617	23.57	23.822	18.464	18.232	18.872	18.565	19.477	19.524	21.259	21.004
Minimum	4.9	4.9	4.9	4.9	4.9	4.9	4.9	4.9	4.9	4.9	4.9	4.9
Model III with 70 wells (Prior to simulation, $V_{DP} = 0.656$, mean = 101.28 md., and SD = 122.20)												
Seed no.	218583				7497676				2904965			
Model type	Gaussain				Gaussain				Gaussain			
Distance (m.)	600	600	900	900	600	600	900	900	600	600	900	900
Nugget value (%)	10	30	10	30	10	30	10	30	10	30	10	30
V_{DP}	0.654	0.659	0.624	0.639	0.663	0.675	0.63	0.656	0.651	0.654	0.62	0.635
Mean	102.29	114.74	88.73	106.65	100.99	111.3	87.332	102.99	96.258	104.9	83.176	98.435
Std.dev.	117.01	126.86	100.14	117.06	120.73	129.6	105.25	118.89	117.01	125.77	100.06	116.46
Coef. of var	1.1439	1.1056	1.1286	1.0977	1.1954	1.1644	1.2051	1.1544	1.2156	1.1989	1.203	1.1831
Maximum	565.05	565.05	565.05	565.05	565.05	565.05	565.05	565.05	565.05	565.05	565.05	565.05
Upper quartile	185	194.5	83.229	189.33	183.35	194.27	81.969	184.69	154.63	184.07	79.442	151.07
Median	41.061	45.339	40.889	43.124	40.884	41.074	40.7	41.065	40.005	40.912	39.811	40.92
Lower quartile	30.854	31.028	30.914	31.041	27.275	30.53	30.218	30.946	27.167	30.773	29.073	31.001
Minimum	10.21	10.21	10.21	10.21	10.21	10.21	10.21	10.21	10.21	10.21	10.21	10.21
Model IV with 58 wells (Prior to simulation, $V_{DP} = 0.590$, mean = 101.80 md., and SD = 102.05)												
Seed no.	6259246				9451304				2895849			
Model type	Spherical				Spherical				Spherical			
Distance (m.)	500	500	800	800	500	500	800	800	500	500	800	800
Nugget value (%)	10	30	10	30	10	30	10	30	10	30	10	30
V_{DP}	0.586	0.594	0.562	0.579	0.587	0.597	0.573	0.588	0.572	0.584	0.562	0.578
Mean	94.188	96.646	85.63	90.673	103.27	108.66	94.306	102.43	95.214	100.21	89.951	96.891
Std.dev.	98.552	102.06	90.497	96.336	101.09	106.29	94.062	101.4	96.333	100.83	91.782	97.611
Coef. of var	1.0463	1.056	1.0568	1.0625	0.9789	0.9782	0.9974	0.99	1.0118	1.0062	1.0204	1.0074
Maximum	403.24	403.24	403.24	403.24	403.24	403.24	403.24	403.24	403.24	403.24	403.24	403.24
Upper quartile	146.96	171.98	81.178	98.508	189.15	194.33	162.23	187.94	154.34	183.59	91.567	179.42
Median	41.056	41.025	40.918	40.929	48.62	51.82	42.036	44.947	42.065	43.372	41.069	42.068
Lower quartile	31.153	31.051	31.188	31.084	33.772	33.785	32.567	33.472	33.568	33.085	32.77	32.532
Minimum	18.91	18.91	18.91	18.91	18.91	18.91	18.91	18.91	18.91	18.91	18.91	18.91

Table 4.4 : SGS results of eight models by varying parameters (continued)

Model V with 49 wells (Prior to simulation, $V_{DP} = 0.551$, mean = 101.82 md., and SD = 91.17)												
Seed no.	69069				7301294				5027296			
Model type	Spherical				Spherical				Spherical			
Distance (m.)	300	300	600	600	300	300	600	600	300	300	600	600
Nugget value (%)	10	30	10	30	10	30	10	30	10	30	10	30
V_{DP}	0.568	0.571	0.551	0.559	0.554	0.559	0.532	0.544	0.562	0.566	0.539	0.55
Mean	108.72	110.49	98.335	102.16	102.04	104.23	91.601	96.55	107.69	108.57	96.244	100.49
Std.dev.	98.631	100.18	89.963	93.849	92.317	94.365	83.655	88.38	96.382	97.89	86.441	91.176
Coef. of var	0.9072	0.9067	0.9149	0.9186	0.9047	0.9053	0.9133	0.9154	0.895	0.9017	0.8981	0.9073
Maximum	339.4	339.4	339.4	339.4	339.4	339.4	339.4	339.4	339.4	339.4	339.4	339.4
Upper quartile	194.35	194.77	183.93	190.29	189.15	192.69	143.69	181.31	194.36	194.44	181.4	187.31
Median	54.28	54.971	49.067	51.306	52.494	52.675	44.808	47.864	54.156	53.416	51.065	51.823
Lower quartile	36.775	36.781	34.148	34.902	36.842	36.78	36.64	36.743	37.521	36.934	37.201	36.925
Minimum	30.43	30.43	30.43	30.43	30.43	30.43	30.43	30.43	30.43	30.43	30.43	30.43
Model VI with 40 wells (Prior to simulation, $V_{DP} = 0.520$, mean = 102.51 md., and SD = 81.05)												
Seed no.	1042094				6160440				8275380			
Model type	Spherical				Spherical				Spherical			
Distance (m.)	600	600	900	900	600	600	900	900	600	600	900	900
Nugget value (%)	10	30	10	30	10	30	10	30	10	30	10	30
V_{DP}	0.524	0.531	0.506	0.519	0.508	0.516	0.493	0.507	0.499	0.515	0.489	0.507
Mean	98.019	102.02	91.746	97.01	102.32	104.79	97.805	101.82	99.798	107.36	97.524	105.09
Std.dev.	79.749	84.151	73.248	79.334	78.108	81.011	73.296	78.031	75.465	80.911	71.613	77.87
Coef. of var	0.8136	0.8249	0.7984	0.8178	0.7633	0.7731	0.7494	0.7663	0.7562	0.7536	0.7343	0.741
Maximum	320.2	320.2	320.2	320.2	320.2	320.2	320.2	320.2	320.2	320.2	320.2	320.2
Upper quartile	187.24	192	174.04	184.47	188.85	193.49	182.66	188.1	185.14	194.21	182.55	192.86
Median	55.776	57.159	53.195	55.401	62.738	62.853	61.677	62.364	62.335	64.739	62.737	64.774
Lower quartile	38.601	39.149	38.657	39.212	40.878	40.863	40.92	40.89	40.918	40.92	40.989	40.972
Minimum	33.5	33.5	33.5	33.5	33.5	33.5	33.5	33.5	33.5	33.5	33.5	33.5
Model VII with 31 wells (Prior to simulation, $V_{DP} = 0.482$, mean = 101.66 md., and SD = 67.12)												
Seed no.	307057				5280856				8326199			
Model type	Spherical				Spherical				Spherical			
Distance (m.)	300	300	600	600	300	300	600	600	300	300	600	600
Nugget value (%)	10	30	10	30	10	30	10	30	10	30	10	30
V_{DP}	0.483	0.484	0.478	0.48	0.485	0.487	0.482	0.484	0.476	0.479	0.468	0.474
Mean	101.65	101.47	99.113	99.479	113.35	114.77	114.77	114.92	101.69	102.34	102.87	102.91
Std.dev.	68.154	68.332	66.85	67.284	70.185	70.555	69.614	69.935	66.946	67.601	66.05	66.879
Coef. of var	0.6705	0.6734	0.6745	0.6764	0.6192	0.6148	0.6066	0.6085	0.6583	0.6605	0.6421	0.6499
Maximum	208.78	208.78	208.78	208.78	208.78	208.78	208.78	208.78	208.78	208.78	208.78	208.78
Upper quartile	193.26	193.62	187.8	189.97	195.94	196.19	195.53	195.9	190.76	192.27	189.66	190.38
Median	64.813	64.645	64.018	63.858	77.632	77.706	78.479	78.286	67.604	67.431	70.04	68.994
Lower quartile	41.066	41.061	41.068	41.06	46.502	46.527	50.033	48.574	41.9	41.476	45.479	43.174
Minimum	38.72	38.72	38.72	38.72	38.72	38.72	38.72	38.72	38.72	38.72	38.72	38.72

As can be seen from Table 4.4, the results show that heterogeneity largely depends upon standard deviation (SD). For example, the simulated base case values give the highest V_{DP} in the range of 0.86 to 0.885 and SD in the range of 159 to 194. While the simulated model VII values show the lowest V_{DP} in the range of 0.478 to 0.487 and SD in the range of 99 to 115. As a result, V_{DP} is mostly characterized by standard deviation. In this study, we deal with a lot of uncertainties by varying random number seed, range and nugget. The comparison of these uncertainties will be explained.

In order to get multiple realizations, random number seeds are used for the study. It was found that the base case still give the highest V_{DP} and SD. On the contrary, model VII gives the lowest V_{DP} and SD. Comparing with the raw data of each model, we observed that all simulated statistical data give wide range of variation. At higher V_{DP} , statistical results give a wide range of all parameters. In other words, the higher variation it has, the more uncertainty will be identified. Furthermore, from the simulated base case data to simulated model VII data, it was found that V_{DP} values decreased gradually from 0.885 to 0.478.

Normally, the size for searching nearby data is relatively difficult to determine. If it is too small, we may not have sufficient samples within the neighborhood to estimate a representative value. If it is too large, we might select samples outside the local stationary region. To minimize the effect of outliers or extreme data, varying ranges are used. As range is decreased, heterogeneity will be increased. In addition, the continuity increases as the range increases. This is because the proximity to the estimated location and data redundancy becomes important.

The nugget effect indicates a total lack of information with respect to spatial relationship. As the nugget effect is increased, the reservoir tends to have a higher value of heterogeneity. Moreover, as the mean and CV increase, SD also increases.

CHAPTER V

RESERVOIR PERFORMANCE PREDICTION

This chapter begins with explanations for preparing data for reservoir modeling, assumptions used in the reservoir simulation and then moves on to study relationships of all results from performance predictions such as V_{DP} and recovery factor at the time of abandonment for both homogeneous and heterogeneity reservoirs.

5.1 Performance of Reservoir Having Different Levels of Heterogeneity

In order to assess reservoir performance at different degrees of heterogeneity, reservoir simulation is conducted. ECLISPE 100, a black-oil simulator, is used to evaluate the performance with the same grid dimensions and block sizes as geostatistics modeling in which grid dimensions are 136 x 100 x 1 blocks and block sizes are equal to 25 x 25 x 7 m. in the x, y and z directions, respectively. After 104 realizations were created using SGS, all data needed to be transferred into ECLISPE. Typically, porosity is one of the important parameters in reservoir modeling. Therefore, as original porosity data from 109 wells were obtained and shown in Table 4.1, we calculated unsampled porosity based on correlation between permeability and porosity for the given field. The correlation that we use to determine porosity value from simulated permeability value was shown in Equation 4.1.

After porosity had been calculated, reservoir models were created. Figure 5.1 shows example of reservoir model with 32 producers.

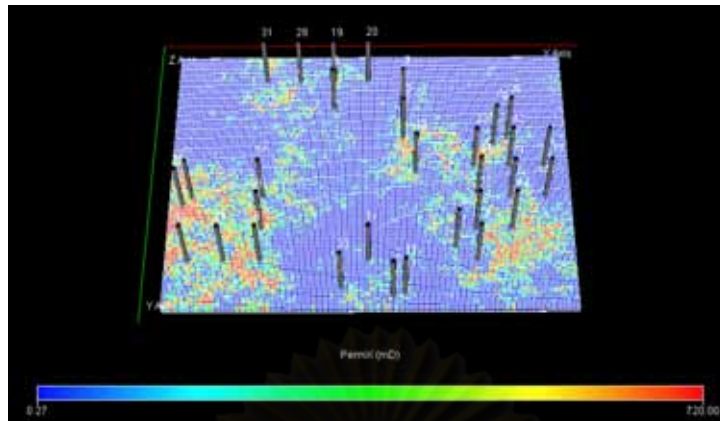


Figure 5.1 : Reservoir model with 32 producers

As sketched in Figure 5.1, the locations of the 32 producers which were the same as the number of wells and well locations of Model VII were fixed to use with all other reservoir models so that the uncertainty in reservoir performance can be easily defined. The reason to select the same number of wells and well locations as in model VII is that we cannot choose at other simulated locations where the permeability is always changed by SGS algorithm. As a result, selecting other simulated locations may cause erratic comparison in the recovery factor. Although other models have more producers than the 32 wells, we assume that all other wells are shut in so that the comparison can be easily investigated.

In this study, homogeneous permeability reservoir which has a mean of 101.74 md. is used to compare with the uncertainties of 104 realizations. Only the primary drive mechanism is studied as the stage of production in which the maximum and minimum production rates of all wells are controlled at 250 stb/day and 5 stb/day, respectively. The minimum reservoir pressure is set at 500 psia, and the pump is assumed to be used with this depletion drive. All other input data in the ECLISPE program are shown in Appendix B.

In this study, we compare the recovery factor at two conditions: (1) at the time to abandonment of homogeneous reservoir and (2) at the time to abandonment of the actual heterogeneous reservoirs.

In the first criteria, the comparison between recovery factor for different V_{DP} 's based on time to abandonment of homogeneous reservoir was performed. To do so, the homogeneous model is first simulated until all the wells are shut in so that the

time to abandonment of homogeneous reservoir can be defined. In this case, all the wells were shut in at the days of 5,160. This time will be used as the maximum producing time of all other models so that the different degrees of heterogeneity schemes can be compared. The schematic comparison of recovery efficiency for different V_{DP} 's at this period is sketched in Figure 5.2.

In the second criteria, the comparison between recovery factor for different V_{DP} 's is performed when all the wells in each of the heterogeneity reservoir had been shut in. Figure 5.3 shows the relationship between oil recovery factor and V_{DP} at abandonment. Moreover, all the results of the second condition are shown in Table B1.



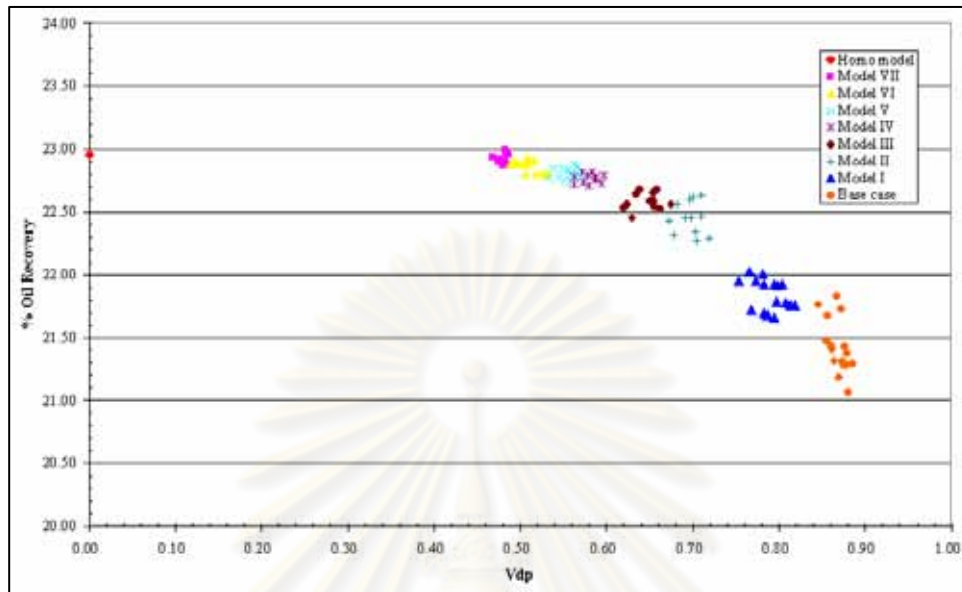


Figure 5.2 : Relationship between oil recovery factor and V_{DP} at 5,160 days

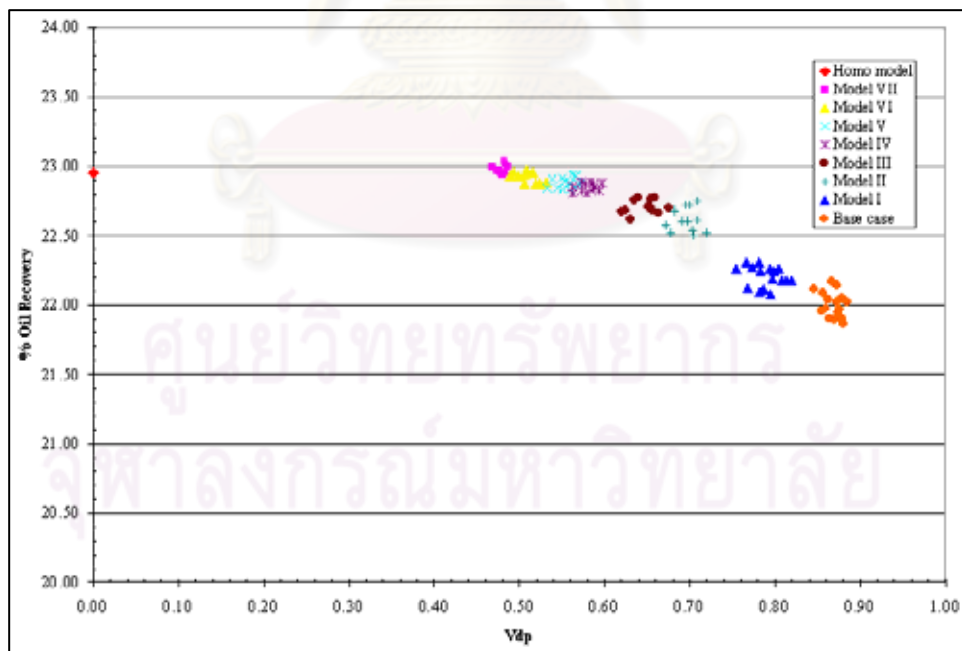


Figure 5.3 : Relationship between oil recovery factor and V_{DP} at abandonment

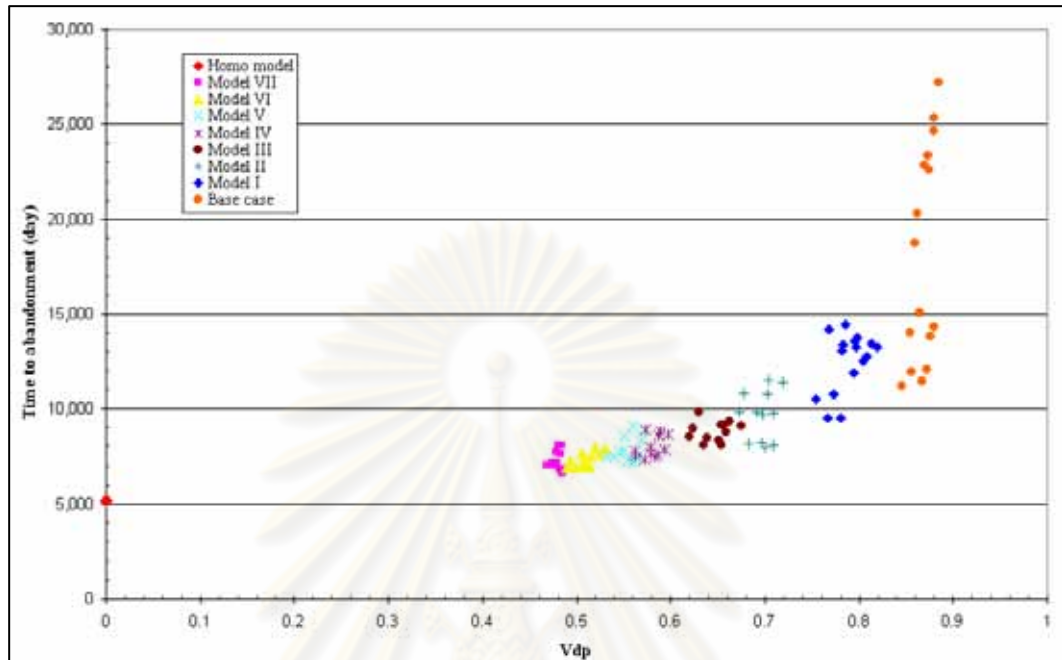


Figure 5.4 : Relationship between time to abandonment and V_{DP}

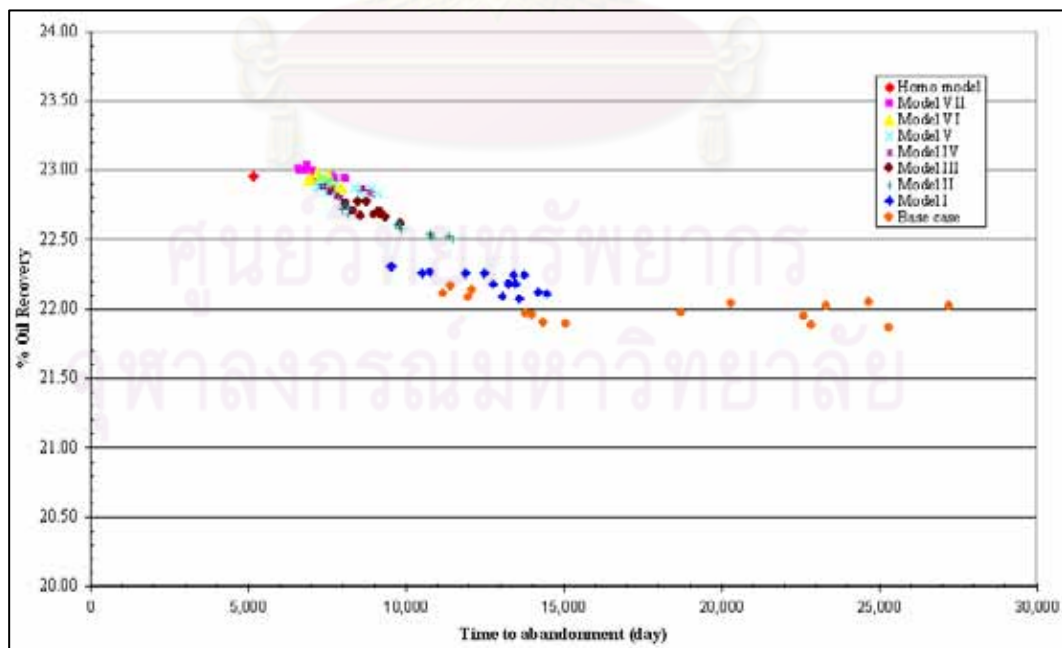


Figure 5.5 : Relationship between oil recovery and time to abandonment

Table 5.1 : Statistical results of oil recovery and reservoir pressure of different models

Model name	Nugget (%) and range (m.)	% Oil recovery at the days of 5,160		% Oil recovery at abandonment		Reservoir pressure (psi) at the days of 5,160		Reservoir pressure (psi) at abandonment	
		mean	SD	mean	SD	mean	SD	mean	SD
Base case	0.1_300	21.48	0.24	22.03	0.10	578	18	509	1
	0.3_300	21.34	0.28	21.98	0.12	588	18	509	1
	0.1_600	21.52	0.16	22.02	0.07	573	13	509	1
	0.3_600	21.37	0.21	21.97	0.10	585	15	509	0
Model I	0.1_600	21.83	0.13	22.20	0.07	556	8	508	1
	0.3_600	21.84	0.16	22.20	0.10	555	7	508	0
	0.1_900	21.85	0.11	22.20	0.06	554	6	508	1
	0.3_900	21.86	0.15	22.21	0.09	554	7	508	1
Model II	0.1_600	22.47	0.14	22.62	0.09	528	7	507	0
	0.3_600	22.46	0.17	22.63	0.11	530	9	507	0
	0.1_900	22.44	0.12	22.60	0.08	529	6	507	1
	0.3_900	22.44	0.17	22.61	0.11	531	8	507	0
Model III	0.1_600	22.56	0.04	22.69	0.03	524	2	507	0
	0.3_600	22.63	0.06	22.74	0.04	524	2	507	0
	0.1_900	22.51	0.06	22.66	0.04	527	3	508	1
	0.3_900	22.62	0.07	22.74	0.05	524	3	507	0
Model IV	0.1_500	22.78	0.03	22.86	0.02	518	1	506	1
	0.3_500	22.78	0.05	22.86	0.04	519	1	506	1
	0.1_800	22.75	0.03	22.83	0.02	519	1	506	1
	0.3_800	22.75	0.04	22.84	0.03	519	1	507	1
Model V	0.1_300	22.83	0.05	22.90	0.04	517	1	507	1
	0.3_300	22.82	0.04	22.89	0.03	518	1	507	1
	0.1_600	22.79	0.05	22.86	0.04	517	1	507	1
	0.3_600	22.78	0.05	22.86	0.04	518	1	507	1
Model VI	0.1_600	22.87	0.06	22.93	0.05	516	2	506	0
	0.3_600	22.87	0.06	22.93	0.04	516	3	506	1
	0.1_900	22.86	0.05	22.92	0.05	516	2	506	1
	0.3_900	22.86	0.05	22.92	0.04	516	3	506	1
Model VII	0.1_300	22.92	0.03	22.98	0.03	515	1	506	1
	0.3_300	22.91	0.03	22.97	0.03	516	1	507	0
	0.1_600	22.94	0.05	22.99	0.05	515	1	507	0
	0.3_600	22.91	0.05	22.97	0.04	514	3	507	0

In this study, we will quantify and mention only the effect of heterogeneity on the recovery at the days of 5,160 and abandonment. As seen from Figures 5.2 and 5.3, a high V_{DP} results in a slightly low recovery factor. That is to say that the reservoir which has a low continuity will obstruct the fluid flow into the well more than the one which has a high continuity. In other words, the fluid will take more time to flow into the well than the one with higher continuity. For example, as shown in Figure 5.4, at V_{DP} of 0, the time to abandonment was 5,160 days or 14.1 years comparing with V_{DP} of 0.879 spent 24,660 days or 67.6 years for the time to abandonment. As a result, the more heterogeneity the reservoir is, the more time will be spent to recover the fluid as shown in Figure 5.5. For example, at the time to abandonment of the homogeneous reservoir, $V_{DP} = 0$, of 5,160 days, oil recovery factor was 22.95% compared with the time to abandonment of the extreme large heterogeneity reservoir, $V_{DP} = 0.885$, of 24,660 days oil recovery factor was 22.02%. The difference of 0.93% could also tell that the higher heterogeneity the reservoir is, the more reduction and obstruction of flow efficiency into the wellbore will be. However, the heterogeneity has a small effect on ultimate recovery but tremendous effect on time to abandonment. Table B1 gives the comparison of oil recovery at the different degrees of heterogeneities. When the range increases, V_{DP} decreases while the recovery factor slightly increases. When the nugget increases, V_{DP} increases while the recovery factor slightly decreases.

As we varied the random number of seeds to get different maps in geostatistical modeling, statistical analysis is used to determine the variation of each model. As shown in Table 5.1, we calculated the mean and SD of realizations at the same nugget and range values so that uncertainties of each simulated model can be compared. In this case, changing nugget had slightly more effect on the recovery factor than range.

Table 5.2 : Comparison of statistical results of oil recovery factor and V_{DP} of each model.

Model name	V_{DP} Prior to simulation	V_{DP} of simulated models				% Oil recovery at the days of 5,160			% Oil recovery at abandonment		
		mean	max	min	SD	max	min	SD	max	min	SD
Base case	0.853	0.869	0.885	0.846	0.011	21.831	21.066	0.218	22.167	21.867	0.092
Model I	0.779	0.789	0.819	0.754	0.018	22.024	21.658	0.122	22.306	22.073	0.075
Model II	0.713	0.697	0.719	0.672	0.014	22.635	22.273	0.129	22.749	22.506	0.086
Model III	0.656	0.647	0.675	0.620	0.017	22.680	22.452	0.068	22.776	22.615	0.050
Model IV	0.590	0.580	0.597	0.562	0.011	22.818	22.706	0.038	22.888	22.802	0.030
Model V	0.551	0.555	0.571	0.532	0.012	22.884	22.740	0.047	22.945	22.830	0.039
Model VI	0.520	0.510	0.531	0.489	0.012	22.929	22.800	0.048	22.981	22.872	0.039
Model VII	0.482	0.480	0.487	0.468	0.005	22.992	22.873	0.038	23.038	22.934	0.038

Generally, if V_{DP} is less than 0.5, it should be simulated as a homogeneous reservoir. This is because it has a small variation which does not have much effect on the recovery factor. In this study, the lowest V_{DP} value is 0.468 due to a lack of information. We can illustrate that at lower V_{DP} , there is less effect on the recovery factor. As seen in Table 5.2, at the lowest average V_{DP} of 0.480, the standard deviations of the recovery factors at 5,160 days and abandonment have the lowest value. Comparing with the highest average V_{DP} of 0.869, the standard deviations of the recovery factors at 5,160 days and abandonment have the highest value. Again, the model that has a high V_{DP} will give a slightly low recovery factor because it is more difficult for the fluid to flow into the well bore.

Figures 5.6, 5.7 and 5.8 compare the production profiles of the homogeneous model and other eight main models where each main model was the realization which has the highest V_{DP} as shown in Table B1 so that the comparison can be easily defined. For example, the base case which has the maximum V_{DP} of 0.885 is used from the realization with seed number of 5209294, nugget effect of 0.3 and range of 300 m., and all other seven models are obtained with the same method. Figure 5.6 shows that the homogeneous model will produce at a constant rate for longer than other models. It seems that the higher heterogeneity, the shorter duration of constant flow rate will be. This is because with higher heterogeneity the fluid will be more difficult to flow from the reservoir to the well bore than with the lower heterogeneity. Figure 5.7 shows the relationship between reservoir pressure and time for different models. It was found that the higher heterogeneity, the slower the pressure will drop

and the longer the production time. Moreover, as the heterogeneity increases, the reservoir pressure will drop faster because it requires more pressure loss to flow the same amount of fluid into the well. When the gas-oil ratio starts to decline, the reservoir pressure of the homogeneous model will drop faster than the reservoir pressure of the heterogeneous models because the higher heterogeneity, the longer time to produce the fluid. Thus, the reservoir still has pressure left in the system. Figure 5.8 illustrates that the lower heterogeneity, the higher the cumulative oil production will be. Although the global permeability mean of all the models is controlled as close as possible to the global permeability mean of the base case of 101.74 md., the global porosity mean of each model obtained from Equation 4.1 does not have the same value due to lognormal distribution of permeability. The higher the heterogeneity, the lower global porosity mean will be. For example, the homogeneous model which has the global permeability mean of 101.74 md. has the global porosity mean of 0.2246 and the base case which has the global permeability mean of 101.74 has the global porosity mean of 0.1897. Therefore, the homogeneous model would give the maximum cumulative oil production. On the other hand, the most heterogeneous case would give the minimum cumulative oil production. As a result, the higher the heterogeneity is, the lower the cumulative oil production and the longer the time to produce fluid will be.

As stated before, the global permeability means of all the models are quite the same but all the models give the different global porosity mean due to the lognormal permeability distribution. Therefore, hydrocarbon pore volumes (HPV) for different reservoir models shown in Figure 5.9 are also slightly different as they depend upon the porosity. In this study, the higher heterogeneity is, the lower global porosity mean and the lower HPV will be.

As the number of producers is reduced from 32 wells to 15 wells which is illustrated in Figure 5.10, oil production rate shown in Figures 5.11 and 5.12 will constantly maintain longer than oil production rate with 32 producers and the effect on reservoir pressure between the homogeneous and heterogeneous reservoirs which is shown in Figure 5.13 is similar to the reservoir pressure with 32 producers as explained before in Figure 5.7 except the time will be different. That is to say that the reservoir pressure of all the models with 15 producers will spend a longer time to

reach abandonment than that with 32 producers. In other words, the higher production is, the faster reservoir pressure will be decreased as shown in Figure 5.14.

Figures 5.15, 5.16 and 5.17 illustrate the comparison of cumulative oil production and time, and oil recovery and time. It was found that reducing the producers from 32 wells to 15 wells would have a slight difference on both cumulative oil production and oil recovery. That is, using 15 producers would increase a little bit both the cumulative oil production and oil recovery. In other words, with 32 producers at below the bubble point, gas which forms in pore space helps maintain the reservoir pressure and will be produced more and faster than the case with 15 producers. As a result, there is not much free gas to support reservoir pressure. For the same reservoir properties and conditions, the higher reservoir pressure and free gas in pore space, the more oil will be produced. Once, much gas is produced to surface at some certain time just before abandonment, gas would decline suddenly. Then, wells would be shut in faster than usual. Therefore, using 32 producers will produce less oil than using 15 producers. In addition, the higher free gas in pore space at below the bubble point, the higher and longer the pressure to lift the fluid to the surface. Once free gas is produced quickly with more producers, the pressure will decrease rapidly.

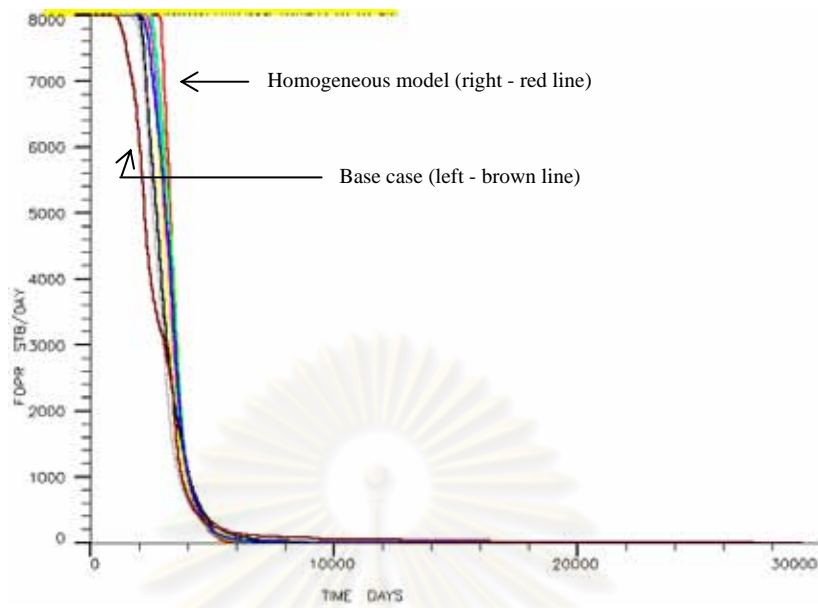


Figure 5.6 : Relationship between field oil production rate and time of 9 models with different values of V_{DP} using 32 producers

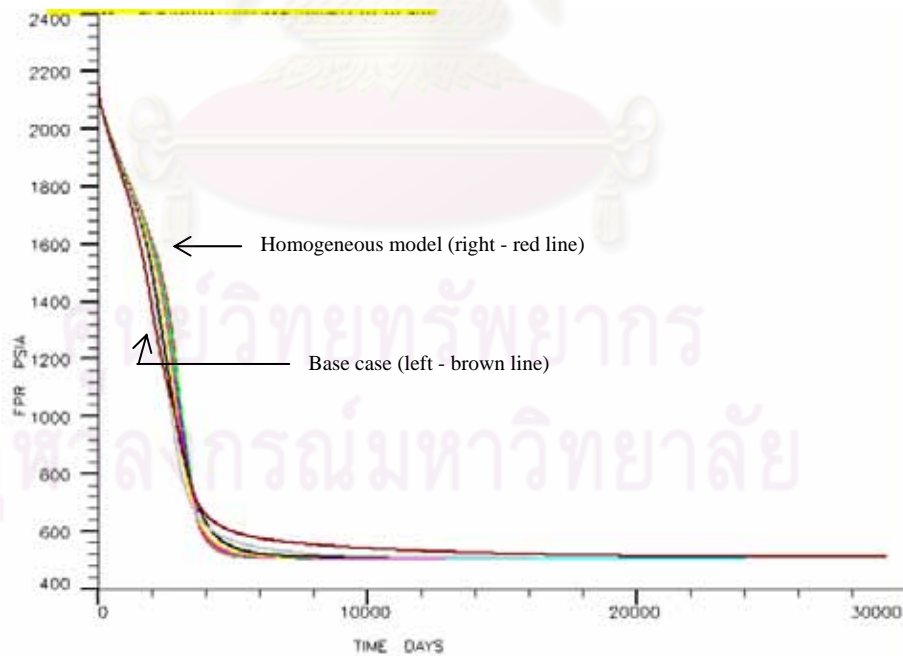


Figure 5.7 : Relationship between reservoir pressure and time of 9 models with different values of V_{DP} using 32 producers

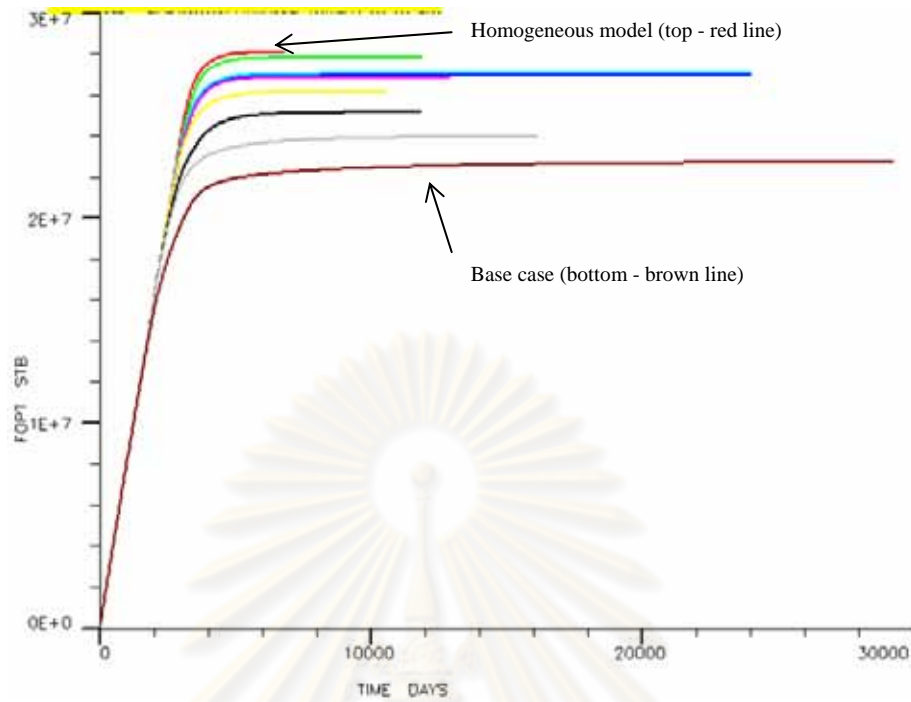


Figure 5.8 : Relationship between cumulative oil production and time of 9 models with different values of V_{DP} using 32 producers

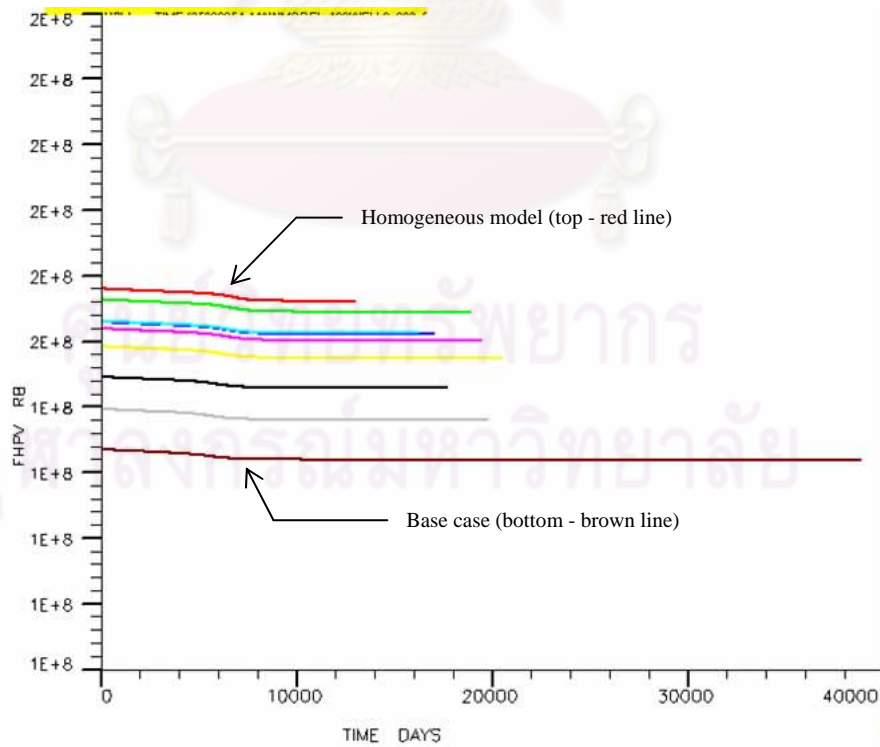


Figure 5.9 : Comparison of hydrocarbon pore volume and time

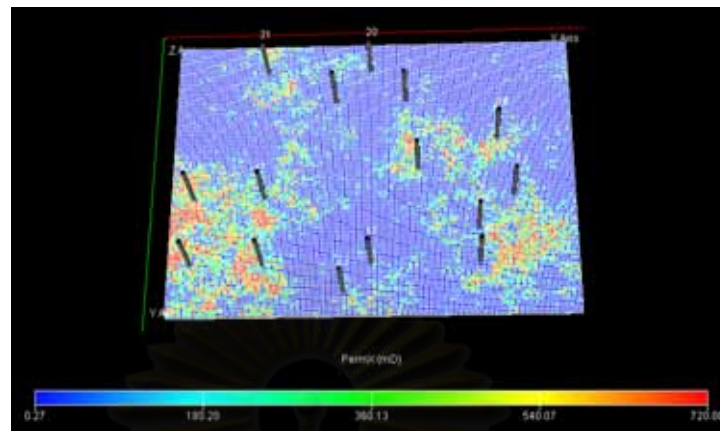


Figure 5.10 : Reservoir model with 15 producers

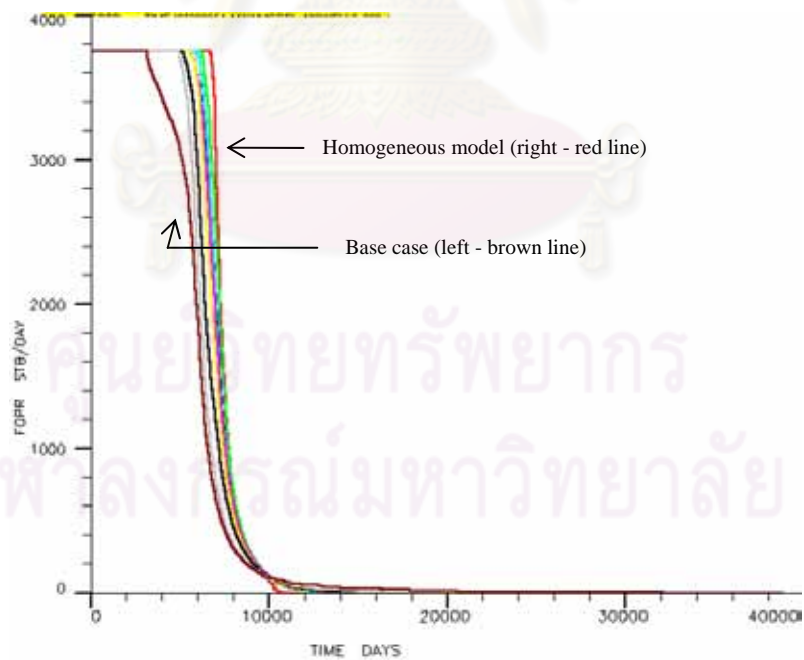


Figure 5.11 : Relationship between field oil production rate and time of 9 models with different values of V_{DP} using 15 producers

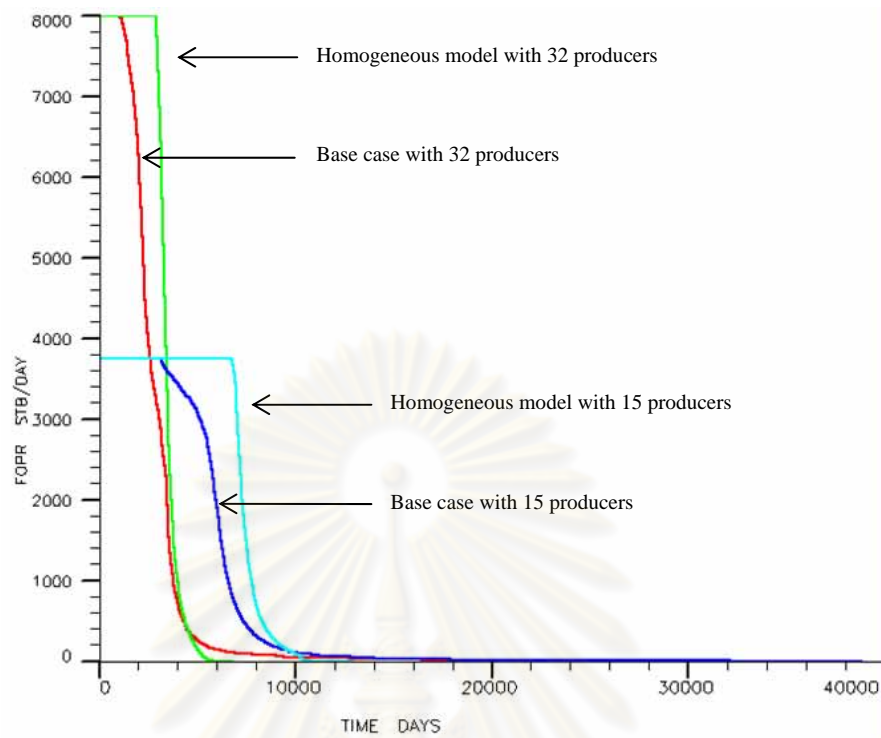


Figure 5.12 : Relationship between field oil production rate and time using 32 and 15 producers

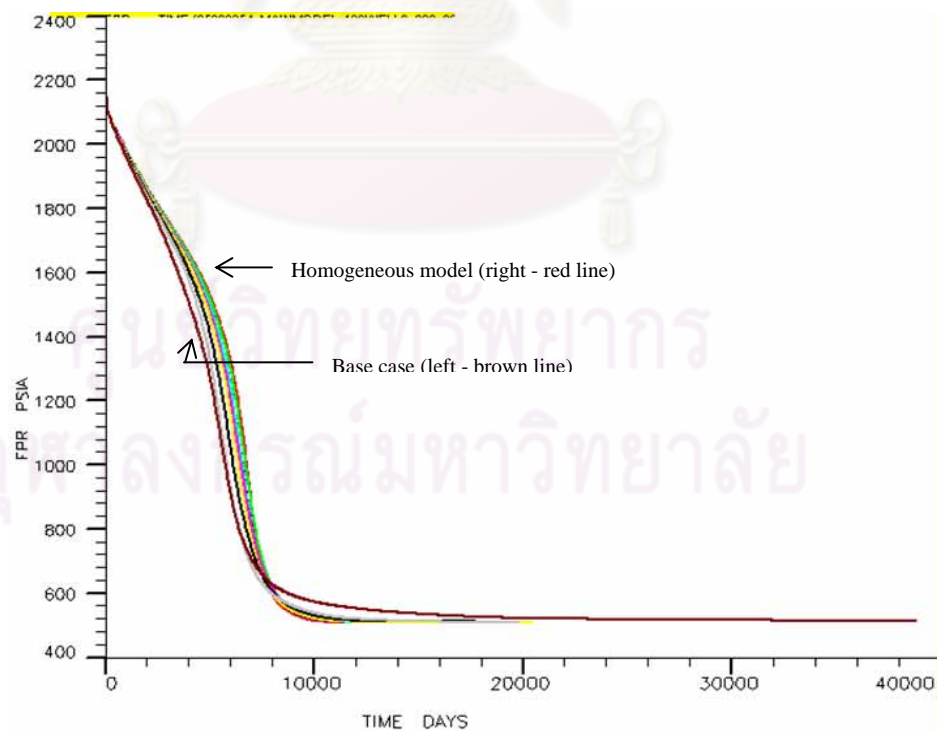


Figure 5.13 : Relationship between reservoir pressure and time of 9 models with different values of V_{DP} using 15 producers

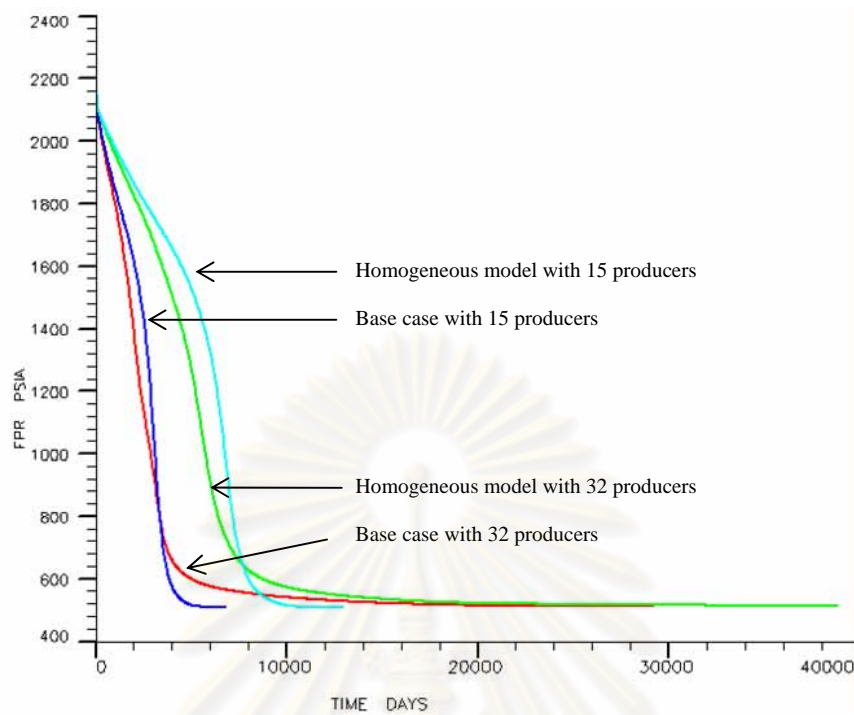


Figure 5.14 : Relationship between reservoir pressure and time using 32 and 15 producers

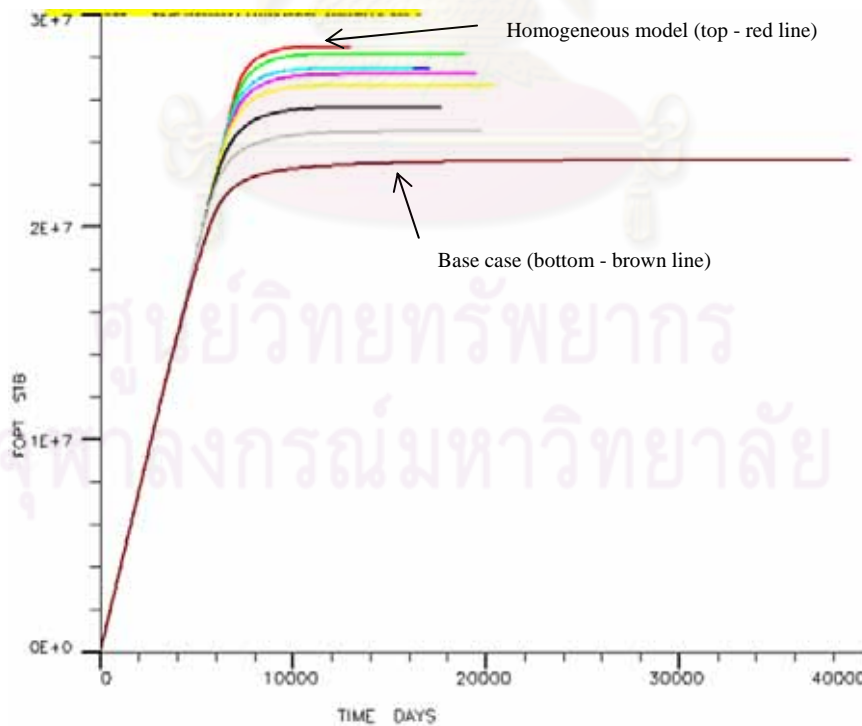


Figure 5.15 : Relationship between cumulative oil production and time of 9 models with different values of V_{DP} using 15 producers

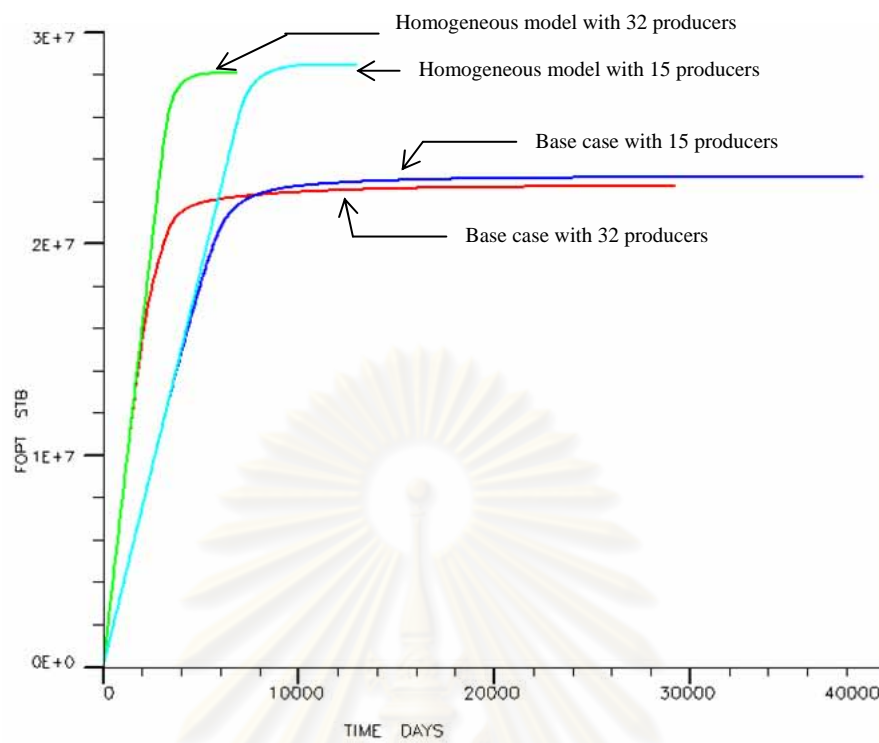


Figure 5.16 : Relationship between cumulative oil production and time using 32 and 15 producers

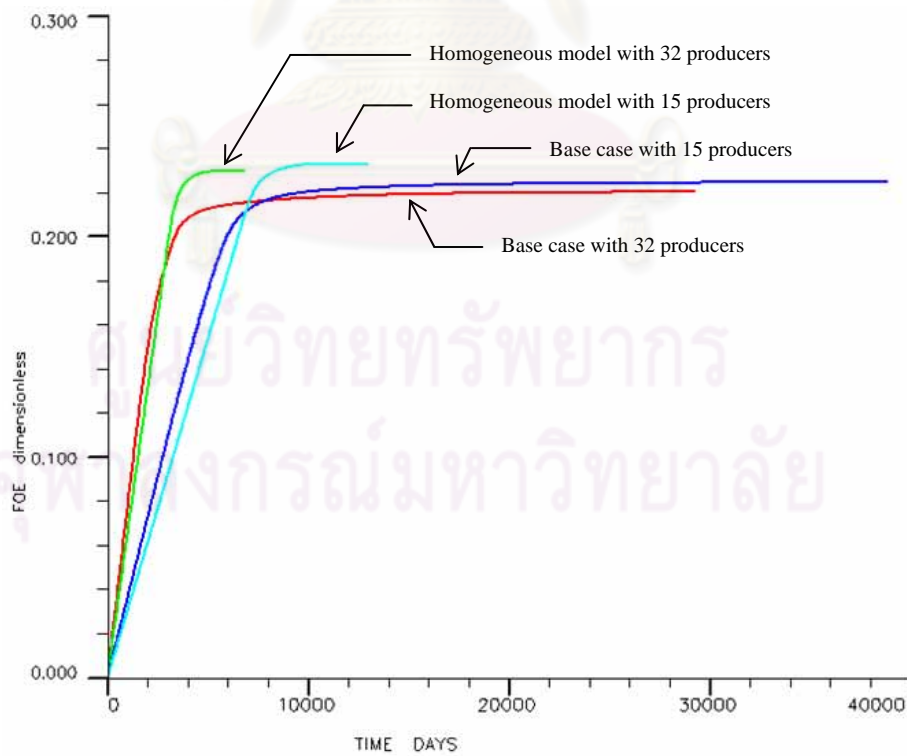


Figure 5.17 : Relationship between oil recovery and time using 32 and 15 producers

CHAPTER VI

CONCLUSIONS AND RECOMMENDATIONS

6.1 Conclusions

To determine the level of heterogeneity in reservoir, we used a statistic measure, namely, Dykstra-Parsons coefficient. In reality, in reservoir evaluation we always deal with uncertainties concerned by amounts of data. The more information we have, the less uncertainty and more accuracy the reservoir prediction will be. As limited data in the petroleum industry are unavoidable due to cost of operations, Geostatistical method can be used to create realization(s) with limited data by using spatial relationships or variograms to describe how neighborhood values are related according to distance and direction. The accuracy of finding the values at unsampled locations depends on how good the variogram model is. That is, minimize the impact of outlier. In this study, spherical and Gaussian variogram models were used. In addition, varying spatial continuity parameters such as relative nugget and range was also used to assess uncertainty. Once, spatial relationship was defined, Sequential Gaussian Simulation was used to generate different maps while preserving the original statistical data. Finally, reservoir simulation was performed in order to investigate the effect of different degrees of reservoir heterogeneities in recovery factor and time to abandonment.

The conclusions of the study are summarized below:

1. V_{DP} mainly depends upon standard deviation (SD) of the data. That is, the higher SD, the higher V_{DP} will be obtained. In this study, the simulated maximum and minimum V_{DP} values are 0.885 and 0.480, respectively.
2. The maximum and minimum oil recoveries in this study are 22.95% and 21.86%. There is only a slight difference on the recovery factor as V_{DP} varies.

3. As the range increases the continuity increases causing the V_{DP} to decrease and the recovery to increase slightly. Conversely, as the nugget increases, the V_{DP} increases and the recovery decreases.
4. At a higher degree of heterogeneity, there is a wider range of variation or more uncertainty on recovery factor than the lower one.
5. Reducing the number of producers slightly increases RF.
6. Considering with the time to abandonment, a reservoir with the highest V_{DP} will take the longest time to produce oil and get the lowest RF. However, there is only a slight decrease in recovery factor.

6.2 Recommendations

Recommendations for future study are as follows:

1. To obtain more accurate results, permeability and porosity need to be jointly investigated within the framework of Sequential Gaussian Cosimulation (SGCOSIM)
2. As some authors state that permeability can be normal distribution and V_{DP} algorithm can be used for both normal and log-normal distributions, uncertainty between these two distributions might be further studied.
3. As the depletion drive did not have much variation on RF, waterflooding would have more pronounced effect on variation of RF. As a result, waterflooding needs to be investigated in the future.

References

- Al-Khalifa, M.A. The Role of Conceptual Geological Models in More Accurately Estimating In Place Hydrocarbon: An Example From the Cooper Basin, South Australia, paper SPE 100956, SPE Adelaide, Australia, September 2006
- Al Rumhy, M.H. A Synergistic Approach to Characterization of Reservoir Permeability: A Conditional Kriging Method, paper SPE 21446, SPE Middle East Oil Show, Bahrain, November 1990.
- Baker, R.O., and Moore, R.G. Effect of Reservoir Heterogeneities on Flow Simulation Requirements, paper SPE 35413, Improved Oil Recovery Symposium, Tulsa, April, 1997
- Jakobsen, S.R. Assessing the Relative Permeability of Heterogeneous Reservoir Rock, paper SPE 28856, European Petroleum Conference, London, U.K., October 1994.
- Jerry Lucia, F., and Graham E. Fogg. Geologic/Stochastic Mapping of Heterogeneity in a Carbonate Reservoir, SPE, University of Texas and California.
- Journel, A.G. Geostatistics for Reservoir Characterization, paper SPE 20750, The 65th Annual Technical Conference and Exhibition, New Orleans, LA, September 1990.
- Journel, A.G. Geostatistics and Reservoir Geology, AAPG Computer Applications in Geology, no. 3, pp. 19-20. Tulsa, U.S.A., 1994.
- Karn B., Jakarrin A. and Atjana L. Comparison of Homogeneous and Heterogeneous Models, Bachelor's Project, Department of Mining and Petroleum Engineering, Chulalongkorn University, 2005.

Kirk B. Hird. Conditional Simulation Method for Reservoir Description Using Spatial and Well-Performance Constraints, SPE, Amoco Production Research.

Larry W. Lake and Jerry L. Jensen. A Review of Heterogeneity Measures Used in Reservoir Characterization, The University of Texas at Austin and Heriott-Watt University, Texas, U.S.A.

Paul J. Hicks. Unconditional Sequential Gaussian Simulation For 3-D Flow In A Heterogeneous Core, The Pennsylvania State University, University Park, U.S.A.

Poquioma, P., and Mohan Kelkar. Application of Geostatistics to Forecast Performance for Waterflooding an Oil Field, S.A. and The University of Tulsa, 1994.

Sahni, A., and Dehghani K. Benchmarking Heterogeneity of Simulation Models, paper SPE 96838. SPE Annual Technical Conference, Texas, U.S.A., October 2005.

Srivastava, R.M. An Overview of Stochastic Model for Reservoir Characterization, AAPG Computer Applications in Geology, no. 3, pp. 3-16. Tulsa, U.S.A., 1994.

Wilhite, G. Paul. Waterflooding, SPE Textbook, Dallas, 1986.



APPENDICES

ศูนย์วิทยทรัพยากร
จุฬาลงกรณ์มหาวิทยาลัย

APPENDIX A

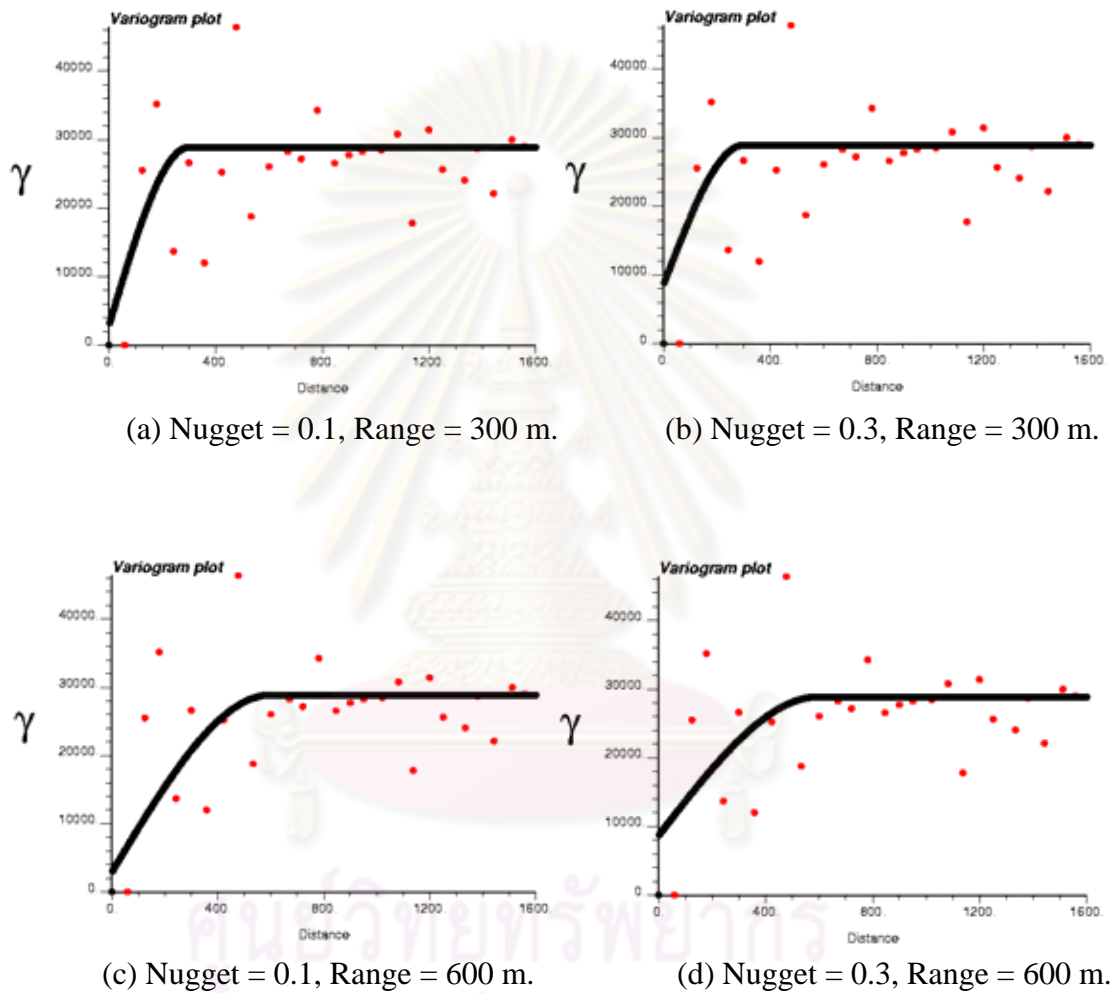
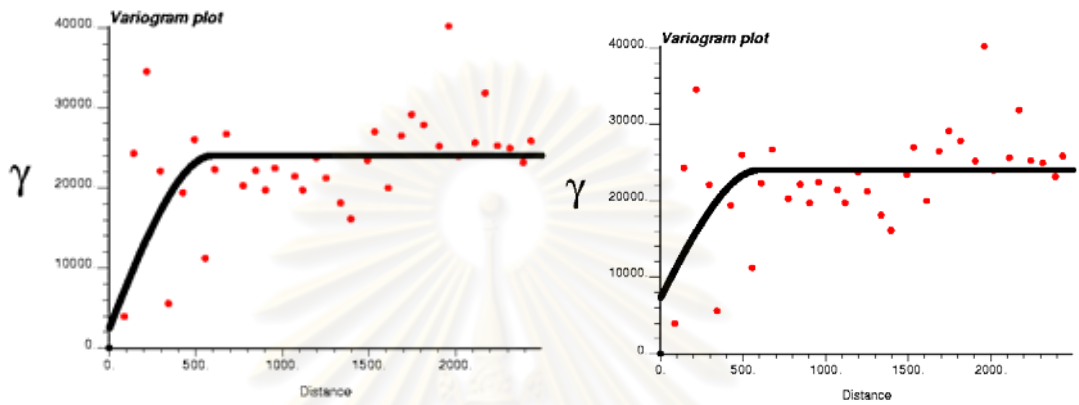
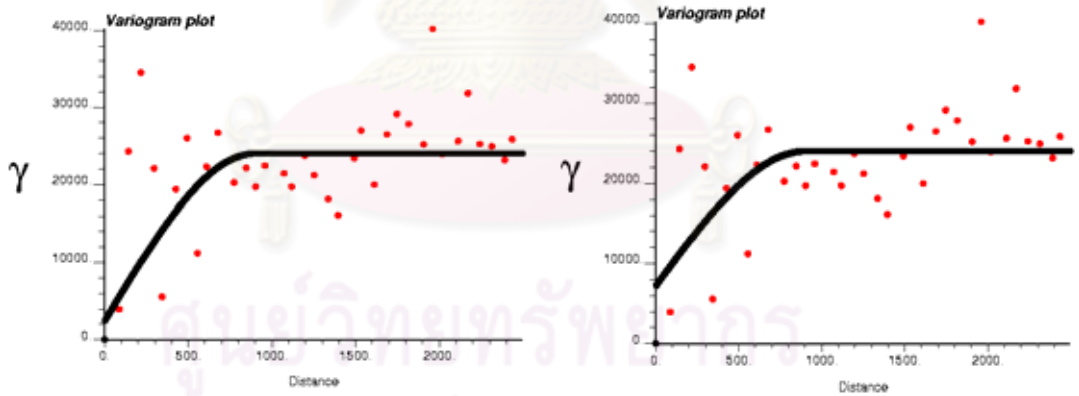


Figure A1 : Omni-directional spherical variograms of base case varied nuggets and ranges using number of lags of 32, lag distance of 60 m.



(a) Nugget = 0.1, Range = 600 m.

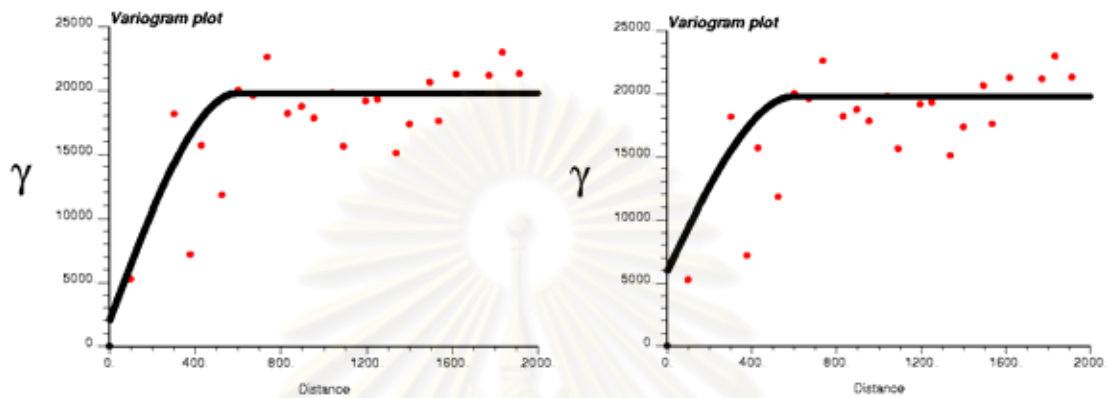
(b) Nugget = 0.3, Range = 600 m.



(c) Nugget = 0.1, Range = 900 m.

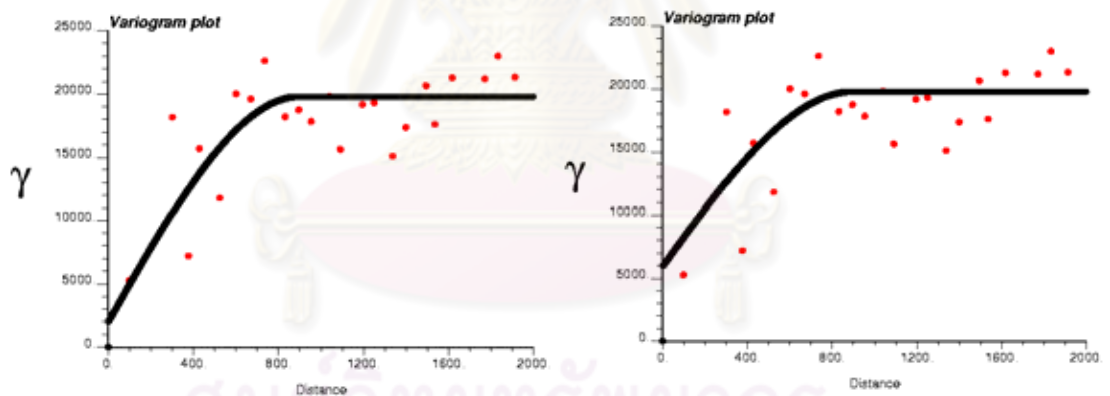
(d) Nugget = 0.3, Range = 900 m.

Figure A2 : Omni-directional spherical variograms of the model I varied nuggets and ranges using number of lags of 35, lag distance of 70 m.



(a) Nugget = 0.1, Range = 600 m.

(b) Nugget = 0.3, Range = 600 m.



(c) Nugget = 0.1, Range = 900 m.

(d) Nugget = 0.3, Range = 900 m.

Figure A3 : Omni-directional spherical variograms of the model II varied nuggets and ranges using number of lags of 35, lag distance of 74 m.

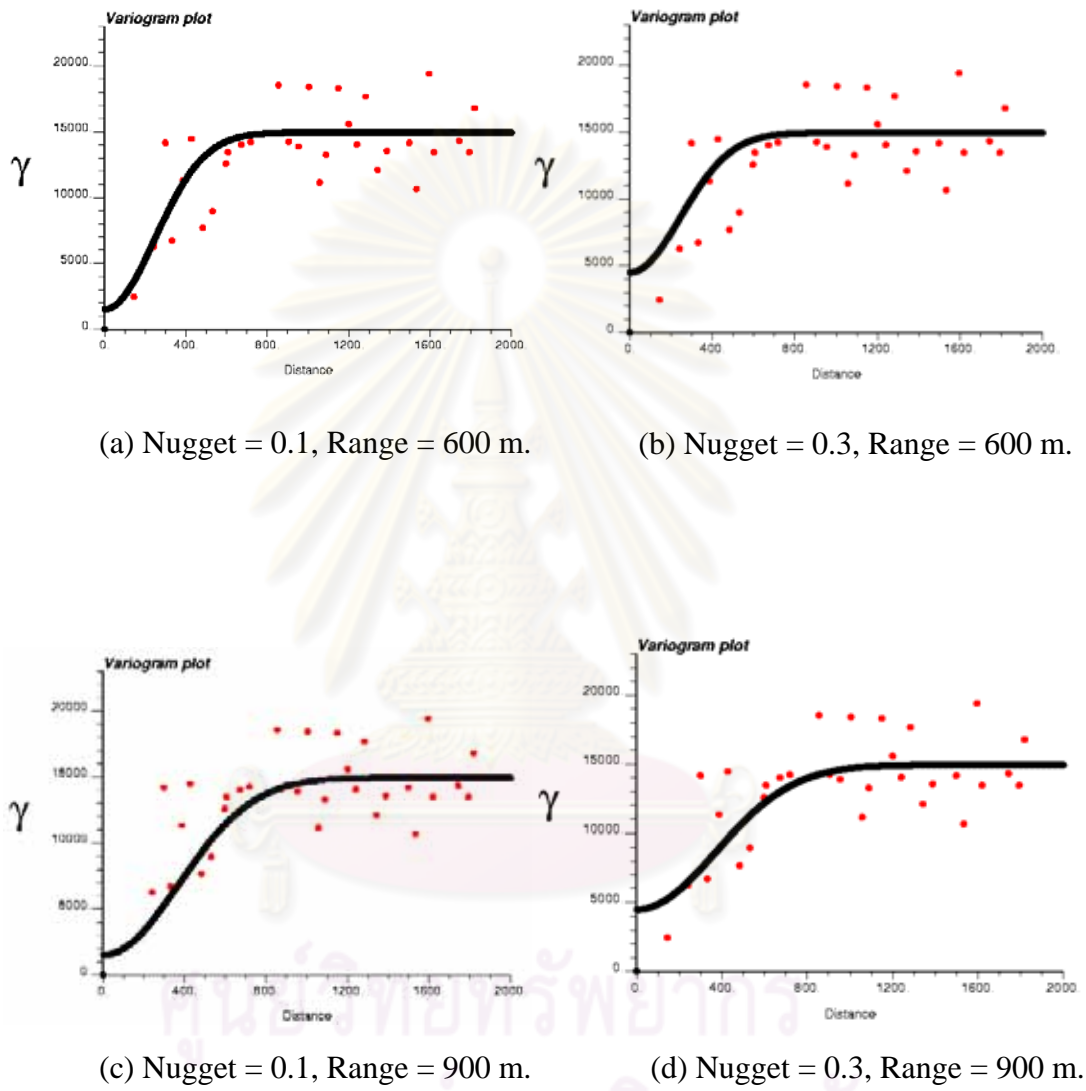


Figure A4 : Omni-directional Gaussian variograms of the model III varied nuggets and ranges using number of lags of 38, lag distance of 48 m.

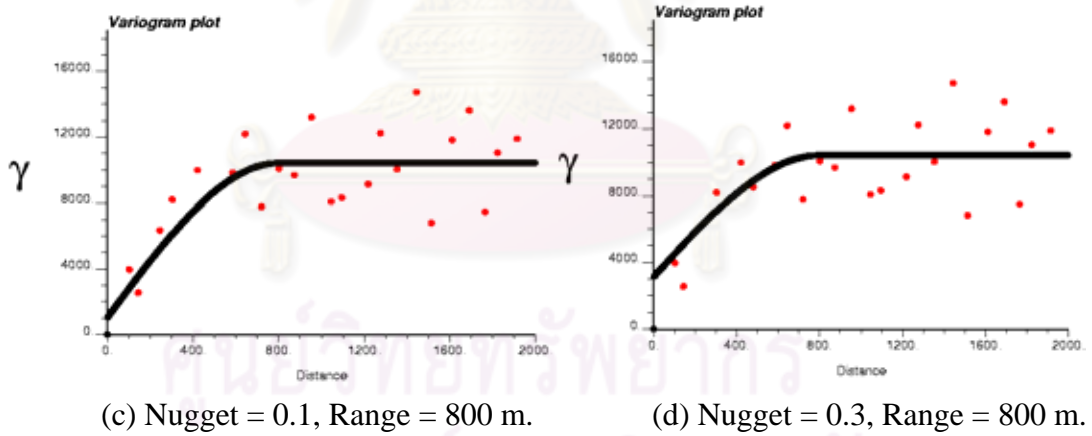
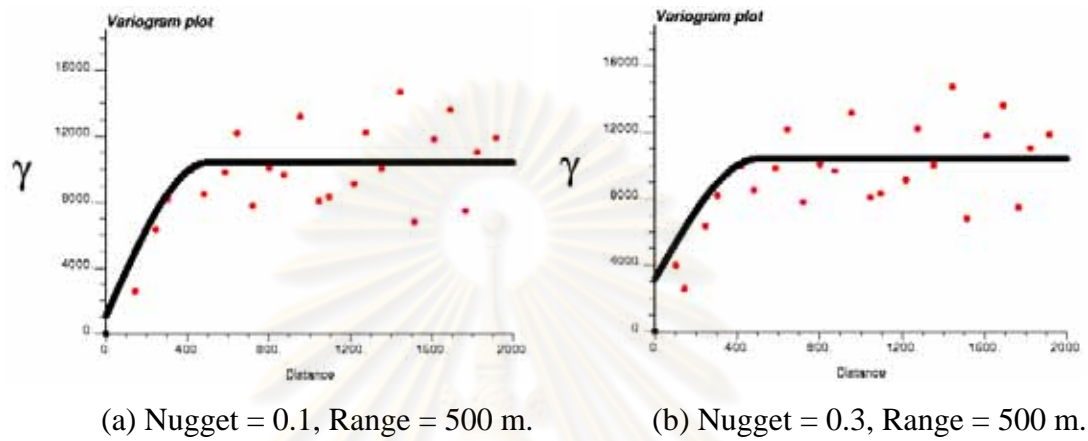


Figure A5 : Omni-directional spherical variograms of the model IV varied nuggets and ranges using number of lags of 37, lag distance of 80 m.

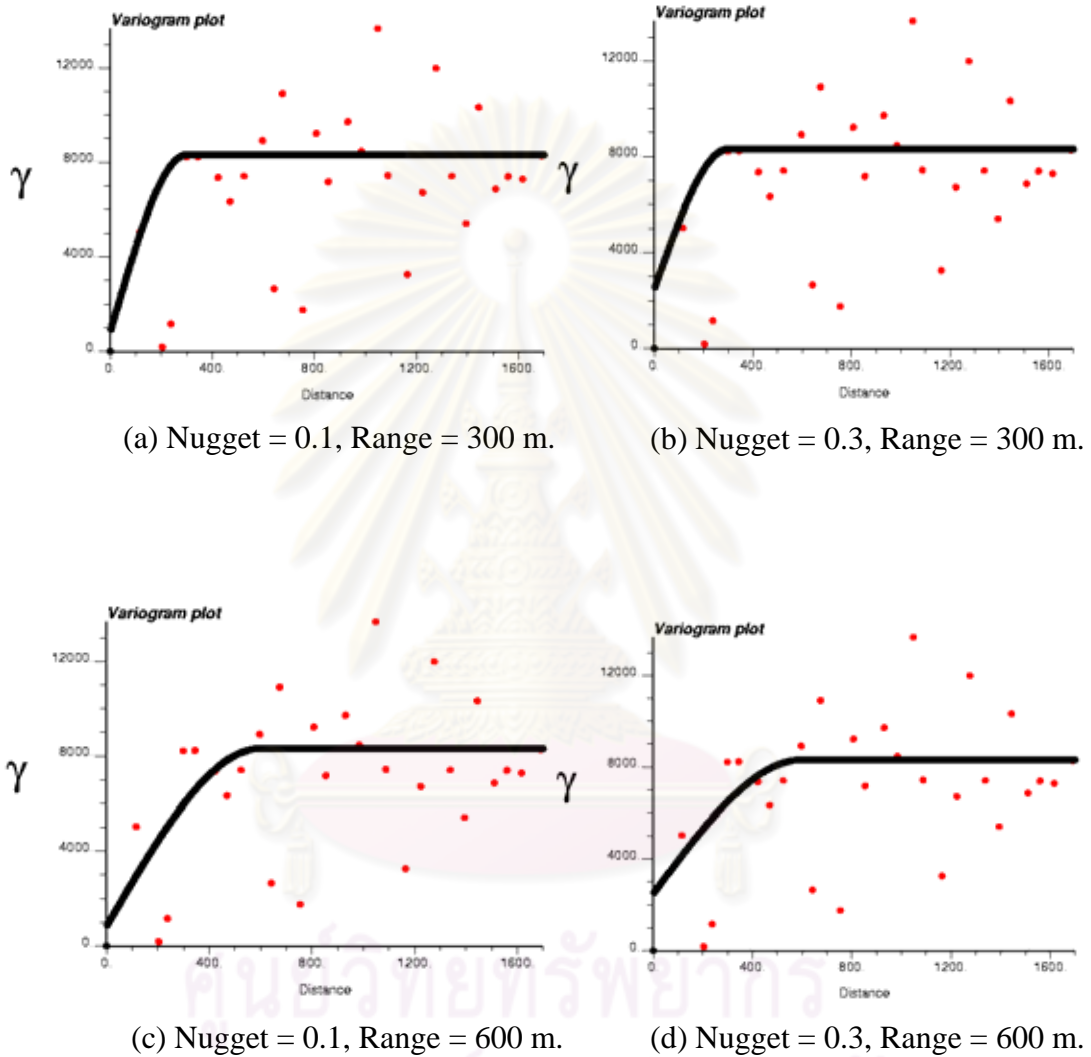


Figure A6 : Omni-directional spherical variograms of the model V varied nuggets and ranges using number of lags of 34, lag distance of 58 m.

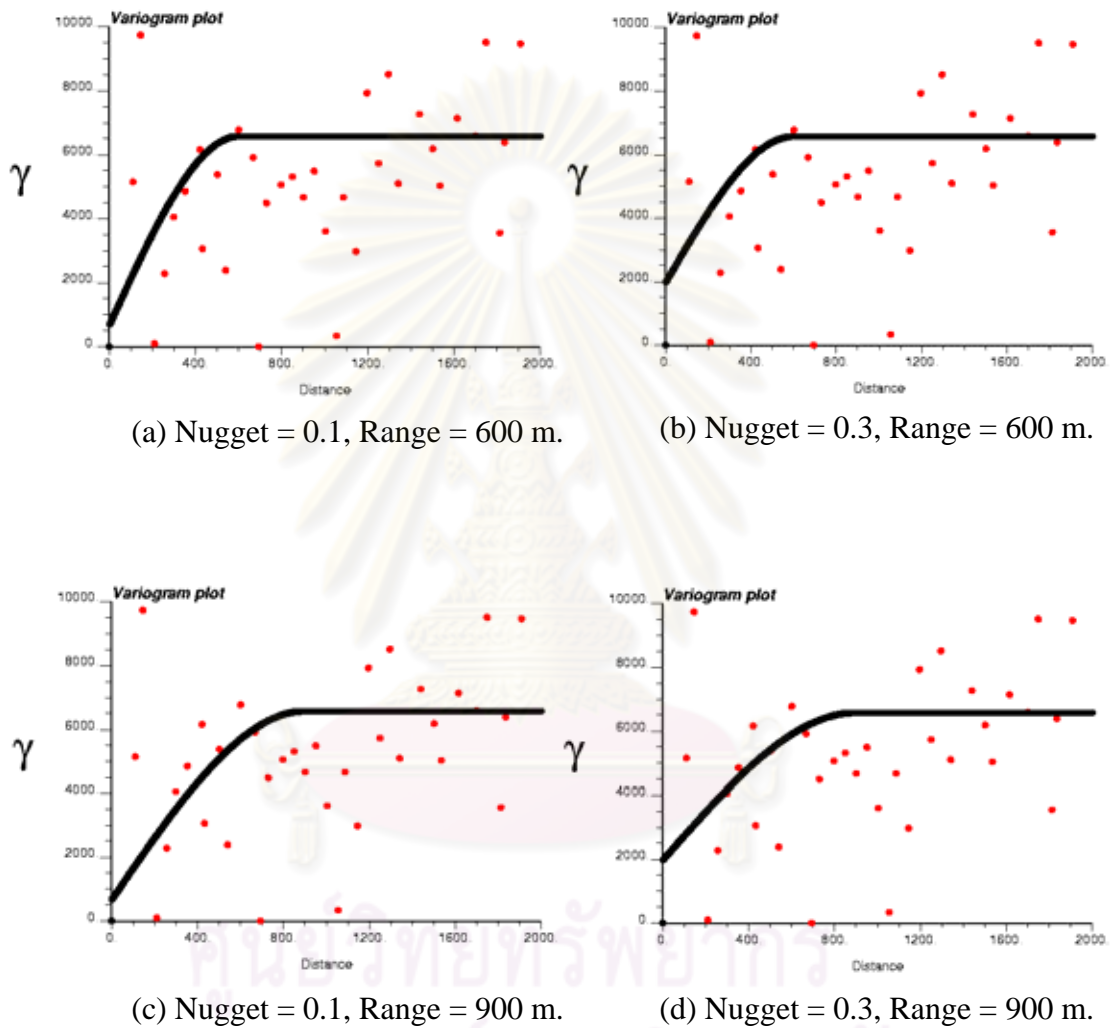


Figure A7 : Omni-directional spherical variograms of the model VI varied nuggets and ranges using number of lags of 40, lag distance of 50 m.

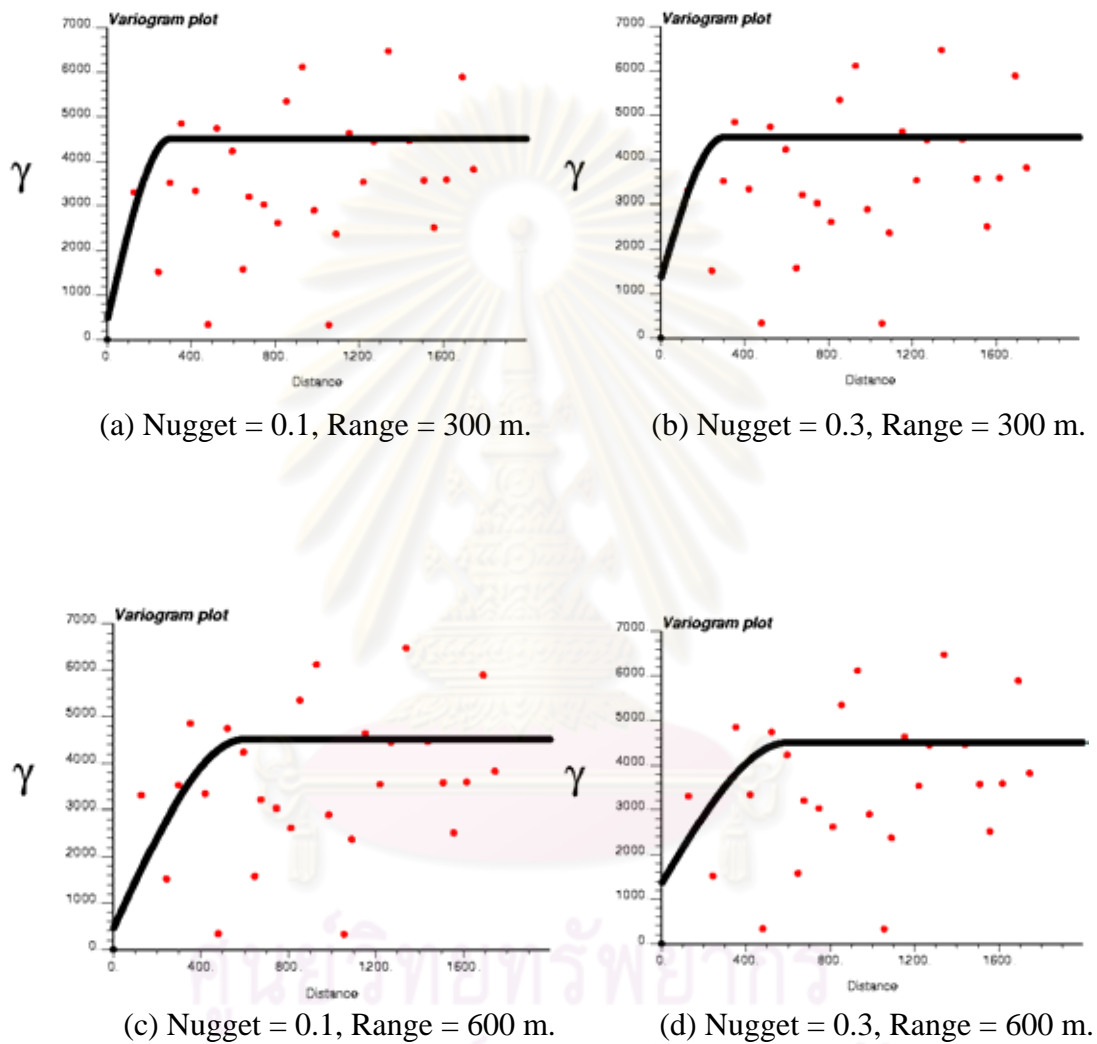


Figure A8 : Omni-directional spherical variograms of the model VII varied nuggets and ranges using number of lags of 30, lag distance of 58 m.

APPENDIX B

B1) Input parameters used in the ECLIPSE program

B1.1) Case Definition

General

- simulator Black Oil
- Simulation Start Date 1 Jan 2009
- Select Model Dimensions
 - o No. of cells in X direction 136
 - o No. of cells in Y direction 100
 - o No. of cells in Z direction 1

Reservoir

- Grid option
 - o Grid type Cartesian
- Geometry option
 - o Geometry type Block Centered

PVT

- Oil-Gas-Water properties Water, Oil and Dissolved Gas

B1.2) Grid

Grid Keyword Section

- Geometry
 - o Grid Data Units Feet
 - o X Grid Block Sizes 82
 - o Y Grid Block Sizes 82
 - o Z Grid Block Sizes 23
 - o Depth of Top Faces 5300

B1.3) PVT

PVT Keyword Section

- Water PVT Properties
 - Reference Pressure (Pref) 3,200 psia
 - Water FVF at Pref 1.0223 rb/stb
 - Water Compressibility 3.5E⁻⁶ /psi
 - Water Viscosity at Pref 0.3 cp

- Live Oil PVT Properties (Dissolved Gas)

R _s (Mscf/stb)	P _{hub} (psia)	FVF (rb/stb)	Viscosity (cp)
0.03	192	1.1363	1.7259
	445.05	1.1336	1.7666
	698.11	1.1309	1.8074
	951.16	1.1282	1.8481
	1204.2	1.1255	1.8889
	1457.3	1.1228	1.9296
	1710.3	1.1201	1.9704
	1963.4	1.1174	2.0111
	2216.4	1.1147	2.0518
	2469.5	1.112	2.0926
	2722.5	1.1093	2.1333
	2975.6	1.1066	2.1741
	3228.6	1.1039	2.2148
	3481.7	1.1012	2.2555
	3734.7	1.0985	2.2963
	3987.8	1.0958	2.337
	4240.8	1.0931	2.3778
4493.9	1.0904	2.4185	
4746.9	1.0877	2.4593	
5000	1.085	2.5	
0.15	575	1.1675	1.4
	807.89	1.165	1.4368
	1040.8	1.1625	1.4737
	1273.7	1.16	1.5105
	1506.6	1.1575	1.5474
	1739.5	1.155	1.5842
	1972.4	1.1525	1.6211
	2205.3	1.15	1.6579
	2438.2	1.1475	1.6947
	2671.1	1.145	1.7316
	2903.9	1.1425	1.7684
	3136.8	1.14	1.8053
	3369.7	1.1375	1.8421
	3602.6	1.135	1.8789
	3835.5	1.1325	1.9158
	4068.4	1.13	1.9526
	4301.3	1.1275	1.9895
4534.2	1.125	2.0263	
4767.1	1.1225	2.0632	
5000	1.12	2.1	

- Live Oil PVT Properties (Dissolved Gas) (continued)

R _s (Mscf/stb)	P _{hub} (psia)	FVF (rb/stb)	Viscosity (cp)
0.215	928	1.195	1.23
	1142.3	1.1924	1.2679
	1356.6	1.1897	1.3058
	1570.9	1.1871	1.3437
	1785.3	1.1845	1.3816
	1999.6	1.1818	1.4195
	2213.9	1.1792	1.4574
	2428.2	1.1766	1.4953
	2642.5	1.1739	1.5332
	2856.8	1.1713	1.5711
	3071.2	1.1687	1.6089
	3285.5	1.1661	1.6468
	3499.8	1.1634	1.6847
	3714.1	1.1608	1.7226
	3928.4	1.1582	1.7605
	4142.7	1.1555	1.7984
	4357.1	1.1529	1.8363
	4571.4	1.1503	1.8742
	4785.7	1.1476	1.9121
	5000	1.145	1.95
0.28	1281	1.225	1.125
	1476.7	1.2229	1.1579
	1672.5	1.2208	1.1908
	1868.2	1.2187	1.2237
	2063.9	1.2166	1.2566
	2259.7	1.2145	1.2895
	2455.4	1.2124	1.3224
	2651.2	1.2103	1.3553
	2846.9	1.2082	1.3882
	3042.6	1.2061	1.4211
	3238.4	1.2039	1.4539
	3434.1	1.2018	1.4868
	3629.8	1.1997	1.5197
	3825.6	1.1976	1.5526
	4021.3	1.1955	1.5855
	4217.1	1.1934	1.6184
	4412.8	1.1913	1.6513
	4608.5	1.1892	1.6842
	4804.3	1.1871	1.7171
	5000	1.185	1.75
0.296	1341	1.23	1.1094
	1533.6	1.2279	1.1392
	1726.2	1.2258	1.1689
	1918.7	1.2237	1.1987
	2111.3	1.2216	1.2285
	2303.9	1.2195	1.2582
	2496.5	1.2174	1.288
	2689.1	1.2153	1.3178
	2881.6	1.2132	1.3475
	3074.2	1.2111	1.3773
	3266.8	1.2089	1.4071
	3459.4	1.2068	1.4369
	3651.9	1.2047	1.4666
	3844.5	1.2026	1.4964
	4037.1	1.2005	1.5262
	4229.7	1.1984	1.5559
	4422.3	1.1963	1.5857
	4614.8	1.1942	1.6155
	4807.4	1.1921	1.6452
	5000	1.19	1.675

- Dry Gas PVT Properties (No Vapourised Oil)

Pressure (psia)	FVF (rb/Mscf)	Visc (cp)
0	173.82	0.011
90	31.126	0.01165
200	15.103	0.0124
400	7.6836	0.01315
600	5.1037	0.0136
725	4.2287	0.01365
950	3.1579	0.01418
1175	2.5033	0.0148
1400	2.0652	0.01549
1625	1.7542	0.01628
1850	1.5245	0.01714
2075	1.3499	0.01807
2300	1.2144	0.01906
2525	1.1073	0.0201
2750	1.0215	0.02116
2975	0.95178	0.02225
3200	0.89446	0.02334
3425	0.84676	0.02442
3650	0.8066	0.0255
3875	0.77244	0.02656
4100	0.74307	0.02761
4325	0.71758	0.02863
4550	0.69526	0.02963
4775	0.67556	0.03061
5000	0.65805	0.03157

- Fluid Gravities at Surface Conditions

- Oil density 51.51 lb/ft³
- Water density 62.5 lb/ft³
- Gas density 0.06 lb/ft³

- Rock Properties

- Reference pressure 2,500 psia
- Rock compressibility 3.5E-6 /psi

B1.4) SCALSaturation

- Water/Oil Saturation Functions

S_w	K_{rw}	K_{ro}	P_c (psia)
0	0	0.9	10000
0.045455	0	0.9	2557.3
0.090909	0	0.9	653.97
0.13636	0	0.9	167.24
0.18182	0	0.9	42.768
0.22727	0	0.9	10.937
0.27273	0	0.9	2.7969
0.31818	0	0.9	0.71526
0.35	0	0.9	0.34262
0.36364	5.19E-05	0.85488	0.18291
0.37333	8.89E-05	0.82279	0.15387
0.39667	0.000711	0.74722	0.083986
0.40909	0.00161	0.7079	0.046776
0.42	0.0024	0.67338	0.038421
0.44333	0.005689	0.60136	0.020549
0.45455	0.008294	0.56769	0.011962
0.46667	0.011111	0.53128	0.009588
0.49	0.0192	0.46328	0.005018
0.5	0.024038	0.43509	0.003059
0.51333	0.030489	0.3975	0.002391
0.53667	0.045511	0.33416	0.001223
0.54545	0.052776	0.3113	0.000782
0.56	0.0648	0.27348	0.000596
0.58333	0.088889	0.21577	0.000297
0.59091	0.098442	0.19813	0.0002
0.60667	0.11831	0.16144	0.000148
0.63	0.1536	0.11107	7.20E-05
0.63636	0.16497	0.098656	5.12E-05
0.65333	0.19529	0.065564	3.69E-05
0.67667	0.24391	0.026627	1.74E-05
0.68182	0.25629	0.020748	1.31E-05
0.7	0.3	2.60E-21	9.19E-06
0.72727	0.35477	2.36E-21	3.35E-06
0.77273	0.44605	1.97E-21	8.56E-07
0.81818	0.53733	1.57E-21	2.19E-07
0.86364	0.62861	1.18E-21	5.60E-08
0.90909	0.71989	7.87E-22	1.43E-08
0.95455	0.81117	3.94E-22	3.66E-09
1	0.90245	0	9.36E-10

- Gas/Oil Saturation Functions

S_g	K_{rg}	K_{ro}	P_c (psia)
0	0	0.9	0
0.05	0	0.73657	0
0.071429	0.000182	0.66892	0
0.092857	0.001458	0.60281	0
0.11429	0.00492	0.53834	0
0.13571	0.011662	0.4756	0
0.15714	0.022777	0.41473	0
0.17857	0.039359	0.35585	0
0.2	0.0625	0.29914	0
0.22143	0.093294	0.24482	0
0.24286	0.13284	0.19316	0
0.26429	0.18222	0.14452	0
0.28571	0.24253	0.099427	0
0.30714	0.31487	0.058693	0
0.32857	0.40033	0.023837	0
0.35	0.5	0	0
0.65	1	0	0

B1.5) Initialization

Initialization Keyword Section

-Initial pressure vs depth

Depth (ft)	Pressure (psia)
5300	2252.57

- Initial Gas Saturation 0
- Initial Water Saturation 0.37
- Initial R_s 0.5 Mscf/stb

B1.6) Schedule

Events-All

- Well specification
 - o Datum depth 5300 ft.
 - o Preferred phase Oil
 - o Inflow equation STD
 - o Automatic shut-in instruction SHUT

- Crossflow YES
- Density Calculation SEG

- Well Connection Data
 - Well (Using 32 wells)
 - I Location (Following Model VII locations)
 - J Location (Following Model VII locations)
 - K Upper 1
 - K Lower1 1
 - Open/Shut Flag Open
 - Well Bore ID 0.583 ft
 - Direction Z

- Production Well Control
 - Well (Using 32 wells)
 - Open/Shut Flag Open
 - Control ORAT
 - Oil Rate 250 stb/day
 - BHP Target 500 psia

- Production Well Economic Limit
 - Well (Using 32 wells)
 - Minimum Oil Rate 5 stb/day
 - Maximum Water Cut 0.9 stb/stb
 - Workover Procedure None
 - End Run No
 - Quantify For Economic Limit Rate
 - Secondary Workover Procedure None

- Print File Output Control
 - Restarts Every Report
 - FIP Reports + Balance Sheet
 - VFP Reports No VFP Table Output

Table B1 : Comparison of oil recovery and reservoir pressure at different degrees of heterogeneity

Model name	Number of original wells	Seed no.	Variogram type	Nugget (%) and range (m.)	V _{DP}	% Oil recovery at the days of 5,160	Time to abandonment (day)	% Oil recovery at abandonment	Reservoir pressure (psi) at the days of 5,160	Reservoir pressure (psi) at abandonment			
Homogeneous at k = 101.74 md					0	22.954	5160	22.954	510	510			
Base case	109	5209254	Spherical	0.1_300	0.879	21.376	24660	22.048	588	509			
				0.3_300	0.885	21.288	27210	22.019	594	511			
				0.1_600	0.862	21.407	20310	22.037	585	509			
				0.3_600	0.873	21.309	23340	22.016	592	510			
		1299460		0.1_300	0.875	21.282	22620	21.946	592	509			
				0.3_300	0.880	21.066	25320	21.867	607	509			
				0.1_600	0.860	21.436	18720	21.974	578	508			
				0.3_600	0.870	21.181	22830	21.890	598	509			
		4211847		0.1_300	0.867	21.831	11430	22.167	552	509			
				0.3_300	0.872	21.729	12090	22.138	564	510			
				0.1_600	0.846	21.76	11190	22.110	554	508			
				0.3_600	0.856	21.675	11970	22.088	563	509			
		1062367		0.1_300	0.876	21.424	13800	21.969	578	508			
				0.3_300	0.879	21.286	14340	21.902	586	509			
				0.1_600	0.855	21.475	14010	21.959	574	510			
				0.3_600	0.864	21.314	15060	21.898	585	509			
model I	95	896078	Spherical	0.1_600	0.773	21.948	10740	22.268	548	507			
				0.3_600	0.781	22.01	9540	22.303	546	508			
				0.1_900	0.754	21.949	10500	22.259	547	507			
				0.3_900	0.766	22.024	9510	22.306	545	508			
		153567		0.1_600	0.798	21.919	13740	22.243	550	507			
				0.3_600	0.804	21.92	12480	22.257	552	508			
				0.1_900	0.783	21.927	13410	22.245	550	507			
				0.3_900	0.794	21.924	11880	22.257	552	508			
		4773049		0.1_600	0.813	21.76	13470	22.181	562	508			
				0.3_600	0.819	21.764	13260	22.179	562	508			
				0.1_900	0.797	21.784	13230	22.185	560	508			
				0.3_900	0.808	21.777	12750	22.179	561	509			
		5237802		0.1_600	0.786	21.682	14460	22.108	562	508			
				0.3_600	0.795	21.658	13590	22.073	560	508			
				0.1_900	0.768	21.722	14190	22.123	559	508			
				0.3_900	0.782	21.697	13050	22.093	559	508			
model II	82	4574483	Spherical	0.1_600	0.703	22.342	10770	22.543	535	507			
				0.3_600	0.719	22.291	11370	22.520	540	508			
				0.1_900	0.678	22.319	10800	22.524	536	507			
				0.3_900	0.704	22.273	11490	22.506	540	508			
		3782386		0.1_600	0.700	22.616	7980	22.726	522	507			
				0.3_600	0.709	22.635	8070	22.749	523	507			
				0.1_900	0.682	22.561	8160	22.681	524	507			
				0.3_900	0.696	22.603	8190	22.723	524	508			
		6768113		0.1_600	0.691	22.45	9810	22.602	527	507			
				0.3_600	0.709	22.461	9750	22.616	527	507			
				0.1_900	0.672	22.426	9840	22.581	527	507			
				0.3_900	0.697	22.451	9690	22.607	528	507			
		model III		70	218583	Gaussian	0.1_600	0.654	22.582	9180	22.702	523	507
							0.3_600	0.659	22.674	8760	22.772	522	508
							0.1_900	0.624	22.558	8970	22.681	524	507
							0.3_900	0.639	22.68	8490	22.776	522	508
7497676	0.1_600		0.663		22.522		9330	22.661	526	507			
	0.3_600		0.675		22.56		9090	22.699	526	507			
	0.1_900		0.630		22.452		9840	22.615	530	508			
	0.3_900		0.656		22.539		9180	22.685	527	507			
2904965	0.1_600		0.651		22.585		8310	22.709	524	507			
	0.3_600		0.654		22.647		8070	22.763	523	507			
	0.1_900		0.620		22.532		8550	22.671	526	507			
	0.3_900		0.635		22.635		8070	22.755	524	507			

Table B1 : Comparison of oil recovery and reservoir pressure at different degrees of heterogeneity (continued)

Model name	Number of original wells	Seed no.	Variogram type	Nugget (%) and range (m.)	V _{DP}	% Oil recovery at the days of 5,160	Time to abandonment (day)	% Oil recovery at abandonment	Reservoir pressure (psi) at the day of 5,160	Reservoir pressure (psi) at abandonment
Homogeneous at k = 101.74 md					0	22.954	5160	22.954	510	510
model IV	58	6259246	Spherical	0.1_500	0.586	22.754	7590	22.837	518	506
				0.3_500	0.594	22.727	7830	22.820	520	506
				0.1_800	0.562	22.721	7770	22.807	519	506
				0.3_800	0.579	22.706	7950	22.802	520	506
		9451304		0.1_500	0.587	22.783	8610	22.870	518	506
				0.3_500	0.597	22.793	8640	22.878	518	506
				0.1_800	0.573	22.733	8880	22.827	519	506
				0.3_800	0.588	22.761	8820	22.852	519	506
		2895849		0.1_500	0.572	22.818	7320	22.884	517	507
				0.3_500	0.584	22.817	7440	22.888	518	507
				0.1_800	0.562	22.783	7560	22.855	518	507
				0.3_800	0.578	22.791	7650	22.867	519	508
model V	49	7301294	Spherical	0.1_300	0.554	22.823	7260	22.888	516	507
				0.3_300	0.559	22.809	7200	22.880	517	507
				0.1_600	0.532	22.773	7470	22.840	517	507
				0.3_600	0.544	22.768	7710	22.842	518	507
		69069		0.1_300	0.568	22.794	8370	22.875	518	506
				0.3_300	0.571	22.78	8880	22.869	519	506
				0.1_600	0.551	22.747	8550	22.830	518	506
				0.3_600	0.559	22.74	9090	22.833	519	506
		5027296		0.1_300	0.562	22.884	7290	22.945	516	507
				0.3_300	0.566	22.865	7530	22.933	517	507
				0.1_600	0.539	22.848	7500	22.911	517	507
				0.3_600	0.550	22.84	7770	22.913	518	507
model VI	40	1042094	Spherical	0.1_600	0.524	22.806	7620	22.876	518	506
				0.3_600	0.531	22.805	7890	22.880	519	506
				0.1_900	0.506	22.802	7680	22.872	518	506
				0.3_900	0.519	22.800	7980	22.875	519	506
		6160440		0.1_600	0.508	22.929	7200	22.981	515	506
				0.3_600	0.516	22.902	7530	22.962	516	507
				0.1_900	0.493	22.906	7260	22.960	515	507
				0.3_900	0.507	22.885	7590	22.947	516	507
		8275380		0.1_600	0.499	22.883	6930	22.929	514	506
				0.3_600	0.515	22.9	6960	22.947	514	506
				0.1_900	0.489	22.883	6900	22.929	514	506
				0.3_900	0.507	22.895	6960	22.942	514	506
model VII	31	307057	Spherical	0.1_300	0.483	22.898	7650	22.954	515	506
				0.3_300	0.484	22.884	8070	22.945	516	507
				0.1_600	0.478	22.89	7740	22.945	515	506
				0.3_600	0.480	22.873	8100	22.934	511	507
		5280856		0.1_300	0.485	22.957	6630	23.005	514	506
				0.3_300	0.487	22.95	6840	23.000	515	507
				0.1_600	0.482	22.992	6870	23.038	514	507
				0.3_600	0.484	22.968	6570	23.016	514	507
		8326199		0.1_300	0.476	22.919	7020	22.975	516	507
				0.3_300	0.479	22.899	7170	22.959	516	507
				0.1_600	0.468	22.933	7020	22.989	516	507
				0.3_600	0.474	22.903	7140	22.964	516	507

VITAE

Sarit Suwanmanee was born on July 23, 1982 in Surat-Thani, Thailand. He received his B.Eng. in Mining and Metallurgical Engineering from the Faculty of Engineering, Prince of Songkhla University in 2004. After graduating, he worked with a mining company for five months and then he resigned his work to study a Masters in Petroleum Engineering at the Department of Mining and Petroleum Engineering, Faculty of Engineering, Chulalongkorn University. Currently, he has worked since he completed all his academic subjects as a field M/LWD engineer with Sperry Drilling Services Department at Halliburton Energy Services.



ศูนย์วิทยทรัพยากร
จุฬาลงกรณ์มหาวิทยาลัย